การผลิตเชื้อเพลิงชีวภาพแบบต่อเนื่องจากน้ำมันปาล์มในแอลกอฮอล์ภาวะเหนือวิกฤต

นางสาววินัฏฐา ศักดาศรี

วิทยานิพนธ์นี้เป็นส่วนหนึ่งของการศึกษาตามหลักสูตรปริญญาวิทยาศาสตรดุษฎีบัณฑิต

สาขาวิชาเคมีเทคนิค ภาควิชาเคมีเทคนิค

คณะวิทยาศาสตร์ จุฬาลงกรณ์มหาวิทยาลัย

ปีการศึกษา 2558

ลิขสิทธิ์ของจุฬาลงกรณ์มหาวิทยาลัย

CONTINUOUS BIOFUEL PRODUCTION FROM PALM OIL IN
SUPERCRITICAL ALCOHOLS

Miss Winatta Sakdasri

จุฬาลงกรณ์มหาวิทยาลัย
CHULALONGKORN UNIVERSITY

A Dissertation Submitted in Partial Fulfillment of the Requirements
for the Degree of Doctor of Philosophy Program in Chemical Technology
Department of Chemical Technology
Faculty of Science
Chulalongkorn University
Academic Year 2015

Thesis Title	CONTINUOUS BIOFUEL PRODUCTION FROM PALM OIL IN SUPERCRITICAL ALCOHOLS
By	Miss Winatta Sakdasri
Field of Study	Chemical Technology
Thesis Advisor	Associate Professor Somkiat Ngamprasertsith, Doctorat de l'INPT
Thesis Co-Advisor	Professor Jean Stephane Condoret, Doctorat de l'INPT

Accepted by the Faculty of Science, Chulalongkorn University in Partial Fulfillment of the Requirements for the Doctoral Degree

.... Dean of the Faculty of Science
(Associate Professor Polkit Sangvanich, Ph.D.)

THESIS COMMITTEE

.... Chairman
(Associate Professor Kejvalee Pruksathorn, Doctorat de l'INPT)

.... Thesis Advisor
(Associate Professor Somkiat Ngamprasertsith, Doctorat de l'INPT)

.... Thesis Co-Advisor
(Professor Jean Stephane Condoret, Doctorat de l'INPT)

.... Examiner
(Professor Pattarapan Prasassarakich, Ph.D.)

.... Examiner
(Associate Professor Chawalit Ngamcharussrivichai, Ph.D.)

.... External Examiner
(Anurak Winitsorn, Ph.D.)

วินัฏฐา ศักดาศรี : การผลิตเชื้อเพลิงชีวภาพแบบต่อเนื่องจากน้ำมันปาล์มในแอลกอฮอล์ภาวะเหนือวิกฤต (CONTINUOUS BIOFUEL PRODUCTION FROM PALM OIL IN SUPERCRITICAL ALCOHOLS) อ.ที่ปรึกษาวิทยานิพนธ์หลัก: รศ. ดร. สมเกียรติ งามประเสริฐสิทธิ์, อ.ที่ปรึกษาวิทยานิพนธ์ร่วม: Prof. Jean Stephane CondoretDoctorat de l'INPT, 142 หน้า.

กระบวนการผลิตเชื้อเพลิงในแอลกอฮอล์ภาวะเหนือวิกฤตเป็นอีกหนึ่งทางเลือกสำหรับการผลิตเชื้อเพลิงชีวภาพ เนื่องจากกระบวนการนี้มีข้อได้เปรียบเหนือกว่ากระบวนการแบบดั้งเดิมซึ่งใช้ตัวเร่งปฏิกิริยาเอกพันธุ์ คือ มีประสิทธิภาพสูงและใช้วัตถุดิบได้หลากหลาย อย่างไรก็ตามการผลิตเชื้อเพลิงชีวภาพในแอลกอฮอล์ภาวะเหนือวิกฤตใช้อัตราส่วนโดยโมลแอลกอฮอล์ต่อน้ำมันพืช 40:1–42:1 เพื่อให้ได้ร้อยละเอสเทอร์สูงสุด ทำให้จำเป็นต้องใช้พลังงานมากเพื่อนำแอลกอฮอล์กลับมาใช้ใหม่ ซึ่งสร้างภาระต่อสิ่งแวดล้อมมากตามไปด้วย ดังนั้นงานวิจัยนี้มีจุดประสงค์เพื่อลดปริมาณการใช้แอลกอฮอล์สำหรับการผลิตเชื้อเพลิงชีวภาพจากชีวมวลลิพิดในแอลกอฮอล์ภาวะเหนือวิกฤต จุดประสงค์แรกของงานวิจัยนี้คือหาภาวะที่เหมาะสมสำหรับการผลิตเชื้อเพลิงชีวภาพในเครื่องปฏิกรณ์แบบแบตช์ จากการศึกษาโดยวิธีการพื้นผิวตอบสนอง (Response surface methodology) พบว่าที่อุณหภูมิ 400 องศาเซลเซียสสามารถลดอัตราส่วนโดยโมลแอลกอฮอล์ต่อน้ำมันพืชเป็น 12:1 จุดประสงค์ที่สองคือ การขยายการผลิตเชื้อเพลิงชีวภาพในเครื่องปฏิกรณ์แบบต่อเนื่อง พบว่าการใช้อัตราส่วนโดยโมลแอลกอฮอล์ต่อน้ำมันพืช 12:1 ที่อุณหภูมิ 400 องศาเซลเซียส ให้ร้อยละการเปลี่ยนของไตรกลีเซอร์ไรด์สูงถึง 99 และให้ร้อยละเอสเทอร์สูงสุดอยู่ในช่วง 80-90 นอกจากนี้ยังพบปฏิกิริยาข้างเคียงของกลีเซอรอลกับแอลกอฮอล์ที่ 400 องศาเซลเซียสและความดัน 15 เมกะพาสคัลส่งผลดีต่อการเพิ่มร้อยละผลได้เชื้อเพลิงในช่วง 2-15 เทียบกับน้ำหนักน้ำมันปาล์มตั้งต้น

ภาควิชา	เคมีเทคนิค	ลายมือชื่อนิสิต
สาขาวิชา	เคมีเทคนิค	ลายมือชื่อ อ.ที่ปรึกษาหลัก
ปีการศึกษา	2558	ลายมือชื่อ อ.ที่ปรึกษาร่วม

5373917223 : MAJOR CHEMICAL TECHNOLOGY

KEYWORDS: BIOFUEL, CONTINUOUS FLOW PROCESS, PALM OIL, USED PALM OIL, SUPERCRITICAL METHANOL, SUPERCRITICAL ETHANOL

WINATTA SAKDASRI: CONTINUOUS BIOFUEL PRODUCTION FROM PALM OIL IN SUPERCRITICAL ALCOHOLS. ADVISOR: ASSOC. PROF. SOMKIAT NGAMPRASERTSITH, Doctorat de l'INPT, CO-ADVISOR: PROF. JEAN STEPHANE CONDORET, Doctorat de l'INPT, 142 pp.

The supercritical alcohol (SCA) process is the one of alternatives to produce biofuel because it has several advantages over the conventional homogeneous catalysts in the term of production efficiency and feedstock flexibility. However, the employing high alcohol to oil molar ratio (40:1–42:1) is the main problem of SCA process due to a requirement of a significant energy in preheating and recovering alcohols. The large energy input also produced a significant environmental load. Thus, this work proposes a novel approach to reduce the alcohol to oil molar ratio in biofuel production from lipid–based biomass in SCA. The first objective was to investigate the optimal conditions of biofuel production in a batch reactor. The investigation was successfully done by the response surface methodology (RSM) and found that alcohol to oil molar ratio can reduce to 12:1 at the optimal temperature of 400 ∘C. The second objective was to scale-up the biofuel production with SCA in the continuous reactor. The results showed that the synthesis of biofuel using a lowered alcohol to oil molar ratio of 12:1 at 400 ∘C provided a triglyceride conversion of up to 99% and the maximum ester content in the range of 80–90%. In addition, the side reaction between glycerol and alcohol at 400 °C and 15 MPa showed a positive effect of increasing fuel yield by 2%–15% based on input palm oil weight.

Department:	Chemical Technology	Student's Signature ....
Field of Study:	Chemical Technology	Advisor's Signature ....
Academic Year:	2015	Co-Advisor's Signature ....

ACKNOWLEDGEMENTS

CONTENTS

LIST OF TABLES

LIST OF FIGURES

จุฬาลงกรณ์มหาวิทยาลัย
CHULALONGKORN UNIVERSITY

CHAPTER I

INTRODUCTION

1.1. Background

The depletion of non-renewable petroleum resources in the near future and the increasing demand for petroleum have focused the world's attention on the search for alternative sources of renewable energy. Biofuels are synthesized from lipid-based biomass, especially biodiesel; offer a promising alternative substitute for petroleum-based fuels. Biodiesel has a potential to sustainably renewable fuel for transportation engines, which can be either directly used or blended with diesel oil [1]. Moreover, biodiesel produces less air pollution (exhaust emissions) than fossil fuels. Biodiesel is commonly produced via transesterification of the triglycerides in vegetable oils or animal fats with alcohols such as methanol or ethanol. Equation (1.1) is representing the overall reaction, 3 moles of fatty acid alkyl ester are produced from each mole of triglyceride. Glycerol is a byproduct of transesterification reaction.

$$\text{Triglyceride} + 3 \text{ Alcohols} \longrightarrow 3 \text{ Fatty acid alkyl esters} + \text{Glycerol} \qquad (1.1)$$

The conventional process to produce biodiesel is a catalyzed chemical reaction between oils and alcohol to yield biodiesel and glycerol, performed at atmospheric pressure and lower temperature than the boiling point of alcohol. However, this process is not suitable to use with oils that have water and free fatty acid contents more than 0.06 wt% and 0.5 wt%, respectively, which lead to saponification and worse characteristics on biodiesel [2]. In addition, the use of homogeneous catalyst requires a lot of steps such as purification of the esters, separation of glycerol, and drying of resultant biodiesel [3].

The supercritical alcohol (SCA) process from vegetable oils is the one of an alternative to resolve the homogeneous catalyst problems because it can be conducted without using any catalysts. This process has a fast reaction rate to give a high yield of biodiesel as well as a high purity of the by-product (glycerol) and it eases to separate the product and by-product. Moreover, the presence of water and acid in the feedstock does not affect the progress of transesterification; the free fatty acid can be esterified

and converted to mono-alkyl esters or biodiesel. The main operating parameters that influence the transesterification under the supercritical condition are temperature, pressure, alcohol to oil molar ratio and the reaction time. The optimal conditions reported in several literature are operating at temperature (280–400 $^\circ$C), pressure (20–35 MPa) and alcohol to oil molar ratio (40:1–42:1) and reaction time (4–30 min), depending on the types of feedstock and reactor, and the FAAEs content has been reported in very high (90–95%) level [4]. However, the use of high alcohol to oil molar ratio (>40:1), compared to the stoichiometric ratio of 3:1, is disadvantages of supercritical alcohol (SCA) process due to a requirement of a large energy input in preheating and recovering alcohols that also produced a significant environmental load [5].

This work proposes a novel approach to reduce the alcohol to oil molar ratio and pressure for produce biofuel from lipid-based biomass via transesterification under supercritical alcohol at 400°C. Some literature reported that the alcohol to oil molar ratio may be reduced from 40:1–42:1 down to 9:1–12:1 by operating at 400–450 $^\circ$C and pressure of 10–15 MPa [6-8]. Moreover, at this temperature, the thermal degradation of triglyceride and glycerol has been generated to several low-molecular-weight compounds that could improve the cold flow properties as well as the viscosity of the biodiesel produced [9].

The first objective of this work is to investigate the optimal conditions of biofuels production in a batch reactor under supercritical methanol and supercritical ethanol at the temperature range of 350–400 $^\circ$C, pressure of 15 MPa and the alcohol to oil molar ratio range of 6:1–15:1, by using refined and used palm oils as feedstock. The second objective is to modify the process, using the chemical kinetics that found in the first objective to design a continuous reactor then perform the experiments and optimize the operating parameters of the continuous reactor.

1.2. Objectives

1.2.1. To investigate the optimal conditions of biofuels production in supercritical methanol and supercritical ethanol in a batch reactor.

1.2.2. To perform the experiments and find out the optimal conditions of the biofuels production in supercritical methanol and supercritical ethanol in a continuous reactor by using refined and used palm oils.

1.3. Scope of dissertation

1.3.1. The effect of alcohol to oil molar ratio is investigated on ester content and triglyceride conversion in a batch reactor.

1.3.2. The kinetic study of palm oil under the supercritical alcohols is developed.

1.3.3. The production of biofuels is investigated from palm oil under supercritical alcohols in a continuous flow reactor.

1.3.4. The effect of water content on the efficiency of biofuel production in the supercritical ethanol.

CHAPTER II
THEORY AND LITERATURE REVIEWS

2.1. Biofuels

Biofuels are defined as a liquid and/or gaseous fuel that derived from the biomass. They offer a promising alternative substitute for petroleum fuels and help to reduce carbon emissions from the transportation sector. Liquid biofuels are the most widely used for the transportation, which can be divided into two principal categories:

2.1.1. Bioethanol

Bioethanol can be derived from alcoholic fermentation of sugars-based biomass such as sugar cane, sugar beet, corn grain maize and wheat straw. Cellulosic-based biomass, such as wood and grasses, is also being developed and employing as feedstocks for bioethanol production. Bioethanol actually used as a petroleum additive by 5 % blending with unleaded gasoline (no engine modification) under the European quality standard EN 228. In addition, high level of bioethanol, for example ethanol blends of 15% (E85), can be used for engine modification [10].

2.1.2. Biodiesel

Biodiesel is defined as fatty acid alkyl ester and is derived from lipid-based biomass i.e. vegetable oil. It can be used directly (B100, 100% biodiesel) or blended with petroleum (B2, B5, B10, and B20) diesel for the diesel engine.

2.2. Lipid-based biomass as feedstocks for biofuel production

Lipid-based biomass, especially vegetable oil, is widely used as feedstocks for biofuel production. For instance, canola oil and rapeseed oil are mostly utilized in European countries and Canada. In the United States of America, soybean oil is the

major feedstock for the biodiesel production. Coconut oil and palm oil are favorable feedstocks in Malaysia, Indonesia, and Thailand.

2.2.1 Palm oil

Compared to other vegetable oil, palm oil is the most promising feedstock for biofuel production due to its low cost and the highest productivity as illustrated in Table 2.1. It can be observed that the palm oil yield has about a twelve-fold, a ten-fold, and fourth-fold more oil than corn, soybean and sunflower, and coconut, respectively.

Table 2.1 The lipid content and productivity of generally edible oil plants

Oil	Lipid content (wt. %)	Oil yield	Price (US$/kg)
Canola	40–45	590.7–663.8	1.23
Corn	3–6	241.9–438.8	1.14
Coconut	65–68	731.3–978.8	0.89
Palm	45–50	3004.0–5006.0	0.82
Soybean	18–20	450.0–506.3	1.14
Sunflower	35–45	516.3–663.8	1.52

In 2013, Thailand was the third world's largest producer with the rate of production about 1.25 million tons [11]. Moreover, the expansion of oil palm plantation constantly increased approximately 9% from the year 2001 to 2010. The Southern Provinces, such as Krabi, Surat Thani, and Chumphorn, are the most important Provinces of oil palm plantation, which is approximately 90% of the total planted area [12]. It is suggested that the ready availability of palm oil to meet the future demand for biodiesel production in Thailand.

Palm oil is edible oil, which derive from the inner wall (mesocarp) of the oil palm fruit. In general, palm oil is orange-red colored because it mainly consists of a high concentration of carotenes. Depending on the raw oil processing, palm oil can be

identified as crude palm oil (CPO) and refined palm oil (RPO). Palm oil contains equal amounts of saturated and unsaturated acids. The fatty acid profiles of CPO and RPO show in Table 2.2.

Table 2.2 The fatty acid composition of palm oil [13].

Fatty acid	Formula	Composition (%w/w)	
		CPO	RPO
Lauric acid	C12:0	N/A	0.1–0.4
Myristic acid	C14:0	0.5–2.0	0.9–1.4
Palmitic acid	C16:0	32.0–45.0	40.0–47.5
Palmitoeic acid	C16:1	0.1–0.7	0.0–0.6
Stearic acid	C18:0	2.0–7.0	0.4–0.45
Oleic acid	C18:1	38.0–52.0	36.4–44.4
Linoleic acid	C18:2	N/A	0.3–11.6
Linolenic acid	C18:3	5.0–11.0	0.1–0.5

N/A is not available

2.2.2. Used or waste cooking oil (WCO)

Currently, the main drawback of biofuel is more expensive than petroleum fuel, approximately one and a half times. In fact, 65–95% of the total production cost is related to the employed feedstocks. Hence, inexpensive feedstocks such as used or waste cooking oil (WCO) are a more competitive economy. The typical costs are two or three times lower than that of refined vegetable oil. Besides, WCO could bring substantial environmental benefits as it provides an alternative way for the waste disposal oil [14].

In food frying process, the vegetable oil was generally operated at a temperature range of 160–190 °C. During this process, the properties of the oil were changed with chemical reactions such as pyrolysis, hydrolysis, polymerization, and oxidation. These

reactions might lead to the increasing of viscosity, FFA content, water content, total polar compounds, polymerized and oxidized compounds and the acid and peroxide values[15]. Moreover, the saponification number and iodine value was also decreased due to the thermal cracking of triglycerides and unsaturated fatty acids

The generation of WCO generated varies in each country; it depends on the consumption of vegetable oil. It has been reported that 0.7–1 and 0.2 million tons of used cooking oil are annually produced in European countries and the United Kingdom, respectively [16]. China and Japan generate about 4.5 and 0.6 million tons of used cooking oil per year [17, 18], respectively. This concern has further raised interest in utilizing WCO as feedstock for biodiesel production.

2.3. Biofuel production processes

Biodiesel is universally produced through the transesterification reactions between triglyceride and short-chain alcohol (typically methanol or ethanol). The products of transesterification reaction are the mixture of fatty acid alkyl ester, which is the chemical name of biodiesel, and glycerol as a by-product. The overall of transesterification reaction shows in Figure 2.1(a). As the transesterification reaction is a reversible reaction, a little excess of alcohol is employed to shift the equilibrium towards the formation of fatty acid alkyl esters. Generally, the transesterification reaction can be divided into 3 steps in which triglyceride reacts with alcohol to produce diglyceride, which further reacts with alcohol to produce monoglyceride. Finally, monoglyceride reacts with alcohol to produce fatty acid alkyl ester and glycerol, as shown in Figure 2.1(b) [19].

(a)

$$CH_2\text{-OOC-R}_1$$
$$CH_2\text{-OOC-R}_2 \quad + \quad 3R'OH \quad \rightleftharpoons \quad R_2\text{-COO-R}' \quad + \quad CH_2\text{-OH}$$
$$CH_2\text{-OOC-R}_3 \qquad\qquad\qquad\qquad R_3\text{-COO-R}' \qquad\qquad CH_2\text{-OH}$$

| Triglyceride | Alcohol | Fatty acid alkyl ester | Glycerol |

(b)

Triglyceride $+$ R'OH $\rightleftharpoons$ Diglyceride $+$ R_1-COO-R'

Diglyceride $+$ R'OH $\rightleftharpoons$ Monoglyceride $+$ R_2-COO-R'

Monoglyceride $+$ R'OH $\rightleftharpoons$ Glycerol $+$ R_3-COO-R'
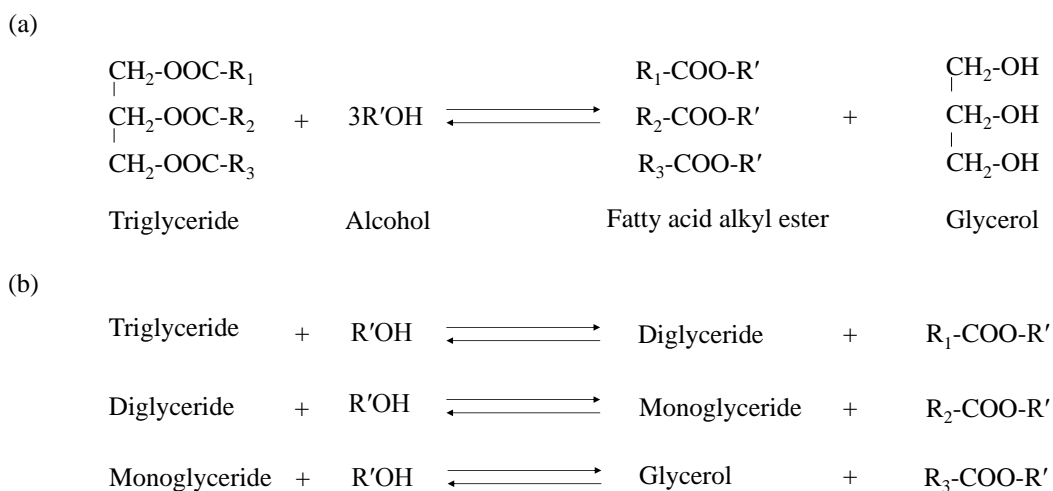
Figure 2.1. Transesterification reaction of triglyceride with alcohol (a) General equation (b) Three consecutive and reversible reactions R_1, R_2, R_3, and R' represent alkyl groups.

The production of biodiesel can be performed by either catalyzed or non-catalyzed transesterification. Different processes of these transesterification reactions will be additionally discussed in the following sections.

2.3.1. Homogeneous-catalyzed processes

As triglycerides (non-polar molecule) and alcohol (polar molecule) are not miscible, the catalysts are introduced in order to promote and improve the surface contact between these two phases and consequently enhance the reaction rate. The homogeneous catalysts were widely used in the commercial biodiesel production plants. Both acid-catalyst and alkali-catalyst have been utilized in either batch or continuous mode. The principally used acid-catalysts are sulphuric acid, hydrochloric acid, and sulfonic acid. For the alkali-catalysts, sodium hydroxide, sodium methoxide and potassium hydroxide are preferred [20].

The biodiesel production with homogeneous catalysts requires several steps on catalyst separation, esters and glycerol purification, product washing and neutralization and alcohol evaporation. For instance, the employment of sodium hydroxide as a

catalyst is illustrated in Figure 2.2. As a requirement of large amount of water in the washing and neutralization steps, the overall costs of production are increased and waste water are significantly produced. Besides, the application of these catalysts is limited only for feedstocks with less than 0.06 wt. % of moisture content or 0.5 wt. % of free fatty acid (FFA). As FFA can be reacted with the alkaline-catalyst to form soap, then the worse characteristics will occur in biodiesel. Thus, low-cost feedstocks of waste or used cooking oil, which is containing high water and FFA values, are not suitable for alkaline-catalyst.
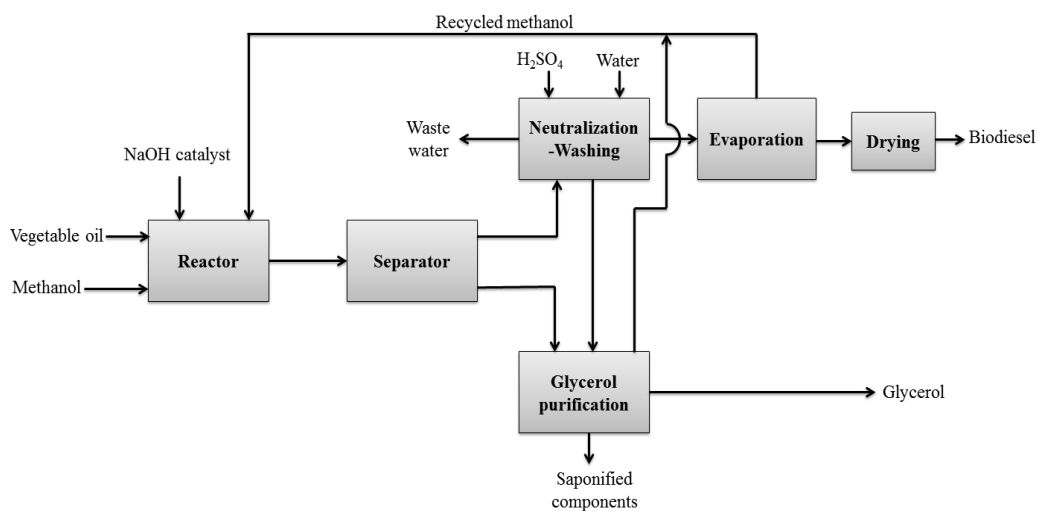
Figure 2.2. Global scheme for typical continuous homogeneous catalyzed processes.

2.3.2. Heterogeneous-catalyzed processes

Compared to homogeneous catalysts those occupy a same phase from the reaction mixture, heterogeneous catalysts occupy the different phase from the reaction mixture. As in a different phase, simple separation and reuse of catalysts are the major advantages of these processes. Moreover, the heterogeneous catalysts present a less corrosive character and can eliminate the formation of soap through free fatty acid neutralization and triglyceride saponification.

Acid and base solid catalysts, such as metal oxides, supported catalysts and zeolites, have been investigated for biodiesel production using heterogeneous catalysts [21]. They include enzyme catalysts such as lipase [22]. The heterogeneous catalysts can be possible applied in either batch or continuous system. A typical process flow diagram of heterogeneous catalytic transesterification process is shown in Figure 2.3.

Nevertheless, these solid heterogeneous catalysts still suffer from mass transfer limitations of two phase regions (liquid–solid) that relate to the requirement of high operating temperature and high alcohol to oil molar ratio. On the other hand, the use of enzyme catalysts in biodiesel production also demonstrates some drawbacks such as enzyme activity losses during the reaction, water deactivation and glycerol inhibition [23].
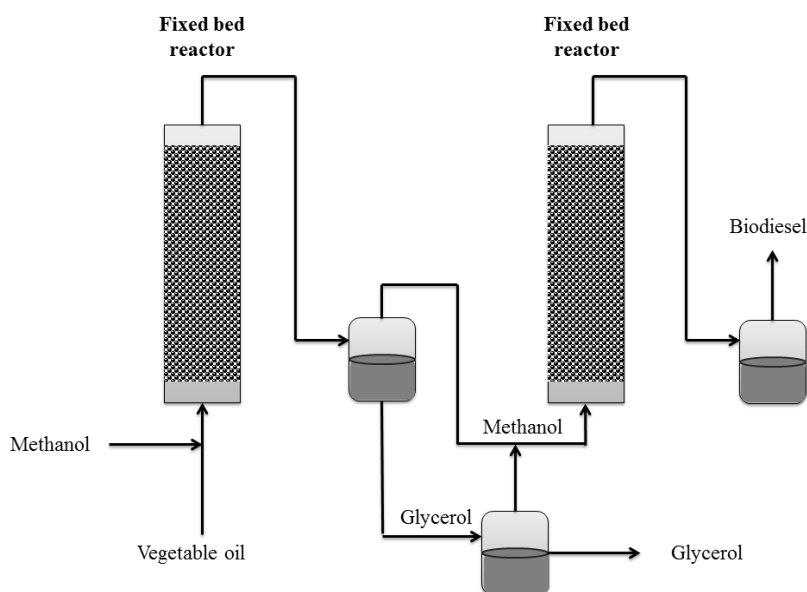
Figure 2.3. Global scheme for a typical continuous heterogeneous catalyzed process

2.3.3. Non-catalyzed supercritical alcohol (SCA) processes

As mentions in previous sections, the utilization of homogeneous-catalyzed processes are still confronted with the problems of feedstock limited, processes complicated, and extremely wastewater generated. The heterogeneous-catalyzed

processes, including solid and enzyme catalysts, were introduced to solve these issues, but they also have some barriers. Hence, the numerous alternative technologies of non-catalyzed processes have been global developed to minimize the problem from the catalyst processes.

Biofuel production with supercritical alcohol (SCA) conditions has been applied for non-catalytic processes. In the conventional condition, oil and alcohol mixture is demonstrated as two immiscible phases; the less density phase (alcohol) and the dense phase contain the oil. The reaction occurs only in the interfacial region between both liquids. Under the SCA condition, these reactants mixture becomes a homogeneous phase due to decreasing dielectric constant and increasing the density of methanol [24]. They would solve the limitations of mass-transfer between these reactants and provide to afford a higher reaction rate. In addition, it was reported that utilized alcohol under the supercritical condition does not only play as reactant, but also plays as an acid catalyst [2].

According to the no catalyst required, the productions can be performed in a minimal number of processing steps and the high purity of product and by-product were simultaneously obtained. A typical process flow diagram for biodiesel production under supercritical methanol (SCM) is shown in Figure 2.4. The SCA is an environmentally friendly process due to the low use of auxiliary chemicals and does not generate significant wastes [24-27]. Furthermore, these non-catalyzed processes have a strong tolerance for the impurities of FFA and water in feedstocks. It has been reported the transesterification and hydrolysis of triglycerides and esterification of fatty acids occur simultaneously under the SCA condition, which is lead to achieve a high yield of biofuel [2, 28]. Hence, these processes are more flexible to various types of feedstocks, especially either waste cooking oil or other inexpensive feedstock.

Although biofuel production with SCA has more remarkable advantages over the catalytic processes, this process is still facing some limitations, which are the requirement of high temperature (320 to 350 °C), high pressure (19 to 45 MPa), and high alcohol to oil molar ratios (40:1–42:1) to get great conversions [24-26]. According

to the severe operating condition requirement, safety issue and energy consumption are necessary to concern. Moreover, the high alcohol to oil molar ratio in the SCA process generates an environmental impact from the large energy input of preheating and recovering the alcohol [5].
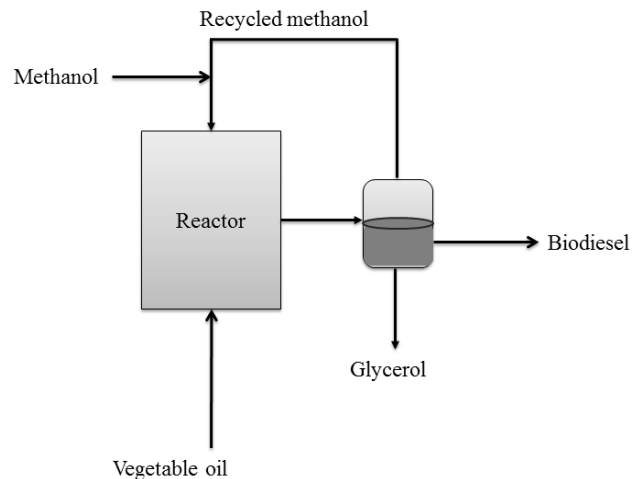
Figure 2.4. Global scheme for a typical continuous non-catalyzed process.

2.4. Chronological research and development of biofuel production with SCA

Among the processes explained above, SCA is one of the promising techniques to the future production of biofuel. Therefore, many researchers around the world are focusing on the exportation of the supercritical biofuel production in the past decade.

2.4.1. Supercritical methanol (SCM)

The earlier research on SCA for biofuel production, methanol is mostly selection as reacting alcohol because of its low cost, and favorable chemical and physical properties [3, 29]. In 2001, the SCM was firstly introduced the world for biofuel production by the Japanese pioneer [25]. They proposed that the SCM could defend the problems of conventional catalytic method. Fatty acid methyl ester (FAME) or biodiesel could be produced in the shorter reaction time, simpler separation, and

purification in the downstream process. In the following years, the SCM was applied to generate biodiesel with six vegetable oils i.e., cottonseed, hazelnut kernel, poppy seed, rapeseed, safflower seed, and sunflower seed by Turkish pioneer [26]. This SCM process with various oil types was successful to producing biodiesel and it also shown remarkableness over the conventional catalyzed method in the term of shorter reaction time. According to the different of chemical structures between methyl ester and petroleum based diesel fuels, thus, the viscosity of this biodiesel was slightly higher than that the no. 2 Diesel fuel.

In during the years 2001–2004, the discovery of biofuel production with SCM was focusing on the feedstock flexibility, especially feedstocks from waste. As wasted feedstocks are mostly consisting with high values of FFA and water, the reaction behavior of FFA under SCM conditions was investigated by Kusdiana and Saka [25]. The results demonstrate that the FFA can be esterified and converted into FAME with the highest yield of 95% at 350 °C. So, transesterification and esterification reaction of triglycerides and FFA could simultaneously occur during the SCM condition. Moreover, the higher reactivity of methyl esterification than that of transesterification also confirmed that the presented FFA in feedstocks would be completely converted to the FAME under the SCM condition [29]. The effect of water on biodiesel production was then investigated by the same researchers [2]. They proposed that the presence of water did not show valuable effect on the yield of biodiesel. Because the reaction rate of the water hydrolysis is faster than transesterification, triglyceride was hydrolyzed by water into FFA and subsequently esterified with methanol to generate FAME under SCM. However, the hydrolysis of FAME can occur under supercritical water at the temperature over 210 °C. The overall reactions, which will involve under SCM condition, while the appearance of FFA and water in feedstocks, are shown in Figure 2.5. Therefore, this finding supported that the biofuel production with SCM is more flexible to a high FFA feedstock i.e. low-grade feedstocks. Waste cooking oil and waste lard were employed for biodiesel production in the SCM condition by some researchers [30-32].

(a)

$$CH_2\text{-OOC-}R_1$$
$$CH_2\text{-OOC-}R_2 \quad + \quad 3CH_3\text{-OH} \quad \longrightarrow \quad R_2\text{-COO-}CH_3 \quad + \quad CH_2\text{-OH}$$
$$CH_2\text{-OOC-}R_3 \qquad\qquad\qquad\qquad R_3\text{-COO-}CH_3 \qquad\qquad CH_2\text{-OH}$$

$R_1\text{-COO-}CH_3$ and $CH_2\text{-OH}$

| Triglyceride | Methanol | Fatty acid methyl ester (FAME) | Glycerol |

(b)

$$CH_2\text{-OOC-}R_1$$
$$CH_2\text{-OOC-}R_2 \quad + \quad 3\ H\text{-OH} \quad \longrightarrow \quad R_2\text{-COO-H} \quad + \quad CH_2\text{-OH}$$
$$CH_2\text{-OOC-}R_3 \qquad\qquad\qquad\qquad R_3\text{-COO-H} \qquad\qquad CH_2\text{-OH}$$

| Triglyceride | Water | Fatty acid | Glycerol |

(c)

$$R_1\text{-COO-}R' \quad + \quad H\text{-OH} \quad \longrightarrow \quad R_1\text{-COO-H} \quad + \quad 3R'OH$$

| Fatty acid methyl ester (FAME) | Water | Fatty acid | Alcohol |

(d)

$$R_1\text{-COO-H} \quad + \quad CH_3\text{-OH} \quad \longrightarrow \quad R_1\text{-COO-}R' \quad + \quad H\text{-OH}$$

| Fatty acid | Methanol | Fatty acid methyl ester (FAME) | Water |

Figure 2.5. Overall reaction with the present of FFA and water under SCM condition. (a) Transesterification reaction (b) Hydrolysis reaction of triglyceride (c) Hydrolysis reaction of fatty acid alkyl ester (d) Esterification reaction. R_1, R_2, and R_3 represent alkyl groups.

In 2004, as previously mentions, the first article of the two-step process was introduced for the biodiesel production with SCM process in order to decrease the operating parameters of temperature, pressure, and alcohol to oil molar ratios [29]. In 2005, the addition of co-solvent i.e. propane [33], and CO_2 [34] has been proposed, and it also demonstrated to reduce those operating parameters. In 2007, the addition catalyst of nano-MgO [35] and NaOH [35] under SCM conditions was successful in producing biodiesel without the occurrence of the soap formation. The FAME yield was archived to the maximum value at milder operating conditions.

Since 2006, numerous researchers introduced the SCM condition in a continuous flow reactor, which is in order to increase the efficiency of biofuel production [6, 9, 36-38]. For instance, Bunyakiat et al. were successful to employ the SCM conditions for continuous transesterification of coconut oil and palm kernel oil with the maximum FAME yield of 95% and 96%, respectively [36]. The optimal conditions are 350 °C, 19.0 MPa, methanol to oil molar ratio of 42:1, and a space-time of 400 s. However, He et al. reported that the maximum yield was only 77% obtained from the continuous transesterification of soybean due to the loss caused by unsaturated FAME from the thermal decomposition.

Since 2008, the thermal decomposition of FAMEs was evidenced during the production of biodiesel under SCM conditions by many groups of researchers [39-41]. The unsaturated FAMEs, i.e. methyl oleate (18:1), methyl linoleate (18:2), and methyl linolenate (18:3), were observed to decompose at the temperature over 300 °C. In addition, they noted that degree of the thermal decomposition strongly depends on the number of double bond in unsaturated FAMEs. Because the double bond is less stable than single bond, the poly-unsaturated FAMEs are more rapidly thermal decompose than that mono-unsaturated. For the saturated FAMEs, i.e. methyl palmitate (16:0) and methyl stearate (18:0), begun to disappear at the temperature over 350 °C. Besides, among the saturated FAMEs, the shorter chain length has higher thermal stability under SCM conditions as reports by Lee-Yong et al. [40]. The decomposition products mostly consist with the small molecular of FAMEs and hydrocarbon (C7–C10) such as methyl undec-10-enoate, methyl heptanoate (7:0) and 1-undecene. However, these decomposition products could improve the viscosity, density and cold flow properties of biodiesel. For example, the thermal decomposition of FAME is illustrated in Figures 2.6. Recently, the biofuel production with SCM are interesting on employ the wet algae [42], waste lard [31], and a non-edible oil i.e. crude Jatropha oil and Krating oil [43] as alternative feedstocks.
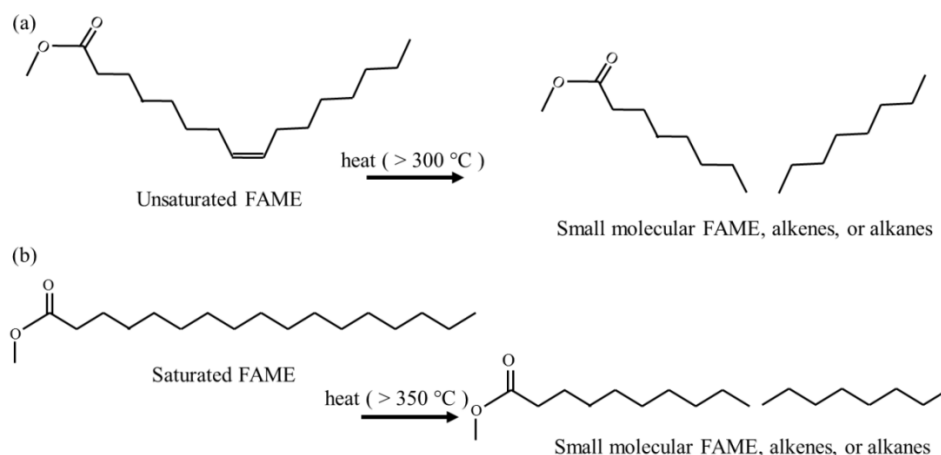
Figure 2.6. The thermal decomposition reaction of (a) unsaturated FAMEs (b) saturated FAMEs under SCM conditions

2.4.2. Supercritical ethanol (SCE)

Ethanol is one of the most promising as a reacting alcohol in place of methanol for biofuel production because it is a renewable source that can be produced from biomass by fermentation. In contrast, methanol is mainly produced from nonrenewable fossil fuels such as methane gas. Therefore, using ethanol provides a 100% renewable basis for biodiesel production feedstocks. Nevertheless, ethanol is currently more expensive than methanol [44].

In 2004, the reactivity of triglycerides and FFA of rapeseed oil was investigated in various alcohol type of supercritical conditions i.e. methanol (SCM), ethanol (SCE), 1-propanol (SCP), 1-butanol (SCB), and 1-octanol (SCO). They observed that the almost 100% yield of alkyl esters was obtained from the shorter alkyl chains of alcohol including SCM and SCE. While, under the same condition, 85% and 62% yield of alkyl esters were produced from SCB and SCO, respectively. A comparative study between SCM and SCE for biodiesel was also investigated in batch [28 , 45, 46] and continuous flow reactors [4, 47, 48]. The conversion of alkyl esters in SCM was observed higher than that SCE in both batch and continuous reactor.

In the years 2007 [49] and 2009 [50], the SCE was introduced to produce biodiesel by employing soybean oil and refined palm oil as feedstocks, respectively. The effects of operating parameters (temperature, pressure, and ethanol to oil molar ratio) on the fatty acid ethyl ester (FAEE) were investigated. For soybean oil, the optimal operating parameters of 623 K, 20 MPa, and ethanol to oil molar ratio of 40:1 within 15 min were reported to achieve the FAEE yield about 80%. For refined palm oil, the operating parameters were optimized by using response surface methodology (RSM). It was inspected that 79.2 wt.% of FAEE obtained from 349 °C, ethanol to oil molar ratio of 33:1 and reaction time of 30 min.

In during the year 2007–2011, the effect of water content on the conversion to FAEE yield with the SCE was investigated in a continuous process by Vieitez et al. [47, 51, 52]. The results showed that 10 wt. % water positively affected by increasing the rate of reaction. In addition, the conversion of oil was almost complete, which was confirmed by the absence of mono-, di-, and tri- glyceride in the final product. However, FAEE content was observed only 77.5% at the operating conditions of 250 ∘C to 350 ∘C and 20 MPa, and ethanol to oil molar ratio of 40:1. This is because of the degradation of the fatty acids with the high operating temperature. Moreover, these finding attract some researchers to employ azeotropic and/or hydrated ethanol (96 wt. % ethanol and 4 wt. % water) for biodiesel with SCE [53, 54].These azeotropic and/or hydrated ethanol is one of an alternative reactant due to its cheaper price than anhydrous ethanol (>99.8 %).

In 2011, the stability of FAEE from soybean was studied with exposed for different periods with SCE conditions at 20 MPa and temperatures between 250 and 375∘C by the same group of Vieitez et al [55]. They noted that the decomposition rate depended on the nature and unsaturation degree of FAME. For instance, ethyl linoleate (C18:2), which is consisting of two double bonds, has a higher rate of decomposition than that ethyl stearate (C18:0). In a year later, the influence of FFA on the process efficiency of the biodiesel production with SCE was investigated in continuous process [56]. The different five oil types, namely soybean oil, rice bran oil, and high oleic sunflower oil were employed as feedstocks. The addition of FFAs positively effects on

the increasing of conversion rate for all type of feedstocks. They concluded that the introduction of FFA in feedstocks could be a useful tool for improving the conversion of oil under the SCA conditions.

Recently, the additional co-solvent of hexane [57] and catalysts of CaO/ Al_2O_3 [58] and NaOH [59] were also presented in order to reduce the operating parameters in biodiesel production with SCE. In addition, the 3rd generation of feedstock, microalgae *Nannochloropsis Salina,* was directly converted to produce FAEE without pretreatment under SCE conditions.

2.5. Reaction parameters affecting biofuel production with SCA

The approach of SCA with various vegetable oil for biofuel production, including in batch and continuous reactors is summarized in Table 2.3. It can be observed that the production is affected by reaction parameters of temperature, pressure, alcohol to oil molar ratio, and reaction time. The effects of these factors are described herein.
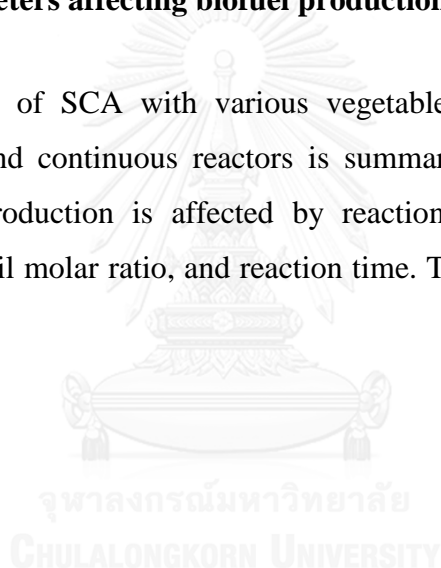
Table 2.3 Summary of literature-reported experimental data using the SCA process.

Year /ref	Oil types	Alcohol	T (°C)	P (MPa)	MR	Time (min)	process type	FAME/ CV (%)
2001 [25]	Rapeseed	Methanol	350	43	42	4	batch	95 % FAME
2002 [26]	Cottonseed, hazelnut kernel, poppy seed, rapeseed, safflower seed, and sunflower seed	Methanol	350	N/A	41	5	batch	95 % FAME
2004 [32]	Canola	Methanol	450	40	11–45	4	continuous	~100 % CV
2004 [45]	Sunflower	Methanol/ Ethanol	400	20	40	40	batch	96 % CV
2006 [36]	Coconut	Methanol	350	19	42	6.67	continuous	95 % FAME

Table 2.3 Summary of literature-reported experimental data using the SCA process.

Year /ref	Oil types	Alcohol	T (°C)	P (MPa)	MR	Time (min)	process type	FAME/ CV (%)
2006 [36]	Palm oil	Methanol	350	19	42	6.67	continuous	96 % FAME
2007 [46]	Castor and Linseed	Methanol/ Ethanol	350	20	40	40	batch	~100 % CV
2007 [60]	Soybean	Methanol	300	32	40	25	continuous	77 % FAME
2007 [49]	Soybean	Ethanol (99.9 %)	350	20	40	15	continuous	80 % FAEE
2008 [4]	Soybean	Methanol/ Ethanol (99.9 %)	400	20	6	1.75	continuous	>98 % CV
2008 [51]	Soybean	Ethanol (99.9 %)	350	20	40	1.5 mL/min	continuous	77.5 % FAEE

Table 2.3 Summary of literature-reported experimental data using the SCA process.

Year /ref	Oil types	Alcohol	T (°C)	P (MPa)	MR	Time (min)	process type	FAME/ CV (%)
2008 [60]	Sunflower Seed oil	Ethanol (99.9 %)	280	N/A	40	5	batch	80 % FAEE
2009 [30]	WCO	Methanol	287	N/A	41	30	batch	99.6 % FAME
2009 [6]	Chicken fat	Methanol	400	30	9	6	continuous	80 % FAME 99 % CV
2010 [28]	Purified palm	Methanol	372	15–25	40	16	batch	81.5 % FAME
2009 [50]	Palm	Ethanol (99.8 %)	349	15–25	33	29	batch	79.2 % FAEE
2010 [7]	Chicken fat	Methanol	400	37.6	6	5	batch	88 % FAME

Table 2.3 Summary of literature-reported experimental data using the SCA process.

Year /ref	Oil types	Alcohol	T (°C)	P (MPa)	MR	Time (min)	process type	FAME/ CV (%)
2011 [9]	Palm olein	Methanol/ Ethanol	400	15	12	10	batch	80 % FAME
2011 [52]	Castor	Ethanol + water	300	20	40	0.8 mL/min	continuous	74.2 % FAEE
2012 [31]	Waste lard	Methanol	335	20	45	20	batch	89.9 % FAME
2012 [61]	Waste canola	Methanol	270	10	80	45	batch	102 % FAME
2012 [62]	Sunflower	Ethanol (99.9 %)	320	15	40	50	continuous	90 % FAEE
2014 [53]	Refined and used palm	Ethanol (96.5 %)	300	30	30	60	continuous	80 % and 73 % FAEE

FAME: % Fatty acid methyl ester content, FAEE: % Ethyl ester content, CV: % Conversion.

The significant digits are the same as in the original sources

2.5.1. Effects of temperature and reaction time

Reaction temperature and time are the critical parameters to determine the reaction rate or the reaction kinetic of oil conversion to biofuel under the SCA conditions. In all reports dealing with SCA shown that an increase in reaction temperature and time improved conversion level, especially at condition beyond the critical point of methanol (239.6 °C) and ethanol (240.6 °C). Although, high temperatures and prolonged reaction time demonstrate the advantage on the yield, the two major drawbacks are thermal degradation and additional energy consumption.

The first article, the influence of reaction temperature for the synthesis of biodiesel was investigated between sub-critical methanol condition (200 °C and 7 MPa) and SCM conditions (350–400 °C and 45–65 MPa) [25]. At 200 and 230 °C, the FAME yield is relatively low due to a sub-critical state of methanol. A complete conversion was observed at a temperature of 350 °C and reaction time of 4 min, the 95 wt. % of FAME was obtained. At 400 °C, the conversion was rapidly complete in 2 min. In addition, the effect of temperature on biodiesel production was also confirmed by discovery in both SCM and SCE at a pressure of 20 MPa, a methanol to oil molar ratio of 40, and reaction time of 40 min [45]. In SCM, the FAME yield was relatively increased from 78% to 96% with the temperature risen from 200 to 400 °C. The similarly trend was also observed in SCE, FAEE yield increased with the temperature.

As previously mention, the thermal decomposition of both FAME and FAEE noted in the temperature over 300 °C. The poly-unsaturated fatty acid, which is containing with 2 or more double bonds, was harshly affected. This thermal decomposition significantly results in the reduction of FAME and FAEE content obtained. Therefore, it was suggested that the treatment of SCA should take place at the temperature less than 270 °C to avoid the thermal decomposition. On the other hand, gradual heating and low residence time have been introduced to solve the thermal decomposition problem in the SCM [62]. The FAME content obtained was observed as 96% with the gradual heating from 100 to 320 °C, compared to 77% obtained from

uniform heating at 310 ∘C. Nevertheless, some studies reported that the decomposition products could improve the viscosity [63] and cold flow [39] properties of biodiesel.

2.5.2. Effect of pressure

As the majority of research in SCA is carried out in batch reactors, the reaction pressure is uncontrolled [29]. In batch type mode reactor, the pressure was dominated by the temperature of the experiment, the alcohol to oil ratio and quantity of reactants. The reacting pressure has been reported to increase at least 5 fold with the increasing temperature further above 320 ∘C [24]. On the other hand, the reacting pressure has been demonstrated to increase with the addition of methanol to oil molar ratio [33]. Hence, the data on the effect of pressure on the synthesis of biodiesel with SCA is not presented in the batch reactor; it is only monitored during the reaction.

In the continuous reactor, the reaction pressure has been controlled by a back-pressure regulator at the reactor outlet. The effect of reaction pressure on FAME yield has been investigated in SCM [37]. The FAME yields rapidly increased with the pressure higher than the critical pressure of the methanol. Nevertheless, when the pressure increased to a specific level, the FAME yield was constant. So, it can indicate that pressure has significant influence on the yield in a certain range. As similarly reported by Bunyakiat et al. [36], the effect of pressure on yield is negligible on the transesterification conversion of coconut oil with SCM.

2.5.3. Effect of alcohol to oil molar ratio

Alcohol to oil molar ratio is strongly affecting transesterification reactions of non-catalyst SCA processes. Most researchers generally concluded that the highest conversions can be obtained from the employment of the highest alcohol, e.g., 40:1–42:1 [24, 46, 64]. In addition, they observed that the product yield was relatively constant at the methanol to oil molar ratios over 40:1.

Because the transesterification is the reversible reaction, the employ of high alcohol to oil molar ratio is necessary to drive the reaction forward. However, the high alcohol to oil molar ratio is not only driven the equilibrium to the product side but also reduces the critical temperature. Therefore, large used of alcohol to oil molar ratio is necessary to reduce the critical temperature of the mixture, which allows a homogeneous supercritical phase at milder operation temperatures. As reported by Bunyakiat et al. [36], the critical points of mixtures between crude coconut oil and methanol decreased with methanol to oil molar ratios, as shown in Table 2.4. This behavior was confirmed by the observation of phase in a high-pressure view cell [4, 65]. The two liquid phases of alcohol and oil are become completely miscible at 350, 180 and 157 ∘C with methanol to oil molar ratio of 24:1, 42:1, and 65:1, respectively.

Although, the relatively high alcohol to oil molar ratio enables easier formation of a homogeneous supercritical phase, it is encountering the following problems:

- The equipment costs increased due to greater volumetric throughput and corresponding pressure increase.
- The biodiesel and glycerol mixtures in the final product are difficult to separate due to the glycerol is favorable to dissolve in alcohol.
- High alcohol to oil molar ratios requires large energy consumption for recycling and recovering of these excess alcohols.

To avoid these problems, the addition of co-solvents has been introduced by Anitescu et al. [4]. In this case, methanol to oil molar ratio can be reduced to 6:1 when employ CO_2 as a co-solvent. On the other technique, the molar ratio has been also observed to reduce from 40:1 to 6:1 by increasing the operation temperature to 400 ∘C. Moreover, almost 100% conversions demonstrate in both techniques.

Table 2.4 The critical point for mixtures of crude coconut oil and methanol using group contribution methods [36].

Methanol to oil molar ratio	Critical point	
	Temperature (∘C)	pressure (MPa)
0:1	629	0.6
6:1	396	3.8
12:1	346	5.1
24:1	306	6.2
42:1	282	6.9

2.4.4. Effect of alcohol types

The most common alcohols used for biofuel production are methanol and ethanol. Among of alcohol types, methanol is more wildly used due to its low price and high activity. However, ethanol is one of the currently promising reactants to produce an entirely renewable fuel because it can be derived from a renewable feedstock. In addition, it has been reported that the longer chain alcohols can assist to improve some properties of biodiesel such as cloud point. The cloud point of an ethyl ester was 3 ∘C lower than that of the methyl ester [29].

The influences of five alcohol types have been investigated on the fatty acid alkyl ester conversion, i.e. methanol, ethanol, 1-propanol, 1-buthanol, and 1-octanol [29]. The results have shown that shorter chain alcohols gave faster reaction rates. At 300 °C, the treatment with methanol required only 15 min to a nearly 100% yield of alkyl esters, while it need 45 min with ethanol and 1-propanol. The similar observation has also reported in some studies, the obtained yield by SCE was lower than that SCM in both of batch and continuous mode reactors [46, 47, 66, 67].

2.6. Process design of biofuel production with SCA

The kinetic and phase behavior studies are a fundamental knowledge for further process development, detailed design, optimization, and scale-up. The investigation of kinetic and equilibrium phase behavior for the biofuel production with SCA are described below.

2.6.1. Reaction kinetics

In the past decade, the determination of kinetic reaction has been investigated in subcritical and supercritical transesterification of triglycerides as shown in Table 2.5. In 1998 [19], the chemical kinetics analyzes of SCM were first proposed by using three consecutive steps of transesterification, as given in Figure 2.1(b). As the high employment of alcohol to oil molar ratio of 42:1, the reverse reaction was ignored and the methanol concentration considered constant. Hence, the reaction was assumed to be the pseudo-first order with respect to each reacting component. The rate constants of three steps were determined by fitting the experimental data as a function of time. The results shown that the conversion rates of tri- and di-glyceride demonstrated were much higher than that monoglyceride, which corresponded to a very slow removal of monoglyceride in the product.

To simplify the evaluation of kinetic reaction, Kusdiana and Saka introduced the overall reaction of transesterification by ignoring the intermediates steps [24], as illustrated in Figure 2.1 (a). The reaction was also assumed to be the pseudo-first order with respect to the concentration of triglyceride alone. The rate constants of this reaction were observed to increase with the increasing reaction temperature in the range between 200 and 487 ∘C, especially sharply rise over the temperature of 270 ∘C. The similar results were observed in the kinetic study of soybean oil by He et al. [37]. They indicated that the steeply increase was due to the transition of a heterogeneous phase to a homogeneous phase.

Several researchers also approached the simplified single step model for determining the kinetics under both SCM and SCE with different vegetable oil types including sunflower [45], palm, groundnut, *Pongamia piñata*, *Jatropha curcas* [68], castor, linseed [46], and waste vegetable oils (WVO) [69]. They found that the reaction rate constant was strongly influenced by the composition of the vegetable oil. The reaction rate constant of saturated fatty acids triglyceride was faster than that for one with unsaturated acids. Also, the reaction rate could be retarded by the increasing number of double bond in polyunsaturated acids.

The activation energy (E_a) of the reaction was evaluated from the rate constant values at various temperatures using the Arrhenius' law. As shown in Table 2.5, the activation energy of SCA was influenced highly dependent on the nature of the oil and the nature of the alcohol.

Table 2.5 Activation energies of non-catalytic vegetable oil with SCA.

Year/ Ref.	Alcohol	Oil type	T ($\circ$C)	P (MPa)	MR	E_a (kJ/mol)
2001 [24]	SCM	Rapeseed	200–270	7–12	42:1	38.48
			300–487	19–105		47.09
2007 [37]	SCM	Soybean	210–230	28	42:1	11.22
			240–280			55.91
2007 [68]	SCM	Palm	200–400	20	50:1	14.94
		Groundnut				10.54
		Pongamia pinata				9.45
		Jatropha curcas				11.37
2007 [46]	SCE	Castor	200–350	20	40:1	35.00
		Linseed				46.5
2011 [70]	SCE	palm olein	270–350	35	40:1	81.37

Year/ Ref.	Alcohol	Oil type	T (°C)	P (MPa)	MR	E_a (kJ/mol)
2013 [69]	SCE	WVO	240–280	20	33.8:1	31.71
2007 [37]	SCE	Soybean	200–375	20	20:1	92.90
					40:1	78.70
2007 [68]	SCE	Palm	200–400	20	50:1	11.10
		Groundnut				11.10
		Pongamia pinata				12.46
		Jatropha curcas				13.38
2007 [46]	SCE	Castor oil	200–350	20	40:1	55.00
		Linseed				70.00

MR: Alcohol to oil molar ratio

2.6.2. Equilibrium phase behavior

In recent years, the production of biofuel with SCA has been focused as advanced and might be the main applied technology in the future. So, the knowledge of equilibria phase behavior at high temperature and pressure is crucial for describing the kinetic of the process and necessary to process design.

As the transesterification is a major reaction for biofuel production, the mixture of products mainly consists of methyl or ethyl esters, the small amount of glycerol, and the large excess of alcohol. In addition, monoglyceride and diglyceride, which are intermediate products, could be present only in traces. The behavior analyst of these multicomponents is extremely complicated. So, the binary mixture systems of methyl or ethyl esters, alcohol, and glycerol or monoglycerides have been investigated to determine the phase equilibrium of biofuel with SCA, as shown in Table 2.6.

Table 2.6 The literature review of phase equilibrium studies for biofuel production with SCA

Ref.	System/ Equilibria	Measurement range		Critical data	Thermodynamic model
		T (°C)	P (MPa)		
[71]	Triolein–methanol/ VLE	60–190	6.0–10.0	Tc= 681 °C, Pc= 0.360 MPa, ω= 1.686	PR EOS and VdW mixing rule
[72]	Glycerol–monoolein–methyl oleate / LLE ,VLLE	60 ,135	N/A	N/A	UNIFAC and UNIFAC–Dortmund
[73]	Sunflower oil–methanol	200–230	2.9–5.6	Tc= 704.7 °C, Pc= 0.334 MPa, ω= 1.9782	RK–ASPEN EOS and VdW mixing rule
[74]	Methyl oleate, glycerol, and methanol/ LLE ,VLLE	40–120	0.1–0.6	N/A	GCA–EOS and UNIFAC
[75]	FAMEs C18 mixture–methanol/ VLE	250–300	2.4–11.4	Tc= 496.8 °C, Pc= 1.356 MPa, ω= 0.857	PR EOS and VdW mixing rule
[76]	Methanol–methyl laurate, Methanol –methyl myristate/ VLE	220–270	2.1–8.4	Tc=508.70 °C, Pc= 1.67 MPa, ω= 0.6849 and Tc= 439.15 °C, Pc= 1.55 MPa, ω= 0.9498	PRASOG model

Ref.	System/ Equilibria	Measurement range		Critical data	Thermodynamic model
		T (∘C)	P (MPa)		
[77]	Methanol– methyl laurate, and Methanol– methyl myristate/ VLE Ethanol–ethyl laurate, and Ethanol–ethyl myristate/ VLE	220–270	2.1–8.4	Tc=508.70 °C, Pc= 1.67 MPa , ω= 0.6849 and Tc= 439.15 °C, Pc= 1.55 MPa, ω= 0.9499 Tc=475.5 °C, Pc= 1.648 MPa, ω= 0.771 and Tc= 439.15 °C, Pc= 1.48 MPa, ω= 0.852	SRK, WS mixing rule, and COSMO– SAC theory
[78]	Glycerol– methanol/ VLE	220–299	2.2–8.7	N/A	PR–SV EOS and VdW mixing rule
[78]	Glycerol– ethanol/ VLE	220–299	2.2–8.7	N/A	PR–SV EOS and VdW mixing rule
[79]	Triolein–ethanol	50–345	2.5, 2.6	N/A	RK EOS

N/A is not available

In addition, the existence of one homogeneous or single phase is important to obtain a high reaction rate for biofuel synthesis with SCA (without the use of a catalyst). Thus, some researchers recently applied a high-pressure view cell for directly observe the behavior of phase under the subcritical and supercritical alcohol conditions [4, 65, 80, 81].

Anitescu et al. and Hegel et al. applied a high-pressure view cell to produce the biodiesel from vegetable oils with SCM [4, 65]. Anitescu et al. found that the transition from a two-phase VL system to a one-phase supercritical system occurred at nearly the critical temperature of 350 ◦C at the molar ratio of 24:1. Whiles, the completely miscible with two liquid phases was observed at the temperature of 180 and 157 ◦C for the methanol to oil molar ratio ranged from 6 to 27, as reported by Hegel et al. They concluded that the increase methanol to oil molar ratios resulted on the decreasing of transition temperature. Therefore, as mention previously, a large excess of alcohol is necessary for the non-catalyzed SCA process in order to reach the partial miscibility of alcohol and vegetable oil.

In order to determine the phase transition, the phase equilibria between methanol and vegetable oil mixture were monitored in a view cell by Glišić and Skala [80]. They found that the distributions of methanol, triglyceride, FAME and glycerol were changed depending on the temperature and pressure of the reaction. The phase transition was dived into three types. The first type is the characteristic of phase transition for temperature up to 170 ◦C and pressure below 1.5 MPa. The second type is phase transition exists at subcritical temperature and pressure of methanol (150–210 ◦C and 1.5–5.0 MPa). The last phase transition type was observed around the critical point at the temperature and pressure over 270 ◦C and 7.5 MPa, respectively. The same phase behavior was also observed in mixtures of ethanol and vegetable oil [79].The possible number of phase and phase composition at these different three conditions is schematically shown in Figure 2.7.
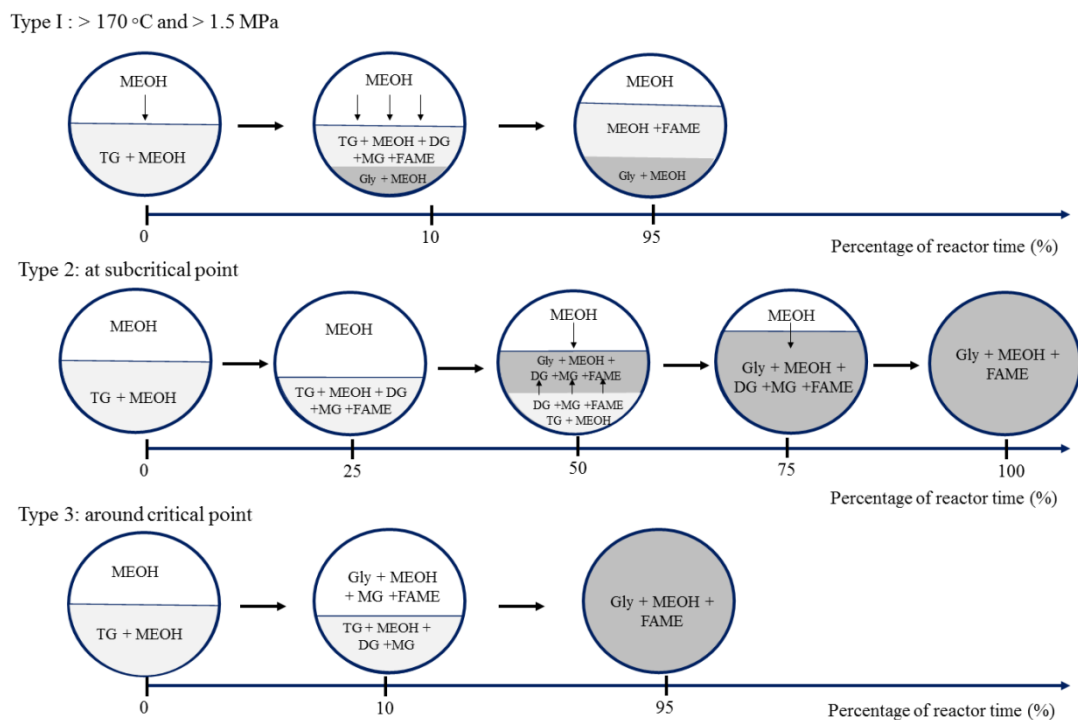
Figure 2.7. The schematic diagram of the possible number of phases and phase compositions at elevated temperature and pressure during the reaction. Note: MEOH is methanol, TG is triglyceride, DG is diglyceride, MG is monoglyceride, and Gly is glycerol.

2.7. Proposed improvements to biofuel production with SCA

As mention earlier, the biofuel production with SCA is still confrontation some limitations such as the requirement of high alcohol to oil molar ratios and high temperature and pressure. Current literature suggested some alternative methods to avoid these problems, which are the two-step process, the addition of co-solvent, the application of micro-reactor in continuous mode.

2.7.1. The two-step process

The alternative two-step or Saka-Dadan process was presented by Minami and Saka for synthesizing biodiesel with SCA in a continuous reactor [82]. This process is comprising hydrolysis of triglycerides in subcritical water and subsequent esterification of FFAs to FAMEs. A simplified process flow diagram is shown in Figure 2.8.
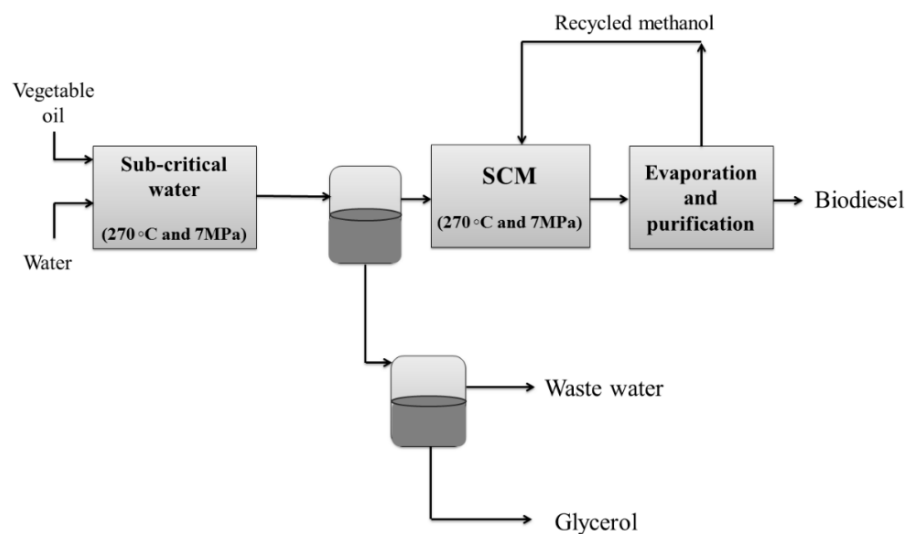
Figure 2.8. Saka-Dadan two step supercritical process

The Saka-Dadan process can be accomplished at milder operating condition (270 ∘C and 7 MPa) than those of the single-step Saka process (350 ∘C and 20–50 MPa), which might reduce the cost of production. This is due to the esterification of FFAs has a faster reaction rate than transesterification of triglycerides at the same condition. So, the almost complete reaction of FFAs was observed at the mild conditions of 270 ∘C and 7 MPa. Moreover, the reaction at milder operating condition is enhanced due to the fatty acids act as acidic catalysts in SCM condition [83]. However, this process has a major disadvantage of the more requirement of energy to heat up large volumes of water in the first stage.

2.7.2. The addition of co-solvent

The addition of co-solvent has been proposed to reduce the harshness of operating conditions of biodiesel production with SCM. This method was assumed to improve the mutual solubility between methanol and triglycerides and might reduce the critical point of the mixture. For this reason, the biodiesel can be synthesized under milder conditions of SCM. The co-solvents such as propane, CO_2, n-heptane and THF have been added for biodiesel production under SCA conditions. The comparative results of this co-solvent are in Table 2.7.

Table 2.7 Comparison of co-solvent results.

Co-solvent	T (∘C)	P (MPa)	MR	Time (min)	Yield (%)	Ref.
None	350	19.0	21:1	8	80	He et al. [62]
Propane	280	12.8	24:1	10	98	Cao et al. [33]
CO_2	280	14.3	24:1	10	98.5	Han et al. [34]
	350–425	10.0–25.0	6:1	2–3	~100	Anitescu et al. [4]
THF	350	N/A	37:1	10	86.5	Sawangkeaw et al. [84]
n-hexane	350	N/A	43.4:1	10	88.1	Sawangkeaw et al. [84]
	295	10.0	45:1	20	85	Muppaneni et al. [85]
	300	10.0	33:1	20	91	Muppaneni et al. [57]

N/A is not available

As shown in Table 2.7, it can be clearly seen that the addition of co-solvents can decrease the optimal operating condition to achieve the highest yield (>98%) when compared with the non-co-solvent process. However, the addition of n-hexane as co-

solvent can be reduced only the reaction temperature and pressure, but did not increase the ester content significantly.

2.7.3. The application of micro-tube reactor

In recent years, the design of micro tube reactor has been studied for the continuous biodiesel synthesis with SCA [47, 86-88]. The mass and heat transfer is greatly intensified in the micro-reactor system due to its small space with a large surface area-to-volume ratio [89]. Consequently, the highest yields can be obtained in short reaction time [90].

Da Silva et al. [86] developed a micro-tube reactor of the biodiesel production with SCE. They found that the higher yield could be achieved at lower temperatures and short reaction times. The appreciable yields of 70% were obtained at the low parameters of 325 ∘C, 20 MPa, and ethanol to oil molar ratio of 20:1. Moreover, the total decomposition of the fatty acid is minimized (<5%) when conduct in this smaller reactor.

The addition of co-solvent was also investigated in a micro-tube reactor in order to increase reaction rates and improved mass transfer by Bertoldi et al. [87] and Trentin et al. [88]. Trentin et al. observed that the FAEE yield increased with the increasing amount of CO_2 and the highest yield obtained at the optimal operating condition of 325 ∘C and 20 MPa, and ethanol to oil molar ratio of 20:1. They concluded that the micro-tube reactor can be solved the mass transfer problem in the tubular reactor.

In 2011, da Silva et al. [91] introduced a micro-tube reactor in the two-step process. The experimental conducted in two-series reactors and a reactor with recycling to obtain the highest FAEE yield about 78% and the total fatty acid composition less than 3 wt. %. The optimal operating conditions are 300 ∘C, 20 MPa, and 45 min with ethanol to oil molar ratio of 40:1. Moreover, a high purity of glycerol (∼ 90 wt. %) was also observed after the steps of ethanol evaporation and simple decantation.

2.8. Literature reviews

It is well known that transesterification is the main path to produce biodiesel under the supercritical condition. However, the actual feedstocks are not composed solely of triglycerides; some side reactions can take place due to the contaminated water and free fatty acids especially the low-grade feedstocks. At the temperature over 210 °C or over 300 °C, the alkyl esters and triglyceride can be produced the respective free fatty acid by hydrolysis reaction in the presence of water; however, those fatty acids are subsequently converted to the desired product (biodiesel) by the esterification reaction [92].

At temperatures over 300 °C and reaction times over 15 min, the unsaturated fatty acids, especially the polyunsaturated fatty acids such as linoleic acid, can be cracked to small hydrocarbon molecules of triglyceride by the thermal cracking reaction [7, 93]. The resultant of thermal cracking reaction can be transesterified afterward to alkyl esters under supercritical conditions. Moreover, at the temperature range of 350–450 °C, the triglycerides are decomposed to fatty acids and some gaseous products [39]. In the same way of thermal cracking at 300–350 °C, the fatty acids product can be esterified under supercritical conditions, but the alkyl ester content is also decreased. However, these small hydrocarbon molecules could improve some fuel properties of biodiesel, such as viscosity, density, and cold flow properties.

The supercritical transesterification was first studied by Saka and Kusdiana [25]. They investigated transesterification reaction of rapeseed oil in supercritical methanol, at temperature of 350 and 400 °C, pressure of 45 to 65 MPa, with methanol to rapeseed oil molar ratio of 42:1, in a 5-mL batch reactor. They add the amount of rapeseed oil (2.00 g) and methanol (3.36 g) in the reactor. Then, the reactor was shaken and quickly immersed into the molten tin bath at 350 or 400 °C and kept for a set time (10 to 240 seconds). At the set time, the reaction vessel was quenched subsequently by the water bath to stop the reaction. The content in the reactor was then allowed to settle for phase separation. The upper and lower portions were analyzed by the HPLC. As expected, the lower portion was glycerol, as noticed by a comparison with standard

glycerol chromatogram, and the upper portion was FAME. The results indicated that the maximum conversion of FAME (95%) was found at a temperature of 350 ∘C, a pressure of 19.0 MPa and 240 seconds, optimal condition for this studied.

Then, they studied the kinetic of transesterification reaction of rapeseed oil in subcritical and supercritical methanol by varying temperature of 200 to 500 ∘C and methanol to rapeseed oil molar ratio 3.5 to 42 [37]. The results showed that the reaction temperature of 350 ∘C was considered as the best condition, with the methanol to rapeseed oil molar ratio being 42 and pressure of 19.0 MPa. The conversion rate of rapeseed oil to FAME increased dramatically in the supercritical state (350 ∘C) while the reaction rates were slow at the subcritical temperature below 239 ∘C.

Marulanda and coworkers [6] investigated on supercritical transesterification of chicken fat for biodiesel production from low-cost lipid feedstock, at the temperature range of 350–400 ∘C, pressure of 100–300 bar, alcohol to oil molar ratio of 3:1–12:1, reaction time of 3–10 min. The results showed that the optimal conditions of decomposition of glycerol from resultant of transesterification reaction to a small hydrocarbon molecules product were found at 400 ∘C, 100 bars, with alcohol to oil molar ratio of 9:1 and 6 min., the decomposition products can improve some fuel properties of biodiesel, and could increase FAME content to more than 84%.

Ruengwit and coworkers studied the biofuel production from palm oil with supercritical alcohols [9]. The effects of mole of alcohol in vegetable oil (3:1–24:1) were studied at the temperature of 400 ∘C, pressure of 10–15 MPa, reaction time of 10 min, in a 4-mL batch reactor. It was reported that the transesterification, esterification and thermal decomposition reaction of triglyceride simultaneous occurred and complete at 400 ∘C of reacting temperature and 10 min of reaction time. The optimal alcohol to oil molar ratio of methanol and ethanol were found at 12:1 and 18:1, respectively. Even though the resultant biofuel had the esters content lower than 96.5%, the value which is specified by International standard of biodiesel, it could be concerned as an alternative biofuel due to its fuel properties.

CHAPTER III
EXPERIMENTAL APPARATUS AND METHOD

3.1. Materials

In this study, refined palm oil (RPO) and used palm oil (UPO) were employed as feedstocks. The RPO was supplied from Morakot Industries Co., Ltd., and the UPO was obtained from a local restaurant near Chulalongkorn University, Bangkok, Thailand. Note that, UPO was filtered through filter cloth and paper to remove food residues before running the reaction.

Analytical-grade methanol (99.5%) was supplied by Sigma-Aldrich, Thailand. Analytical-grade ethanol (99.8 %) and glycerol were provided by Fisher, Thailand. For the analysis of samples using gas chromatography (GC), analytical grade n-heptane (Fluka, Thailand) was used as the solvent and methyl heptadecanoate (99.5%, Fisher, Thailand) was selected as the internal standard.

3.2. Experimental setup and procedure

In this study, the fourth different experimental apparatus were applied to produce biofuel under supercritical alcohols (SCA) conditions. To give a better understanding, fourth experimental apparatus and procedures are described in more details in this section.

3.2.1. Biofuel production in batch reactor

The reactions of palm oil and glycerol with SCA were investigated in a constant-volume batch reactor. The batch reactor was constructed from stainless steel tubing (closed at both ends) of 9.52-mm outside diameter, 1.24-mm thickness, and 110-mm length with a volume of 4-mL. The fluidized sand bath (OMEGA Model FSB-3, USA) was used to heat the reactor to the desired temperature. K-type thermocouples

(VSC Advance Co., Ltd, Thailand) and a proportional-integral-derivative controller (Sigma Model SF48, USA) were employed to monitor and control the temperature, respectively.

Initially, the amounts of alcohol and palm oil sample were calculated using the Redlich-Kwong equation of state at a constant alcohol to oil molar ratio to obtain a system pressure of 15 MPa, including the amount of alcohol and glycerol at the molar ratio of 9:1. Note that the effect of the initial air which could cause oxidation at supercritical conditions, could be neglected due to the total volume of reactants was generally over 3-mL in the 4-mL reactor. A given amount of alcohol and palm oil sample was added to a tube reactor, recapped, and immersed in the fluidized sand bath. The reactor was manually shaken periodically to ensure uniform mixing. At the end of the reaction, the reactor was then quenched in a water bath to stop the reaction. Excess ethanol was removed by rotary evaporation at 50 °C and 1.5 kPa for 30 min. Finally, glycerol was removed by gravity separation (>24 h settling time). The biofuel products were collected for analysis by gas chromatography (GC), from which the triglyceride conversion level (%X_{TG}) and the ester content (%FAME and %FAEE) were obtained.
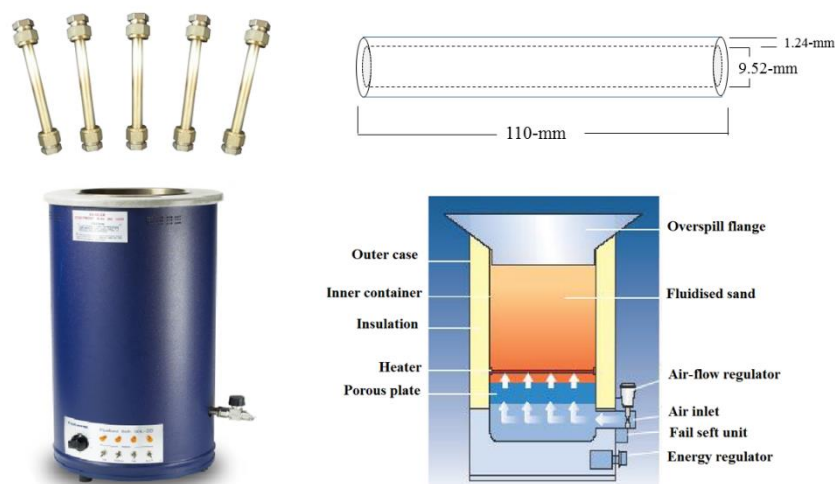
Figure 3.1. Batch reactor and the fluidized sand bath (OMEGA Model FSB-3) [94]

3.2.2. Biofuel production in continuous flow reactor

The experimental apparatus continuous flow reactor is schematically illustrated in Figure 3.2. Oil and alcohol were delivered to the pre-heater by two high-pressure liquid pumps (Jasco, model PU-1580 and PU-2080). In order to check the mass flow rate of the methanol and oil mixture in real-time, the weighing and timing method was applied. Both reactants were separately pumped into coiled pre-heaters (stainless steel (SUS316) tubing of 3.17-mm o.d., 0.71-mm thickness, and 150-cm length) and passed through a coiled tubular reactor (stainless steel (SUS316) tubing of 6.35-mm o.d., 0.89-mm thickness, and 600-cm length). Both the coiled pre-heaters and the tubular reactor were immersed in a fluidized sand bath (OMEGA Model FSB-3, USA). The K-type thermocouples (VSC advance Co., Ltd, Thailand) and a PID controller (Sigma Model SF48, USA) were employed to monitor and control temperature, respectively. After the outlet flow rate was steady, the back-pressure regulator (Swagelok, UK) was adjusted to increase the system pressure. A double-pipe heat exchanger was placed at the reactor outlet to cool the obtained product by flowed through a shell-side with external cooling water. Finally, the liquid product was collected in a glass flask and placed into a rotary evaporator at 50 °C and 1.5 kPa for 30 min to remove excess methanol. The biofuel samples were then quantitatively analyzed by GC.
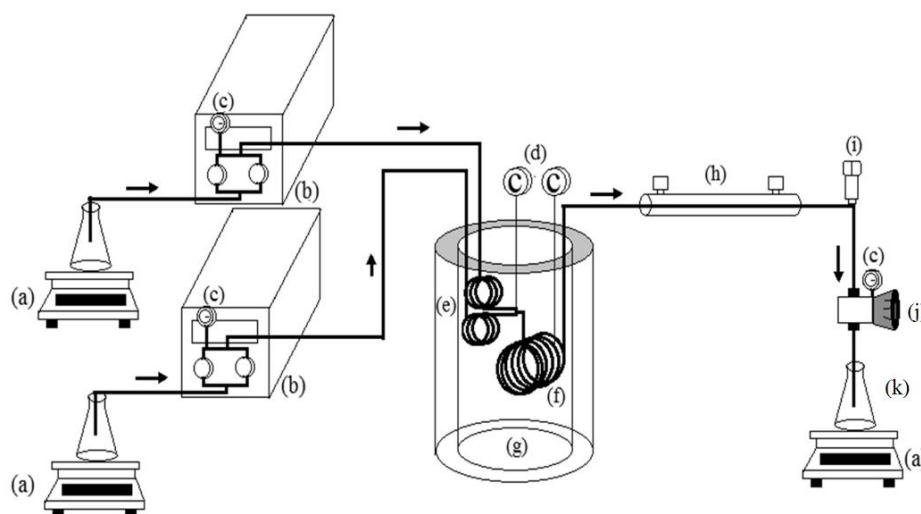
Figure 3.2. Schematic diagram of the lab-scale tubular reactor showing the (a) analytical balance, (b) high pressure pump, (c) pressure gauge, (d) thermocouple, (e) preheater, (f) reactor, (g) fluidized sand bath, (h) double pipe heat exchanger, (i) relief valve, (j) back-pressure regulator and (k) sampling flask

3.2.3. Density measurements in a constant-volume batch reactor.

The density of the reacting mixtures at supercritical condition was measured in a constant-volume cell, "using an isochoric method". The reactor was constructed from stainless steel tubing (closed at both ends) of 9.52-mm o.d., 1.24-mm thickness, and 58-cm length, with a volume at room temperature of 22.58-mL. The pressure was measured with a Wika Pressure Gauge (63.50mm, Lower Mount, 6.35mm NPT fitting, and 0–5000 psi working pressure). A K-type thermocouple was fitted directly into the reactor to monitor the temperature. The mixture of alcohol and oil at a constant molar ratio of 6:1 to 15:1 was added into the cell while global density values (mass/reactor volume) were varied between 0.447 to 0.891 g/cm^3. The measuring reactor was placed in an electric oven and slowly heated at a rate of 2 °C/min to the desired temperature. The pressure was recorded with the increasing temperature from 100 °C to 420 °C to obtain the pressure-temperature, or isochoric, line.
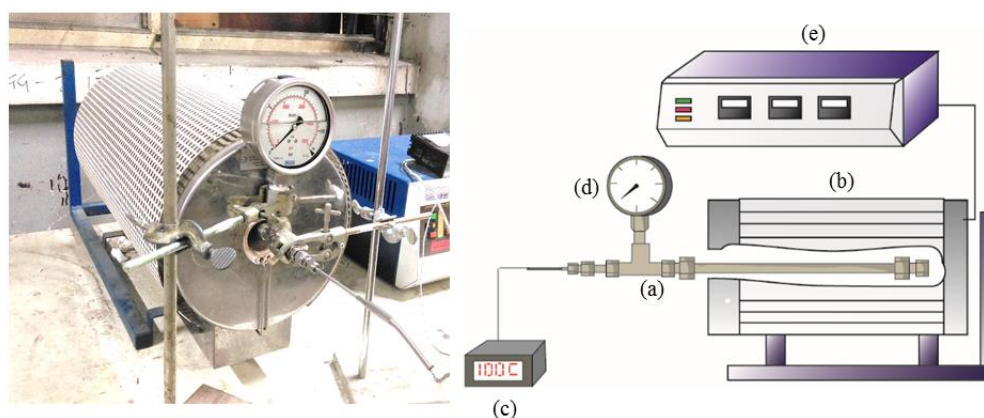
Figure 3.3. Scheme of the isochoric apparatus: (a) constant-volume cell, (b) electric oven, (c) temperature sensor, (d) pressure gauge and (e) process control equipment.

3.2.4. Phase equilibrium in high pressure view cell

The phase behavior of methanol-tripalmitin (palm oil) system was measured in a high-pressure variable-volume cell (Top Industries S.A., France). This set-up is classically used with the objective of determining fluid-liquid phase transition of mixtures, based on the synthetic method [95] as described thoroughly elsewhere [96]. However, for the purpose of this study with low mutual solubility of compounds, the cell has been adapted in order to determine in-situ concentration of phases at equilibrium thanks to Fourier transform infrared (FT-IR) spectroscopy method. This technique allows direct determination of the solubility of methanol in palm oil rich phase. A diamond attenuated total reflection (ATR) fiber probe was set at the top of the cell in such a way that the fiber is in contact with the palm oil rich phase. All spectra were recorded using a Bruker Tensor 27 FT-IR spectrometer (Bruker Optics Inc.) in the wave number from 580 to 3600 1/cm. The experimental setup is shown in Figure 3.4.

The bottom of the cell was first filled with approximately 12.0 mL to 15.0 mL of palm oil, corresponding to a half of the total cell volume, and a magnetic bar was placed inside the cell. A tip of diamond ATR fiber probe was then immersed in palm

oil and a consecutive spectrum of the background of palm oil was recorded. Next, approximately 12.0 mL to 15.0 mL of methanol was filled into the cell. The cell was tightly closed and was heated up to the desired temperature by heating bath circulation thermostats (model series CC-304B, Huber Inc.). A pressure was increased by the manually moving piston. The system was kept at the fixed temperature and pressure for at least 3 hr. By doing this, FT-IR spectra of methanol in palm oil rich phase were obtained. During the stabilization of the measuring conditions, the small decrease in the pressure between 1 and 5 bars that was controlled by the turning of piston wheel. The equilibrium had been reached when at least three consecutive spectra scanned within 30 min interval did not show any significant difference of absorbance. The solubility experiments were performed in the temperature range of 363–393 K and pressures up to 4 MPa.
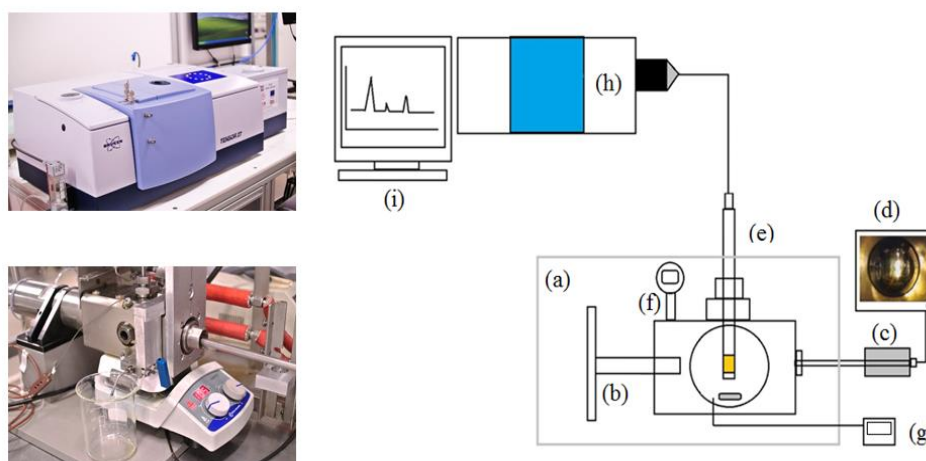
Figure 3.4. Schematic diagram of the experimental apparatus (a) high-pressure cell, (b) piston, (c) CCD Camera, (d) monitor, (e) ATR) fiber probe, (f) pressure gauge, (g) thermocouple, (h) FT-IR measurements, and (i) monitor with FT-IR spectrum.

3.2.4.1. Data processing for the determination of solubility of methanol in palm oil

The volumic concentration of methanol in palm oil rich phase was calculated from FT-IR results, according to the Beer-Lambert law, as shown in Equation (3.1).

$$A = \varepsilon \times L \times C \tag{3.1}$$

Where; A is the sample absorbance, ε is the molar extinction coefficient (L/mol cm) of the compound of interest, L is the optical path length (cm), and C is the sample concentration (mol/L). An aqueous solution of methanol with known concentrations was firstly measured by FT-IR to determine the multiplication of the molar extinction coefficient and the optical path length ($\varepsilon \times L$) for methanol. Based on the FT-IR spectrum of methanol, the peak height at wave number about 1010 1/cm was selected for concentration determinations. We emphasize that the signal of the FT-IR spectrum of methanol at the wave number of 1010 1/cm was the same in palm oil rich phase. Note that the peak height was used as analytical respond instead of peak area to minimize the error from the baseline correction of the integrated area.

Finally, mole fraction of methanol in the palm oil rich phase for phase equilibrium data was calculated as follows:

$$x_{MeOH} = \frac{C_{MeOH}}{C_{MeOH} + C_{palm\ oil}} \tag{3.2}$$

where C_{MeOH} is the concentration of methanol as determined by FT-IR measurements and $C_{palm\ oil}$ is the concentration of palm oil obtained from the literature [97] by considering molar density of palm oil as a function of the temperature. This calculation assumes no change in the molar density of palm oil due to methanol solubilization in the palm oil rich phase.

3.3. Design of experiments

The design of experiments is a statistical method used to minimize the number of experiments required to study a process, which estimates experimental error and eliminates systematic error [98]. In this study, a central composite design (CCD) was chosen to design the experiments and evaluate the influence of operating temperature (A), methanol to oil molar ratio (B), and reaction time (C) on $\%X_{TG}$ and %FAME.

The CCD experimental data was used to develop a mathematical model, e.g., second-order polynomial equation, to correlate both $\%X_{TG}$ and %FAME as the responses. The general form of the second-order polynomial equation is shown in Equation (3.3) [99].

$$y = \beta_0 + \sum_{(j=1)}^{k} \beta_j X_j + \sum_{(i<j)} \Sigma \beta_{ij} X_i X_j + \sum_{(j=1)}^{k} \beta_{jj} X_j^2 + \varepsilon, \qquad (3.3)$$

where y is the value of the response, X_j and $X_i X_j$ are the terms of the main effects and interaction effects, respectively, β_0 is the overall mean, β_j, β_{jj}, and β_{ij} are the coefficients of linear, quadratic, and interaction effects, respectively, and ε is random error.

Statistical analysis was performed using the Design-Expert® 9.0.4 software package, Trial-version (Stat-Ease Inc., Minneapolis, USA,). The quality of the developed model was determined using the coefficient of determination (R^2). Statistical analysis of variance (ANOVA) was then performed to evaluate the significance of the model. To obtain the optimal operating parameters, response surface methodology (RSM) was used to generate the response surface by presenting the response as a function of two factors while keeping the third constant.

3.4. Feed analysis

For feed analysis, the UPO was filtered through filter cloth and paper to remove food residues before examining the composition. The physical properties of the RPO and UPO sample were analyzed using standard testing methods, including the water content (EN ISO 12937), iodine value (ASTM D5554), and acid value (ASTM D664).

In determining the distribution of fatty acid, the American Oil Chemists' Society standard (AOCS Ce2-97) was applied to prepare FAME and FAEE sample. Physical and chemical properties of both oils are presented in Chapter IV.

3.5. Product analysis

The characterizations of biofuel sample were determined using standard testing methods, including density (ASTM D4052), kinematic viscosity (ASTM D445), flash points (ASTM D93), and higher heating value (HHV) (ASTM D240). In addition, the other equipment for product analysis in this study are described below.

3.5.1. Gas chromatograph, GC

Triglyceride conversion and ester content of biofuel samples were determined using a gas chromatograph, Varain Technology Model CP3800, equipped with a capillary column (Rtx®-65TG, 30 m length, 0.250 mm I.D.) and a flame ionization detector. The ester content in each biofuel samples was determined from the peak area obtained from GC based on the European standard method EN 14103:2003 [100]. The temperature program for GC in this study is shown in Table 3.1.

Table 3.1 GC condition for determination of triglyceride conversion and ester content in this study

Condition	Value
Carrier gas (He) flow rate	1.5 mL/min
Makeup gas (He) pressure	28 kPa
Hydrogen pressure (for FID)	30 kPa
Air pressure (for FID)	300 kPa
Detector temperature (FID)	250 °C
Split ratio	Off
Inject volume	0.1 μL

Condition	Value
Injection port temperature	360 °C
Temperature program rate	150 °C for 3 min,
	increased to 350 °C at 15 °C/min,
	370 °C for 5 min

3.5.2. Gas chromatography-mass spectrometer, GC-MS

The identification of compounds in the samples was performed with GC-MS (Shimadzu, GCMS-QP2010). An Agilent J&W DB-5 ms column with dimensions of 20 m × 0.1 mm × 0.1 µm was used, with ultra-pure helium as the carrier gas. The temperature program for the biodiesel samples and the glycerol–methanol reaction products are shown in Table 3.2.

Table 3.2 GC-MS condition for determination of identification in this study

Condition	Value	
Molecular weight scan range	50-850 m/z	
Solvent cut time	1.75 min	
Injection port temperature	250 °C	
Ion source temperature	200 °C	
Interface temperature	230 °C	
Temperature program rate	Biodiesel samples	Glycerol–Alcohol products
	60 °C for 2min, increased to 270 °C at 20 °C/min, 270 °C for 2 min	60 °C for 2 min, increased to 115 °C at 5 °C/min, 220 °C for 10 min at 5 °C/min

3.5.3. High-performance liquid chromatography, HPLC

The concentration of glycerol before and after reaction with methanol at supercritical condition was analyzed by High-performance liquid chromatography (HPLC, Shimadzu, and LC-10ADvp) with a RID-10A refractive index detector. The analytical column was an Aminex HPX-87C (300×7.8 mm), and the mobile phase was 65:35 (v/v) 5 mH_2SO_4/acetonitrile at the flow rate of 0.7 mL/min.

3.5.4. Distillation Gas Chromatograph, DGC

According to the ASTM D2887:2008 standard test method [101], the determining of distillation characteristic was analyzed by DGC, Agilent Technology Model 6890 N, equipped with a capillary column (5-m length $\times$ 0.53-mm o.d. $\times$ 0.09-µm film thickness, SIMDIS HT750, Analytical Controls) and a flame ionization detector. The temperature program was held at 30 °C and was then increased to 320 °C at 10 °C/min. The holding time at the final temperature (320 °C) was 20 min.

CHAPTER IV
BIOFUEL PRODUCTION IN SUPUPERCRITICAL ALCOHOL
USING BATCH REACTOR

As the lower proportion of alcohol required is reflected in a lower energy requirement for alcohol preheating, pumping, and recovery compared with conventional SCA processes with a 42:1 alcohol to oil molar ratio [58]. Thus, in this chapter, biofuel production from palm oil in SCM was investigated using a low methanol to oil molar ratio. The experimental was preliminary performed in a 4-mL batch reactor as described in Chapter III. The operating temperature in the range of 350–400 °C, alcohol to oil molar ratio of 9:1–12:1, and reaction time of 2–10 min were selected on the basis of previous reports [9]. Note that the operation pressure was set as 15 MPa. The effect of each operating parameters, their reciprocal interactions, and regression model on the triglyceride conversion (%X_{TG}) and ester content (%FAME) were evaluated by using the analysis of variance (ANOVA). Finally, the optimum process conditions were determined through the use of response surface methodology (RSM).

In addition, the optimum process conditions were applied to synthesizing the biofuel production in SCE. Ethanol is a promising reacting alcohol for biofuel production because it can be derived from biomass by fermentation. Thus, the employing of ethanol provides an entirely renewable fuel. The effects of reaction times and molar ratio on triglyceride conversion (%X_{TG}) and ester content in SCM and SCE were also compared, including the mass balance the chemical kinetics were also investigated to explore the utility of SCA process and its potential to scale-up to a continuous flow process (Chapter V).

4.1. Properties of Feedstocks (RPO and UPO)

The use of RPO as feedstock for biofuel production has been successfully investigated in our previous study [9]. Thus, in this study, UPO was selected as

feedstock in this preliminary study in a batch reactor. Table 4.1 shows the comparison of the RPO and UPO samples in the term of physical and chemical properties. It can be clearly seen that the UPO differs in physical properties from RPO, especially in the acid value. This is because of the higher level of FFA produced from the hydrolysis reaction during the cooking process [102]. According to ASTM D664, levels of FFA in the samples are directly related to the acid value and its can be determined by calculation. From the acid value of this UPO is 9.62 mg KOH/g, therefore, the % FFA can be derived as 4.50 wt. %.

The FFA levels in feedstock are required below 0.50 wt. % for the alkali-catalyzed biodiesel production. Because the FFA can react with the alkali-catalyst to form soaps, which reduces ester yield in the product [103]. Thus, it is clear that a pre-treatment process would be required to use UPO as a feedstock. However, the FFA does not significantly affect the supercritical transesterification with methanol and ethanol [2, 104, 105]. The FFA can be esterified to produce fatty acid alkyl ester under supercritical conditions to increasing the ester yield and process efficiency [9]. Furthermore, the approximately 10 wt. % of FFA in the feedstocks shows the catalytic activity, which results in higher conversions in both SCM and SCE processes [83, 105].

The water content in the feedstocks could affect the conversion in the transesterification reaction using the conventional acid-catalyzed method, as reported by Kusdiana et al. [2]. However, the water content in RPO and UPO are very low, as indicated in Table 4.1; thus, the effect of water is negligible in this study.

With regard to the fatty acid composition, palmitic acid (C16:0), oleic acid (C18:1), and linoleic acid (C18:2) were observed as the main compound of UPO, which can be transesterified to a major product, i.e., fatty acid alkyl esters in biofuel. It has been proposed that the conversion of a fatty acid ester from oleic acid is a suitable candidate for improving fuel properties. Since, oleic acid has high oxidation stability compared with other fatty acids containing two or three double bonds [106]. In addition, it can be noted that the level of linoleic acid is higher than that for RPO, possibly due to contamination during the cooking process, e.g., by chicken fat, which

contains 36.60 wt. % oleic acid and 27.0 wt. % linoleic acid [7]. The increasing linoleic acid (C18:2) content in UPO results in a slightly higher iodine value than that of RPO. In addition, UPO also contained higher levels of lauric acid (C12:0) and myristic acid (C14:0), most likely resulting from the decomposition of high-molecular-weight fatty acids, especially polyunsaturated fatty acids.

Table 4.1 The physical and chemical properties of RPO and UPO samples.

Physical–chemical properties	Samples	
	RPO (wt. %)	UPO (wt. %)
Fatty acid profiles		
Lauric acid (C12:0)	0.45 ± 0.12	5.72 ± 2.53
Myristic acid (C14:0)	1.10 ± 0.24	4.41 ± 1.64
Palmitic acid (C16:0)	46.14 ± 2.43	35.33 ± 3.61
Stearic acid (C18:0)	4.43 ± 0.13	4.42 ± 0.91
Total saturated fatty acids	52.12 ± 2.92	49.88 ± 8.69
Palmitoeic acid (C16:1)	N/D	N/D
Oleic acid (C18:1)	37.12 ± 4.64	39.96 ± 1.51
Linoleic acid (C18:2)	11.10 ± 1.04	11.51 ± 1.42
Linolenic acid (C18:3)	0.21 ± 0.11	0.34 ± 0.22
Total unsaturated fatty acids	48.43 ± 5.79	51.81 ± 3.15
Acid value (mg KOH/ g)	0.21 ± 0.05	9.62 ± 1.51
Water content (g/ 100g)	0.04 ± 0.05	0.14 ± 0.04
Iodine value (g/ 100g)	53.60 ± 5.00	68.47 ± 5.00
Molecular weight	850	858

N/D is not detected.

4.2. Process optimization

4.2.1. Design the experiments

In this section, CCD was chosen to design the experiments and evaluate the influence of operating temperature (A), methanol to oil molar ratio (B), and reaction time (C) on $\%X_{TG}$ and %FAME. The operating parameters and their ranges were determined at three levels; namely, low (−1), central (0), and high (+1), as summarized in Table 4.2. Note that code factors of each operating parameters derived from Equation (4.1) to (4.3).

$$A = \frac{Temperature(\circ C) - 375}{25} \qquad (4.1)$$

$$B = \frac{Methanol\ to\ oil\ molar\ ratio - 3}{3} \qquad (4.2)$$

$$C = \frac{Reaction\ time(min) - 6}{4} \qquad (4.3)$$

Table 4.2 Ranges of operating parameters and their levels for central composite design.

Factor	Operating parameter	Units	Levels		
			−1	0	1
A	Temperature	°C	350	375	400
B	Methanol to oil molar ratio	-	9	12	15
C	Reaction time	min	2	6	10

Table 4.3. shows the experimental conditions including the actual factor and code factor and the experimental results including $\%X_{TG}$ and %FAME. The complete design of 30 experiments comprised duplicates of eight factorial points, six axial points, and a central point. The experimental sequence was randomized to minimize the effects of uncontrolled factors.

Table 4.3 Experimental design matrix of triglyceride conversion (%X_{TG}) and methyl ester content (%FAME) as the two responses

| Run | Actual (Code) process variables | | | X_{TG} (%) | FAME (%) |
	Temperature (°C) (A)	MR (B)	Reaction time (min) (C)		
1	350 (−1)	9 (−1)	2 (−1)	19.64 ± 0.37	6.58 ± 0.59
2	400 (+1)	9 (−1)	2 (−1)	40.55 ± 0.36	20.64 ± 2.50
3	350 (−1)	15 (+1)	2 (−1)	15.51 ± 1.22	4.60 ± 0.41
4	400 (+1)	15 (+1)	2 (−1)	54.30 ± 1.06	20.14 ± 6.01
5	350 (−1)	9 (−1)	10 (+1)	51.56 ± 1.60	38.52 ± 4.93
6	400 (+1)	9 (−1)	10 (+1)	99.99 ± 0.01	60.16 ± 1.60
7	350 (−1)	15 (+1)	10 (+1)	80.87 ± 3.67	52.58 ± 1.60
8	400 (+1)	15 (+1)	10 (+1)	99.99 ± 0.01	65.63 ± 0.01
9	350 (−1)	12 (0)	6 (0)	59.10 ± 0.22	34.75 ± 1.36
10	400 (+1)	12 (0)	6 (0)	95.46 ± 0.87	57.50 ± 1.61
11	375 (0)	9 (−1)	6 (0)	52.90 ± 0.39	29.67 ± 0.38
12	375 (0)	15 (+1)	6 (0)	51.79 ± 1.29	46.77 ± 1.28
13	375 (0)	12 (0)	2 (−1)	35.63 ± 0.82	14.09 ± 0.81
14	375 (0)	12 (0)	10 (+1)	84.69 ± 2.74	56.77 ± 1.14
15	375 (0)	12 (0)	6 (0)	57.44 ± 0.39	45.28 ± 0.39

4.2.2. Regression model and statistical analysis

The results of the analysis of variance (ANOVA) for both %X_{TG} and %FAME are shown in Table 4.4 and Table 4.5, respectively. The p-value less than 0.05 indicated the significant of each term in the models. As shown in ANOVA table, it is clearly seen that all three individual operating parameters have significant impact on the progress of %X_{TG} and on increasing %FAME. Meanwhile, the interection term of methanol to oil molar ratio with reaction time (BC) has lesser but significant effect on yield of FAME.

The quadratic effect (A^2, B^2, C^2) indicated that the optimal conditions were located within the experimental range [107].

Table 4.4 The ANOVA table for the response surface quadratic model of %X_{TG}

Source	Sum of squares	Df	Mean square	F Value	p-value
Model	19741	9	2193.5	54.9	< 0.0001
A	5353.7	1	5353.7	134.1	< 0.0001
B	419.8	1	419.8	10.5	0.0041
C	12650.5	1	12650.5	316.8	< 0.0001
A^2	562.7	1	562.7	14.1	0.0012
B^2	563.5	1	563.5	14.1	0.0012
C^2	228.1	1	228.1	5.7	0.0268
AB	32.7	1	32.7	0.8	0.3763
AC	15.4	1	15.4	0.4	0.5413
BC	97.1	1	97.1	2.4	0.1346

Table 4.5 The ANOVA table for the response surface quadratic model of %FAME

Source	Sum of squares	Df	Mean square	F Value	p-value
Model	12290.8	9	1365.7	108.1	< 0.0001
A	1795.1	1	1795.1	142	< 0.0001
B	357.6	1	357.6	28.3	< 0.0001
C	9310.1	1	9310.1	736.6	< 0.0001
A^2	54.2	1	54.2	4.3	0.0516
B^2	111.6	1	111.6	8.8	0.0075
C^2	285.1	1	285.1	22.6	0.0001
AB	0.1	1	0.1	0	0.9349
AC	40.8	1	40.8	3.2	0.0874
BC	227.2	1	227.2	18	0.0004

The responses of both %X$_{TG}$ and %FAME were statistically analyzed and observed to fit with the quadratic regression model in terms of code factors, as follows:

$$\%X_{TG} = 64.94 + 16.36A + 4.58B + 25.15C - 10.46A^2 - 10.57B^2 - 6.66C^2, \qquad (4.4)$$

$$\%FAME = 43.36 + 9.47A + 4.23B + 21.58C - 3.25A^2 - 4.66B^2 - 7.45C^2 + 3.25BC, \quad (4.5)$$

As previously described, only the significant model terms, which have probability values of the p-value less than 0.05, are included in both regression models. These significant model terms have a large effect on the model, whereas insignificant model terms are excluded [108].

The predicted %X$_{TG}$ and %FAME from regression models versus experimental results are shown in Figure 4.1(a) and Figure 4.1(b), respectively. The R^2 values of both mathematics models were observed as 0.9514 and 0.9575, respectively. As the coefficient of determination (R^2) provides a measure of how well the experimental data fit with a statistical model [109]. Therefore, it can be indicated that both regression models provided an accurate description of the experimental data. Moreover, the quadratic models show that the probability value of the p-value is less than 0.001 for all responses, indicating that they are significant, with only a 0.01% chance of an unusual event occurring.
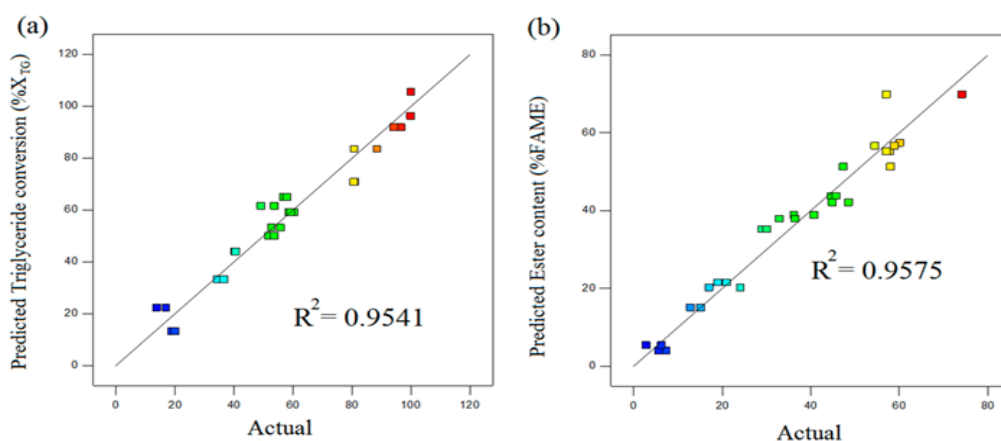
Figure 4.1. Plot of the actual and predicted responses for (a) %X$_{TG}$ and (b) %FAME.

4.2.3. Effects of process parameters

Considering Equation (4.4) and (4.5), reaction time (C) was found to be the major effect on both responses followed by temperature (A) and then molar ratio (B), as indicated by its coefficient. It has been reported that an increase in temperature expedites the transesterification reaction in supercritical condition, while increasing the reaction time allowed the reaction to proceed toward complete conversion, resulting in increasing ester yields [25, 26, 64, 70]. These effects can be clearly seen in Figure 4.2(a). The increment of $\%X_{TG}$ is enhanced two-fold with increasing reaction temperature from 350 °C to 400 °C with methanol to oil molar ratio of 9:1. Meanwhile, $\%X_{TG}$ rapidly increased at the beginning of the reaction, it reached a plateau of close to 99% after 10 min. For the progress of %FAME, similar results from the effect of process parameters were observed in Figure 4.2 (b). However, the ester contents were not sufficiently high at the highest temperature of 400 °C. This is because the thermal decomposition of polyunsaturated methyl esters at temperatures above 350 °C with a prolonged reaction time [39]. These results were in agreement with our previous study using RPO as feedstock [9].
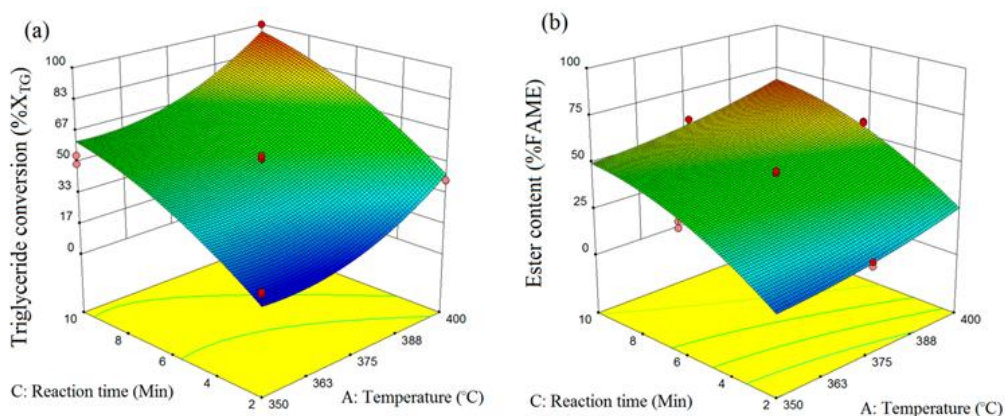
Figure 4.2. Response surface plot demonstrating the effect of temperature (A) and reaction time (C) on (a) $\%X_{TG}$ and (b) %FAME at a constant methanol to oil molar ratio of 9:1. Data are shown as the mean ± 1 SD and are derived from duplicates.

With regards to the effect of methanol to oil molar ratio (B), the change in $\%X_{TG}$ and %FAME is illustrated in Figure 4.3 (a) and (b) at 400 °C and a reaction time of 6 min. The minimal change in $\%X_{TG}$ and %FAME was observed with the increase of B from 9:1 to 15:1. This observation can be explained by the fact that methanol and oil at molar ratio of 9:1 are in a homogeneous state at 400 °C and 15 MPa, as confirmed by phase transition study in Chapter VI. At these conditions, the reaction reached equilibrium and near completion; thus, the increase of B from 9:1 to 15:1 did not lead to any evident effect on either response.
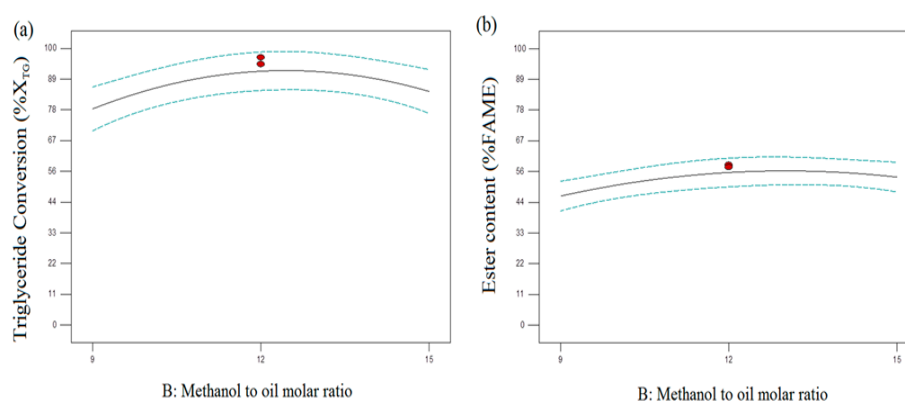
Figure 4.3. Effect of the methanol to oil molar ratio at 400 °C and 6 min on (a) $\%X_{TG}$ and (b) %FAME. Data are shown as the mean ± 1 SD and are derived from duplicates

As presented in Table 4.5, only the interaction of the methanol to oil molar ratio with reaction time (BC) was found to have a synergistic effect on the %FAME. The interaction between B and C shows in Figure 4.4 at a fixed reaction temperature of 400 °C. It can be observed that the increase of methanol to oil molar ratio from 9:1 to 15:1 at 2 min had minimal effect on the %FAME, which is similar at 10 min. Conversely, it can be said that %FAME was scarcely affected by methanol to oil molar ratio greater than 9:1.
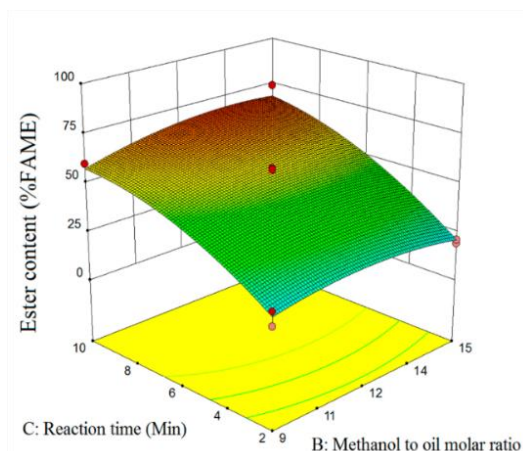
Figure 4.4. Response surface plot of %FAME with the interaction effect of methanol to oil molar ratio (B) and reaction time (C) at 400°C.

4.2.4. Optimization by RSM

The optimization of biofuel synthesis was performed to seek an appropriate combination of individual operating parameters as well as interaction between parameters to enhance the conversion of triglyceride and allow for maximum ester content. With the prospect of a low methanol to oil molar ratio, the variables (9:1–12:1) were set to a minimum while temperature and reaction time were in the range of 350°C to 400 °C and 2 to 10 min, respectively. The optimum operating parameters were carried out with the assistance of the optimization function embedded in the Design-Expert software. The optimum conditions obtained were as follows: temperature of 395.15°C, methanol to oil molar ratio 12:1, and reaction time of 8.82 min, which correspond to the predicted $\%X_{TG}$ and %FAME of 100% and 63.67%, respectively.

The predicted $\%X_{TG}$ and %FAME were verified by carrying out experimental runs under the suggested optimum conditions in triplicate. The mean values of the actual experiments were $99.99 \pm 0.01\%$ and $70.93 \pm 1.50\%$ for $\%X_{TG}$ and %FAME, respectively. Both actual values were close to the predicted values, especially $\%X_{TG}$ with less than 0.01% error. It can be indicated that the predicted optimum parameters are valid for this study. However, the %FAME from UPO was less comparable to that obtained using RPO as feedstock, which has a maximum yield of $74.50 \pm 2.00\%$ [9].

4.3. Comparative study of biofuel production in SCM and SCE

4.3.1. Effect of reaction times

Reaction times are an important parameter in achieving a complete conversion of triglyceride and to give maximum yields of esters. In this chapter, the effect of reaction times on that both responses was investigated from 0.5 to 10 min. Figure 4.1 shown the variation of the ester content levels with reaction time at fixed molar ratio of 12:1. It demonstrated that the total ester content increases steadily with reaction times and then tends to decrease after the reaction time of 6 min and 8 min for SCM and SCE, respectively. The reduction of the total ester content is mainly derived from decreasing of alkyl oleate (C18:1), alkyl linoleate (C18:2) and alkyl palmitate (C16:0). This observation indicates that the thermal decomposition of alkyl ester with excessive reaction times at high temperature, as previously reported in the literature [9, 39]. Since the alkyl linoleate contained two double bonds was observed to have more rapidly decomposed, with a downslope after 5 min for both SCM and SCE. It has been reported that the polyunsaturated fatty acid is increasingly unstable at higher temperatures compared with the mono-unsaturated and saturated ones [39]. The small compounds, i.e., alkane hydrocarbons in the range of C9-C10 are the products from this thermal decomposition, which was measured by GC-MS as shown in Table 4.8.
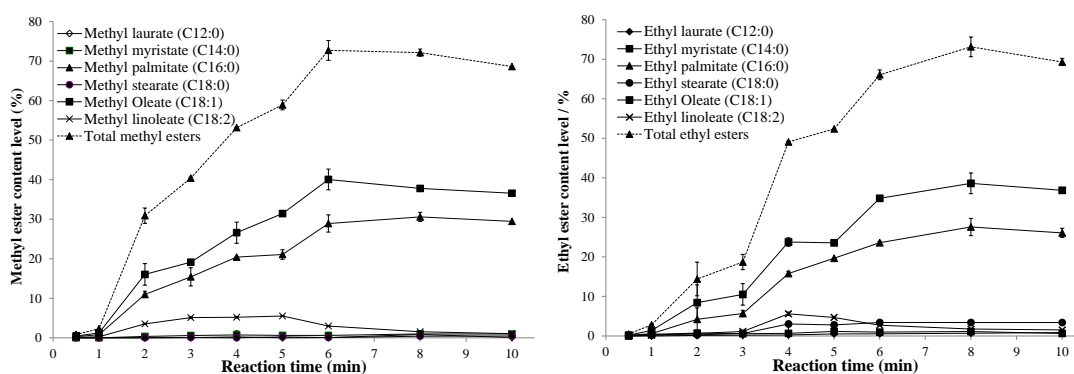
Figure 4.5. Ester contents of biofuel samples from UPO as a function of reaction time with (a) SCM and (b) SCE (Reaction conditions: 400 °C, 15 MPa at 12:1 of alcohol to oil molar ratio).

In order to minimize the glycerides content as specified by The European Standard (EN 14214), the effect of reaction time on the $\%X_{TG}$ was also investigated. Figure 4.6 shows the change of triglyceride with reaction time in both SCM and SCE. It can be observed that the conversion of triglyceride increased rapidly at the beginning of the reaction and then getting to a plateau of approximately 99 % at a reaction time of 10 min for all the alcohol to oil molar ratios. From this observation, hence, it can be concluded that a reaction time of 10 min is suitable to ensure the complete transesterification reaction with SCA at 400 °C and 15 MPa.
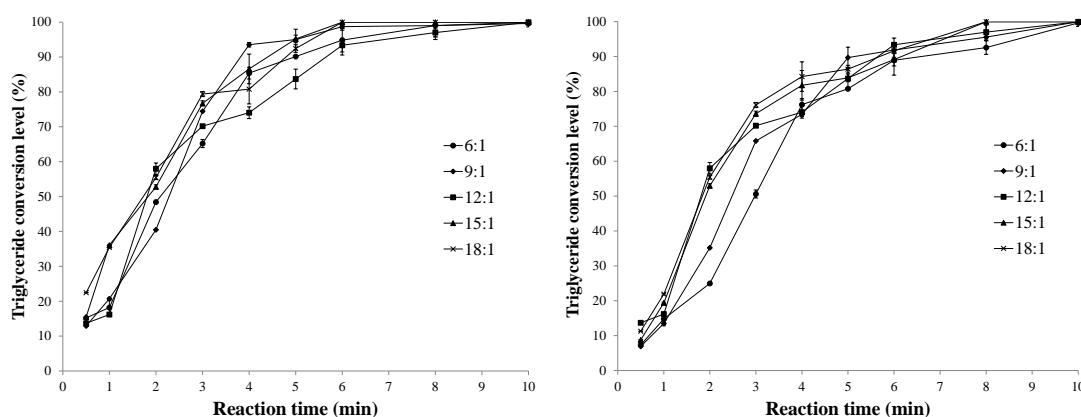
Figure 4.6. Triglyceride conversion level ($\%X_{TG}$) of biofuel samples from UPO as a function of reaction time with (a) SCM and (b) SCE at 400 °C and 15 MPa.

4.3.2. Effect of molar ratio

As previously described in Chapter II, the alcohol to oil molar ratio is one of the most important variables affecting the yield of fatty acid alkyl in SCA conditions. Hence, the influence of the alcohol to oil molar ratio was investigated in this chapter. Note that the alcohol to oil molar ratio 2–6 folds higher than the stoichiometric requirement (3:1) was considered to driven the equilibrium to the product side and also reduced the critical temperature of the mixture. Moreover, it has been reported that ethanol is consumed by multiple reactions such as the transesterification of triglycerides, esterification of FFA, and etherification reaction of glycerol [9].

Figure 4.7 illustrated the change of triglyceride conversion and the total ester content with the variation of the alcohol to oil molar ratio at a fixed reaction time of 10 min. The ester content was found to increase with the increasing of alcohol to oil molar ratio from 0:1 to 12:1 both SCM and SCE. It is due to the critical point of the UPO-alcohol mixture decreased with increasing alcohol content. In addition, the ester contents were observed to be constant at the alcohol to oil molar ratio between 12:1 and 18:1. This finding confirmed that alcohol to oil molar ratio between 12:1 and 18:1 has the small impact on the ester yield, as observed in the ANOVA table.
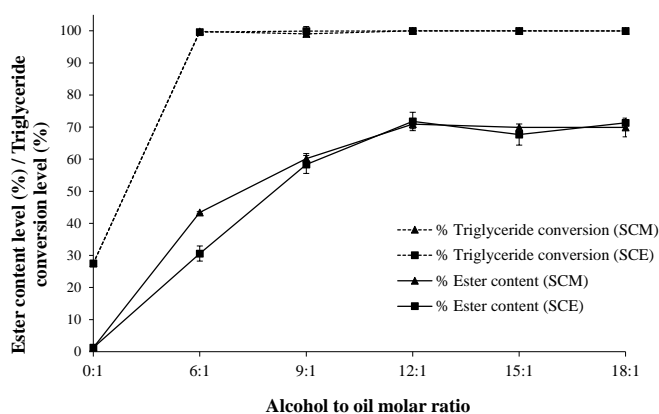
Figure 4.7. Ester content and triglyceride conversion of biofuel samples from used palm oil (UPO) as a function of alcohol to oil molar ratio (reaction conditions: 400 °C at 15 MPa, and 10 min reaction time).

According to the decomposition of alkyl ester observed at this reaction temperature (400 °C), consequently, the ester yield could not be maximized to meet the 96.5% of the biodiesel standard value. Therefore, the reduction of the remaining glycerides in biofuel samples should be considered to controlling the quality of biodiesel. The levels of remaining glycerides in the samples produced in this study are presented in Figure 4.8. The EN 14214 requires levels of mono-, di-, and triglycerides below 0.80, 0.20, and 0.20 mass%, respectively. It was found that the glyceride levels in biofuel samples produced using alcohol to oil molar ratios from 9:1 were within the requirements of this specification. In accordance with the highest ester content and the

glyceride levels under the standard, the molar ratio of 12:1 for both SCM and SCE is the optimal ratio to abstain from the excess of alcohol.
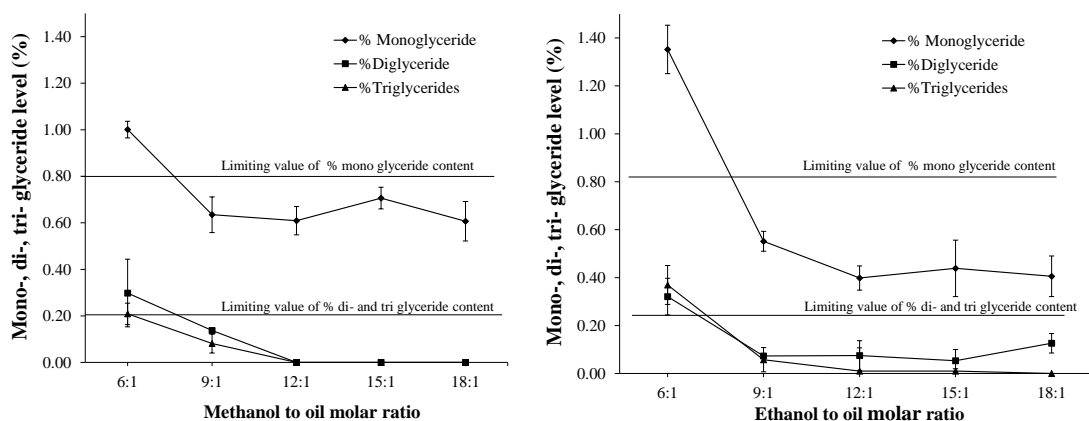
Figure 4.8. Glycerides levels in biofuel samples from UPO as a function of alcohol to oil molar ratio with (a) SCM and (b) SCE (reaction conditions: 400 °C at 15 MPa, and 10 min reaction time).

4.3.3. Mass balance

The mass balance of the optimal molar ratio was investigated based on the transesterification reactions involved in the process. In 100 kg of oil feed, the transesterification reaction of a stoichiometric mixture of triglyceride (TG) with both methanol (MeOH) and ethanol (EtOH) is present in Equation (4.6) and (4.7), respectively. Note that the average molecular weight of triglyceride (TG) for UPO is 858 which were calculated based on the fatty acid composition of UPO.

100.00 kg TG + 11.23 kg MeOH = 99.88 kg FAMEs +11.35 kg glycerol   (4.6)

100.00 kg TG + 16.14 kg EtOH = 99.63 kg FAEEs + 16.51 kg glycerol   (4.7)
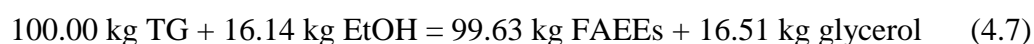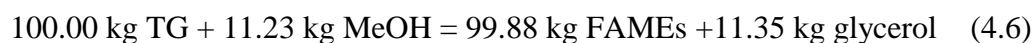
However, there is not only the transesterification reaction but also the esterification reactions will occur due to the present of FFA (4.5 wt. %) in UPO. Therefore, 100 kg of UPO feedstock will react as follows:

95.50 kg TG + 10.69 kg MeOH = 95.08 kg FAMEs + 11.11 kg glycerol   (4.8)

4.50 kg FFA + 0.54 kg MeOH = 4.80 kg FAME + 0.24 kg H_2O (4.9)

95.50 kg TG + 15.38 kg EtOH = 95.16 kg FAEEs + 15.72 kg glycerol   (4.10)

4.50 kg FFA + 0.76 kg EtOH = 4.47 kg FAEE + 0.79 kg H_2O (4.11)
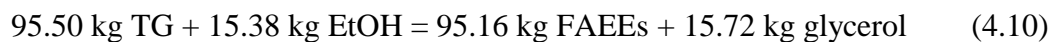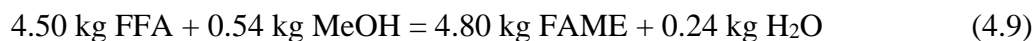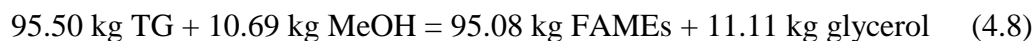
Hence, the mass balance of the overall reaction with the theoretically obtained values of the molar ratio of 12:1 is illustrated in Figure 4.9.

The experimental mass balance of biofuel samples from SCM and SCE are summarized in Table 4.6. It can be seen that the fuel yield of SCM and SCE increases about 6.09 wt. % and 8.05 wt. %, respectively, which was indicated by the mass of the fuel phase divided by the mass of UPO. In addition, the production of glycerol and water phase is approximately 5-8 folds lower than the theoretically obtained values. This observation indicated the etherification of glycerol and supercritical alcohol at 400 °C 15 MPa. Moreover, the slight decrease of outlet alcohol also confirmed the consumption of alcohol in etherification reaction. The product identification of this etherification reaction is present in Table 4.8.

(a)

(b)
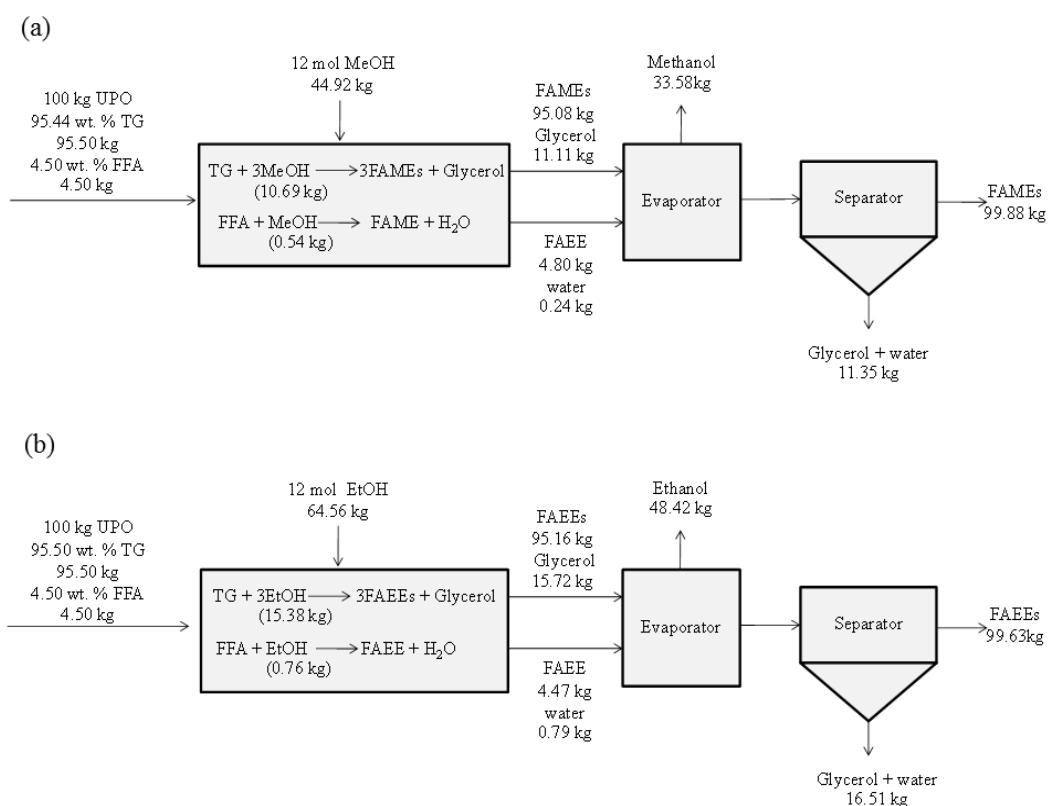
Figure 4.9. Flow sheet of the process with mass balance of biofuel production under the optimal molar ratio of 12:1 with (a) SCM and (b) SCE

Finally, the gas phase displays 5.35 wt. % and 11.21 wt. % for SCM and SCE, respectively, due to the thermal decomposition of the alkyl esters. However, there are not identification of the gas phases in this Chapter due to the small volume obtained from the 4-mL reactor. These gaseous products may consist of methane, ethane, and carbon dioxide, as reported in our previous study of biofuel production from palm olein oil [9].

Table 4.6 Simplified mass balance of biofuel production from UPO with SCA at 400 °C, 12:1 alcohol to oil molar ratio, and 15 MPa as observed in the experiment

Process	Feed (kg)		Outlet (kg)			
	UPO	Alcohol	Fuel phase	Alcohol	Glycerol + water phase	Gas phase
SCM	100	45.45	106.09	31.12	2.89	5.35
SCE	100	64.56	108.15	42.88	2.32	11.21

4.3.4. Reaction between supercritical alcohol and glycerol

The reaction of alcohol and glycerol at 400 °C 15 MPa was also measured in the 4-mL reactor in order to confirm the occurrence of etherification under these supercritical conditions. The possible compounds obtained from the etherification of glycerol with methanol were illustrated in Figure 4.10. When glycerol is etherified with methanol, the hydroxyl groups in the glycerol molecule are reacted to form five different types of ether isomers.
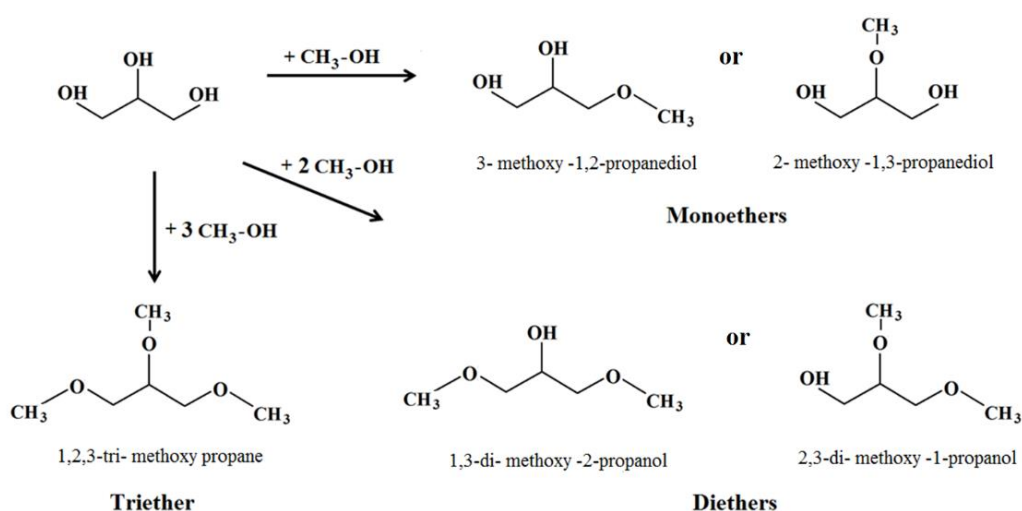
Figure 4.10. Reaction scheme for the etherification of glycerol with methanol.
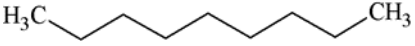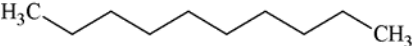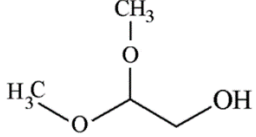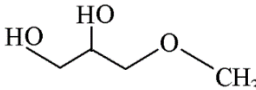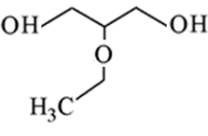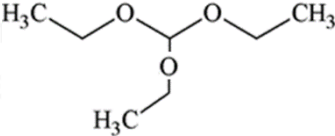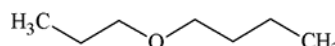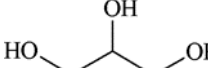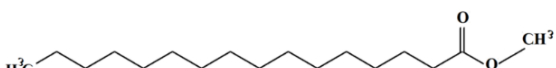
The alcohols to glycerol molar ratios were fixed at 9:1 for both SCM and SCE because this was the molar ratio when the triglyceride conversion was 100% complete. The glycerol content at the beginning and after the reaction time of 10 min was analyzed by HPLC, as shown in Table 4.7. The results demonstrated that glycerol content dramatically decreased from 2.30 g to 0.26 and 0.28 g for SCM and SCE, respectively, which confirmed that the etherification reaction occurred in the supercritical condition.
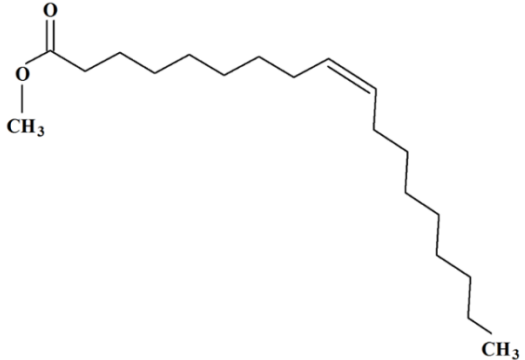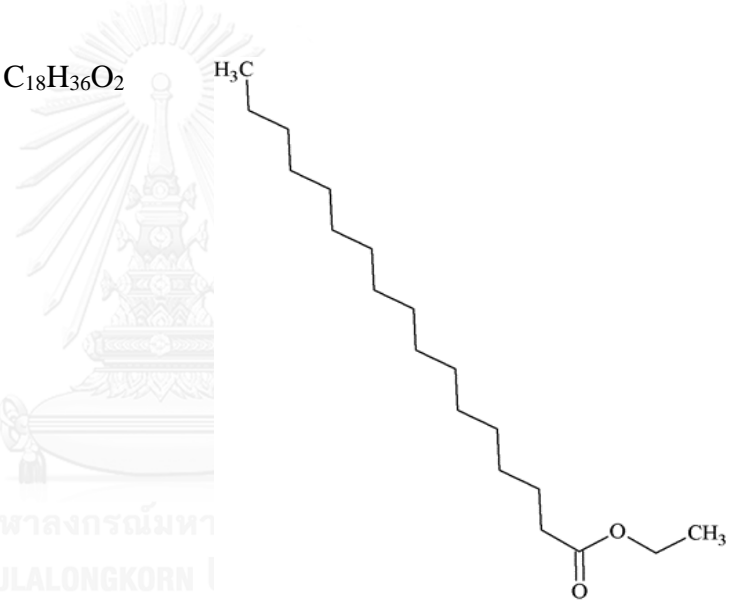
Table 4.7 Glycerol content of the glycerol reaction in SCM at 400 °C and 15 MPa.

Materials (Molar ratio)	Reaction time (min)	Glycerol Content (g)
Glycerol	0	2.31±0.006
Methanol: Glycerol (9:1)	10	0.26±0.008
Ethanol: Glycerol (9:1)	10	0.28±0.012

The product compounds from this reaction were identified by GC-MS analysis. As shown in Table 4.8, the products of SCM–glycerol reaction are 2-methoxy-1-propanoland 3-methoxy-1, 2-propanediol, while 2-ethoxypropane, 1, 1-diethoxy propane, and 2-propoxybutane was observed as the products of SCE–glycerol reaction. Moreover, the compounds of 3-methoxy 1, 2-propanediol, 1, 1-diethoxypropane, and 2-propoxybutane also present in the biofuel product. Thus, it can be implied that the products between the alcohol and glycerol can miscible in the fuel phase and consequently increase the fuel yield. Marulanda et al. [7] reported that the etherification products of glycerol and methanol are completely miscible with biodiesel and they have the improvement of some fuel properties.

Table 4.8 Identified compounds in the product of the alcohol–glycerol reaction and product of biofuel based on GC–MS.

Name	Formula	Structure
[b] Nonane	C_9H_{20}	
[b] Decane	$C_{10}H_{22}$	
[a] 2,3-dimethoxy-1-propanol	$C_5H_{12}O_3$	
[a,b] 3-Methoxy-1,2-propanediol	$C_4H_{10}O_3$	
[a, b] 2-Ethoxy-1,3-propanediol	$C_5H_{12}O_3$	
[a,b] 1,2,3-Triethoxypropane	$C_9H_{20}O_3$	
[a] 2-Propoxybutane	$C_7H_{16}O$	
[a] Glycerol	$C_3H_8O_3$	
[b] Methyl hexadecanoate	$C_{17}H_{34}O_2$	

Name	Formula	Structure
[b]Methyl-9-octadecenoate	$C_{19}H_{36}O_2$	
[b] Ethyl hexadecanoate	$C_{18}H_{36}O_2$	

[a] Appearance in the product of methanol or ethanol–glycerol reaction.

[b] Appearance in the biofuel sample.

4.3.5. Chemical kinetics studies

The transesterification reactions is a reversible reaction, however, an employ of a large amount of alcohol were used to shift the reaction to the right side. This reaction was assumed to be a pseudo-first-order reaction as a function of the concentration of triglyceride, as reported by several researchers [110, 111]. Therefore, the reaction rate can be given by Equation (4.12).

$$rate = -\frac{d\,(TG)}{dt} \tag{4.12}$$

where TG is concentration of triglyceride and t is the reaction time (min). Considering to the terms of conversion, the differential rate can be obtained:

$$\frac{dX_{TG}}{dt} = -k(1 - X_{TG}) \tag{4.13}$$

where X_{TG} is triglyceride conversion and k is the intrinsic rate constant (1/s). The Equation (4.14) was then rearranged and integrated:

$$kt = -ln(1 - X_{TG}) \tag{4.14}$$

Therefore, the intrinsic rate constant of the reaction can be obtained from the plots of $-ln(1-X_{TG})$ versus reaction time (t), as shown in Figure 4.11. In this study, the temperature was varied between 350 °C and 400 °C for the optimal alcohol to oil molar ratio of 12:1 to determine the chemical kinetics.
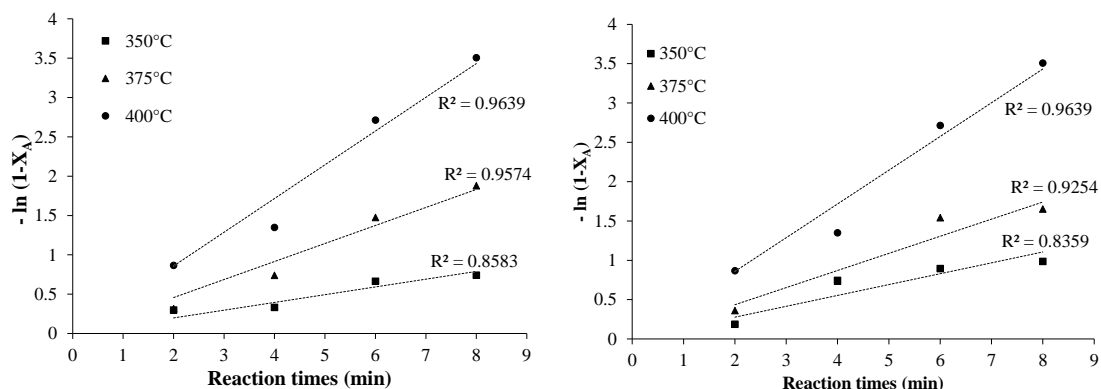
Figure 4.11. Relationship between $-\ln(1 - X_{TG})$ and reaction time from the pseudo-first-order kinetics model at an alcohol to oil molar ratio of 12:1 of (a) SCM and (b) SCE. The linear regression best-fit line and correlation coefficient (R^2) are also shown.

Considering Figure 4.11, all the linear regression lines pass through the origin with R^2 values as high as 0.90; thus, the intrinsic chemical kinetics of this work follows the pseudo-first-order model assumption. The rate constants for each reaction temperature are tabulated in Table 4.9. It is evident that the intrinsic rate constants were sensitive to temperature and also increasing with temperature.

Table 4.9 Rate constants and activation energy of biofuel samples obtained from Figure 4.11 and Figure 4.12, respectively

Temperature (°C)	Rate constant (1/s)		Activation energy, E_a (kJ/mol)	
	SCM	SCE	SCM	SCE
350	0.1383	0.0987		
375	0.2176	0.2290	78.80	92.88
400	0.4289	0.4231		

Based on the results in Figure 4.11, the corresponding Arrhenius plot for the activation energy value (E_a) is presented in Figure 4.12. The results indicated activation energy of 78.80 and 92.88 kJ/ mol for SCM and SCE, respectively.
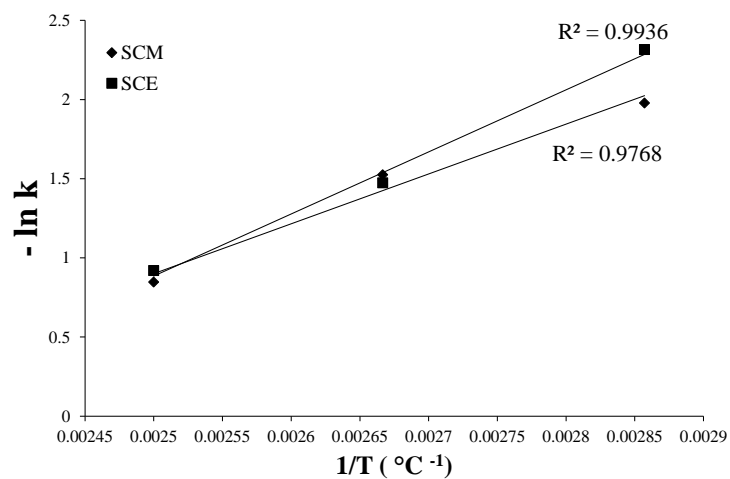
Figure 4.12 Arrhenius plot of the pseudo-first-order kinetics model at an alcohol to oil molar ratio of 12:1
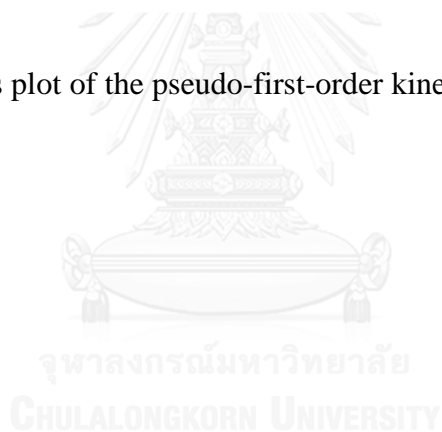
CHAPTER V
BIOFUEL PRODUCTION IN SUPERCRITICAL METHANOL
USING CONTINUOUS REACTOR

Since the SCA process conducted at 400 °C and 15 MPa shown the ability to markedly reduce the alcohol to oil molar ratio to 12:1 in batch reactor, as described in Chapter IV. To scale-up the process, thus, the biofuel was synthesized in SCM using continuous reactor at the selection condition of 400 °C and 15 MPa. In addition, the temperature over 400 °C and pressure in the range of 10-40 MPa are proper to use with low methanol to oil molar ratio, as reported in the previously study (Table 5.1). The low alcohol to oil molar ratio was varied between 6:1 and 15:1. The effects of residence time on triglyceride conversion (%X_{TG}) and ester content (%FAME) was also investigated by regulating the reactant flow rate. Note that the residence time was accurately calculated from the density of each reacting mixtures. It was measured by the isochoric method as described in Chapter III. Finally, the RPO and UPO were employed as feedstock and were also compared.

74

Table 5.1 Summary of literature-reported experimental data using the SCM process.

Oil types	T (°C)	P (MPa)	MR	Residence time (min)	process type	FAME/ CV (%)	ref
Coconut	350	19	42	6.67	continuous	95% FAME	[36]
Palm oil	350	19	42	6.67	continuous	96% FAME	[36]
Soybean	300	32	40	25	continuous	77% FAME	[37]
Palm oil	372	15–25	40	16	batch	81.5% FAME	[104]
Palm olein oil	400	15	12	10	batch	80% FAME	[9]
						~100 % CV	
Chicken fat	400	37.6	6	5	batch	88% FAME	[7]
Rapeseed	350	43	42	4	batch	95% FAME	[25]
Castor	350	20	40	40	batch	~100 % CV	[46]

Table 5.1 Summary of literature-reported experimental data using the SCM process.

Oil types	T (°C)	P (MPa)	MR	Residence time (min)	process type	FAME/ CV (%)	ref
Linseed	350	20	40	40	batch	~100% CV	[46]
Sunflower	400	20	40	40	batch	96% CV	[45]
Chicken fat	400	30	9	6	continuous	80 % FAME	[6]
						99% CV	
Soybean	400	20	6	1.75	continuous	>98% CV	[4]
Canola	450	40	11-45	4	continuous	~100% CV	[32]
Waste cooking oil	287	N/A	41	30	batch	99.6% FAME	[30]
Waste canola oil	270	10	50	45	continuous	~102% FAME	[61]

MR: Methanol to oil molar ratio, FAME: % Ester content, CV: % Conversion.

The significant digits are the same as in the original sources.

5.1. Density of reacting mixtures and residence time calculation

Residence time was precisely determined using Equation (5.1), considering to a mass flow-rate and density of reacting mixture (methanol and oil).

$$\tau_r = \frac{V}{M / \rho_M} \qquad (5.1)$$

where τ_r is the residence time (min), V is the reactor volume (mL), M is a mass flow-rate at ambient conditions (g/min), and ρ_M is the density of reacting mixtures (g/mL).

In supercritical conditions, the isochoric method was applied to measure the density of the palm olein oil and methanol mixture. It has been reported that the isochoric method is a simple way to obtain accurate densities and an indirect way to provide the conditions of phase transition [112-115, 116]. In the biodiesel production with SCA, the isochoric method was first employed to measures the density of coconut and sunflower oils with methanol by Velez et al. [116], including density of sunflower oil and ethanol [117].

Figure 5.1 shows the experimental results obtained by an isochoric method of methanol to oil molar ratio between 6:1 and 15:1 with global density values of 0.477 to 0.891 g/cm^3. In the molar ratio of 9:1 to 15:1, it can be noticed that the pressure-temperature lines are the linear functions with 3 different slopes, which are similar to the results from Velez et al. [117]. They reported that the isochoric results are not only for determining density but also for finding out the phase transition from the heterogeneous region to the homogeneous region. The pressure-temperature lines were separated by slope into three sections. In the low-temperature range (<230 °C), the pressure was observed to increase following the vapor pressure of methanol [118]. This section indicates the liquid-liquid-vapor (LLV) equilibrium of liquid methanol, liquid oil, and vapor methanol. In the second section, the slope of pressure-temperature lines has more planar than the first section at the temperature over the critical point of methanol (~230 °C). Methanol becomes to complete miscibility in a liquid phase of oil, as proposed by Velez et al. [117]. Moreover, they also claim that a high conversion of the transesterification between methanol and vegetable oil to fatty esters and glycerin starts to occur. Either the liquid phase or the vapor phase, depending on the global

density of the mixture, increases up to a point at which the whole mixture becomes homogeneous (via a bubble or dew point for the liquid or vapor phase, respectively). Finally, the third section presents the homogeneous at the highest temperature (approximately 300 to 450°C). The intersection point of second and third sections indicates the phase change from the heterogeneous to the homogeneous region, which is called the "phase transition point". For example in Figure 5.1 (b), the transition point takes place at 450 °C and 9 MPa for the global density of 0.651 g/cm^3. Besides, the phase transition also confirmed that the homogeneous phase can occur in the continuous reactor at the selection condition of 400 °C and 15 MPa.
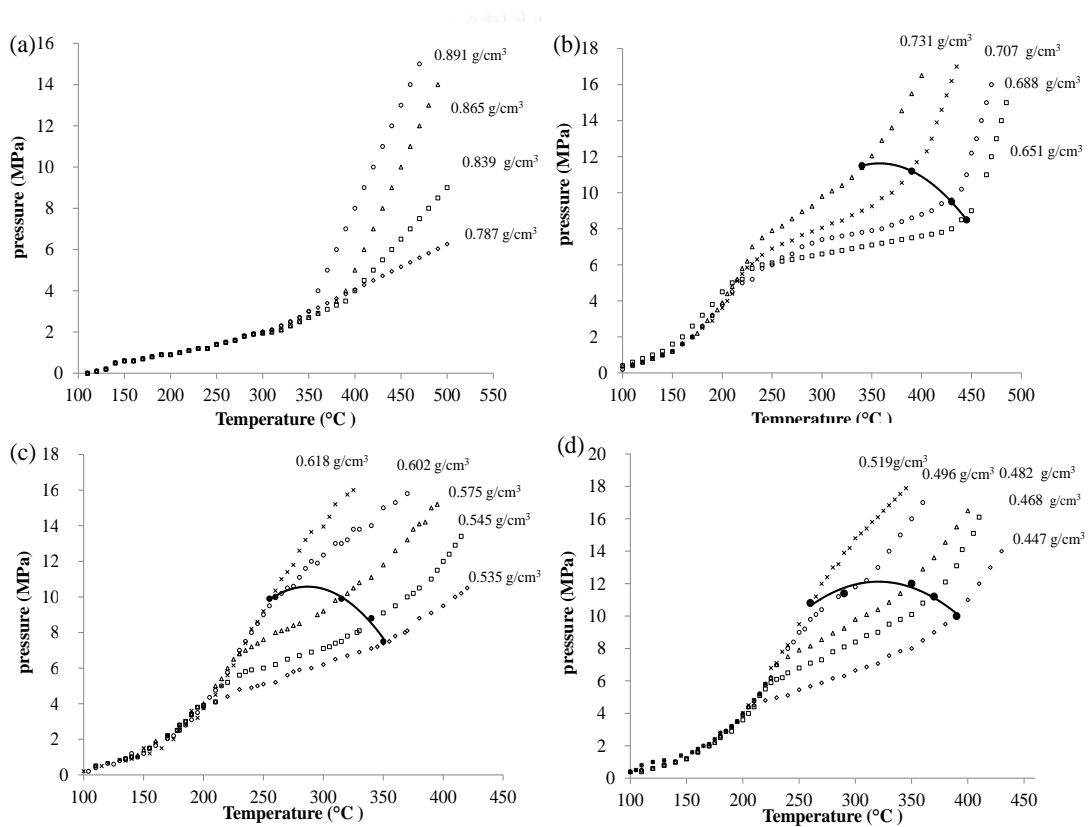
Figure 5.1. Pressure vs. temperature for the methanol and palm olein oil system with a molar ratio of (a) 6:1, (b) 9:1, (c)12:1 and (d) 15:1 and (symbol ●) the and phase transition point.

With regard to the molar ratio of 6:1, the difference behavior the pressure-temperature lines were observed. They were separated into two sections; consequently, both of the intermediate and the transition point were not obtained. The pressure speedily increases with the increasing temperature at the second section. Since the liquid phase of the mixtures expands to filling up the volume of the reactor. As reported by Barrufet and Eubank [119], this case was corresponded to the collinearity phenomenon of the heterogeneous and homogeneous isochoric lines at the maximum temperature point (cricondentherm, CT) of the phase envelope of a mixture. Therefore, it could be said that the transition point for molar ratio lower than 6:1 might not possible to detect by using of isochoric technique.
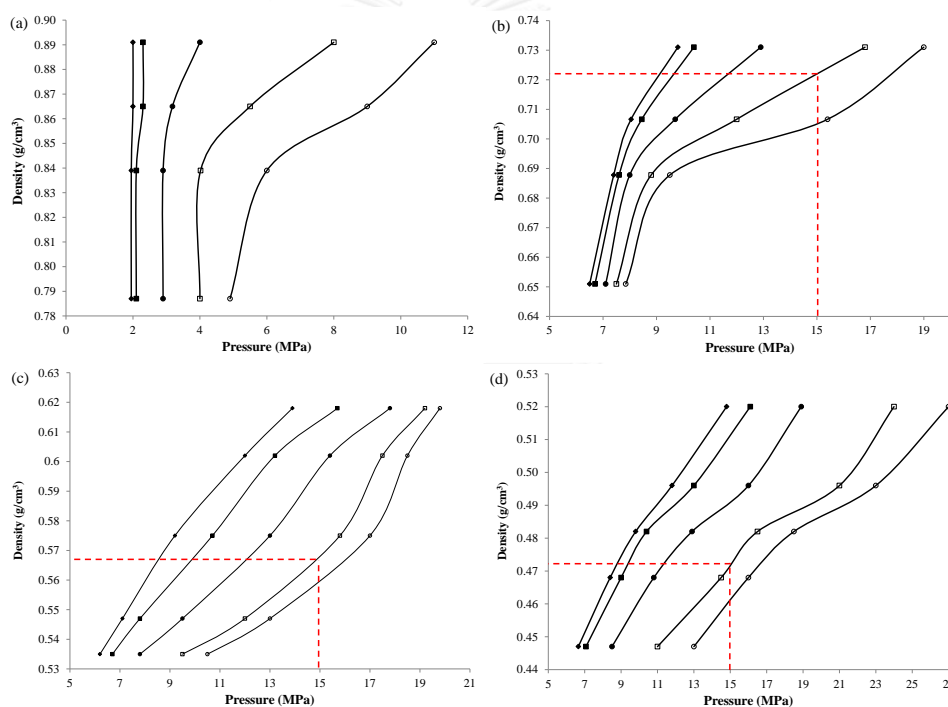
Figure 5.2. Densities of homogeneous reacting mixtures of methanol and palm olein oil of (a) 6:1, (b) 9:1, (c) 12:1 and (d) 15:1 as a function of pressure, at temperatures of (♦) 300, (■) 320, (●) 360, (□) 400, and (○) 440°C. Data are shown as means ± 1 SD, derived from 3 independent repeat measurements.

Considering to Figure 5.1, the data above the phase transition points are replotted in order to simplify the determination of the mixture densities. As illustrated in Figure 5.2, the vertical dashed line was projected from the reacting pressure of 15 MPa to the temperature line of 400 °C for evaluating the mixture densities. The reacting mixture densities are 0.722, 0.568 and 0.472 g/cm^3 of the methanol to oil molar ratio of 9:1, 12:1 and 15:1, respectively. However, the reacting mixture density cannot determine for the methanol to oil molar ratio of 6:1 because of collinearity phenomenon as mention earlier. According to Equation (5.1), the density was subsequently employed to calculate the residence times in the continuous reactor at operating conditions of 400 °C and 15 MPa. The residence times of all alcohol to oil molar ratios are shown in Table 5.2.

Table 5.2 Actual mass flow rate of reactants in biofuel production from RPO and UPO with SCM at 400 °C and 15 MPa.

Oil type	Methanol to oil molar ratio	M, Mass flow rate (g/min)			τ_r, residence time (min)
		Oil	Methanol	total	
RPO	9:1	2.51	0.84	3.35	20.58
	12:1	3.18	1.30	4.48	10.13
		1.94	0.90	2.84	15.98
		1.65	0.76	2.41	18.84
		1.55	0.63	2.18	20.87
		1.40	0.60	2.00	22.69
		1.20	0.54	1.74	25.97
	15:1	1.40	0.78	2.18	20.65
UPO	12:1	2.87	1.33	4.20	10.81
		1.94	0.91	2.85	15.92
		1.64	0.76	2.41	18.86
		1.57	0.64	2.21	20.50

5.2. Effects of molar ratio

To minimize the use of methanol in SCM at 400 °C and 15 MPa, the effect of methanol to oil molar ratio on $\%X_{TG}$ and %FAMEs were examined by varying from 9:1 to 15:1. Figure 5.3 presents the triglyceride and ester content change with the various molar ratios at the residence time of 20 min. It can be clearly found that both $\%X_{TG}$ and %FAMEs increase with the methanol to oil molar ratios from 9:1 to 12:1 and relatively constant at 15:1. This is because of the critical points of mixtures was reduced with the addition of methanol content in the reaction mixture. As presents in Figure 5.2, the phase transition region at the molar ratio of 9:1 is 300–450 °C and 10.0–12.0 MPa while the higher than that region of 250–370°C and 8.0–11.0 MPa was observed at 12:1. According to the constant of both values at 15:1, therefore, the 12:1 was chosen as the optimal molar ratio to elude the surplus of alcohol usage.
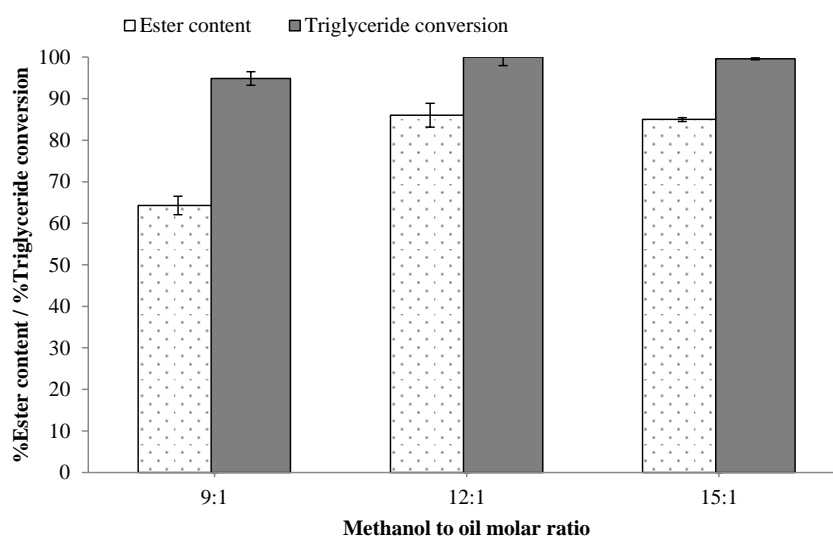
Figure 5.3 Ester and triglyceride contents of biofuel samples from RPO as a function of methanol to oil molar ratio (reaction conditions: 400 °C at 15 MPa, and 20 min of residence time). Data are shown as means ± 1 SD, derived from 3 independent repeat measurements.

5.3. Effects of residence time

It has been reported that the residence time is an important factor to achieve a complete conversion of triglyceride and to obtain the maximum yields of methyl esters. Thus, the influence of residence time on $\%X_{TG}$ and %FAMEs was investigated by varying from 10 to 25 min at 400 °C and 15 MPa with the fixed molar ratio of 12:1. At this conditions, the $\%X_{TG}$ significantly increased with residence time as shown in Figure 5.4. After 18 min, the conversion was almost complete with the value of 99%. However, the of FAMEs yield was observed with the highest values only of 90% at a residence time of 18 min. The ester content sharply increased with residence time from 10 to 18 min, whereas it rapidly decreased with a longering residence time. This observation implied that the thermal decomposition of esters in the supercritical condition at 400 °C at prolong residence times. As shown in Figure 5.5, the biofuel samples changed to a deep brown color after 20 min. This behavior was supported by various previously reported [39, 46, 55], they proposed that the decomposition of ester occurred at long reaction times and high temperature, especially above 350 °C. In addition, the decomposition products are small compounds such as alkanes and alkene hydrocarbons in the range of C7 to C14, which is similar observed in bach reactor (Chapter V). Therefore, a residence time of 18–20 min is recommended for the biofuel production of 400 °C at 15 MPa in order to avoid decomposition of the ester and to achieve a near complete conversion at the same time.

Figure 5.4. Ester and triglyceride contents of biofuel samples from RPO as a function of residence time (reaction conditions: 400 °C at 15 MPa, and 12:1 molar ratio of methanol to oil).

Figure 5.5. Biofuel samples from RPO under SCM conditions at 400 °C, 15 MPa, and a molar ratio of 12:1 at different residence times. The sequence of vials from left to right is residence times of 10, 15, 18, 20, 23, and 25 min, respectively.

Figure 5.6 shows the influent of residence time on the percent change of glycerides levels, namely monoglycerides (MG), diglycerides (DG), and triglycerides (TG). The TG and DG were observed to reduce with residence time while the MG increased in the initial resident time and then tend to decrease. These obtained results are in agreement with the report of Diasakou et al. [19]. The transesterification reaction can be divided into 3 steps in which TG reacts with methanol (MeOH) to produce DG, which further reacts with MeOH to produce MG. In the last step, MG reacts with alcohol to produce FAME and glycerol, as shown in Equation (5.2), (5.3), and (5.4).

$$TG + MeOH = FAME + DG \qquad (5.2)$$

$$DG + MeOH = FAME + MG \qquad (5.3)$$

$$MG + MeOH = FAME + glycerol \qquad (5.4)$$

Therefore, the overall reaction is as follows:

$$TG + 3MeOH = 3FAMEs + glycerol \qquad (5.5)$$

Which regard to the required levels of remaining glycerides in the European Standard for biodiesel (EN 14214), the MG, DG and TG levels were below 0.8, 0.2, and 0.2 mass%, respectively after a residence time of 20 min, as also presented in Figure 5.6.
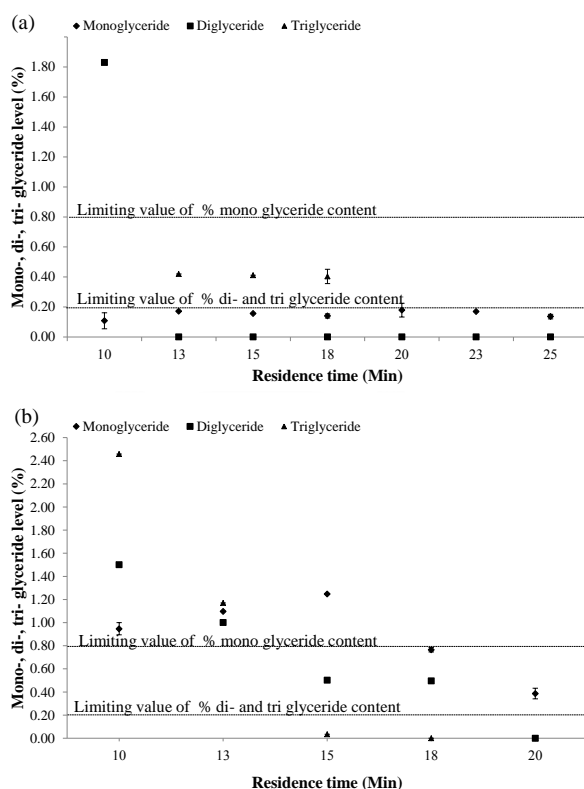
Figure 5.6. Glyceride levels: % monoglycerides (♦), diglycerides (■), and triglycerides (▲) in biofuel samples from (a) RPO and (b) UPO as a function of the residence time (reaction conditions: 400 °C at 15MPa, and 12:1 methanol to oil molar ratio).

5.4. Effects of type of oil

The comparative study of RPO and UPO was investigated in this section. UPO has been recommended as an alternative feedstock and has abundant availability to meet future demand for biodiesel production. In Asian countries, such as China, Malaysia, Indonesia, Thailand and India, used cooking oil was generated more than 40,000 tons per year [120]. The physical and chemical properties of the RPO and UPO used in this work are presented in Table 5.3. Compared to RPO, the level of FFA of UPO is higher than that around five times due to the hydrolysis reaction during the cooking process [102]. Moreover, unsaturated fatty acid levels (C18:1, C18:2 and C18:3) in UPO were observed higher than in RPO. It is possible owing to the contamination during the cooking process (e.g., by chicken fat, which includes with 36.6% of C18:2 and 27.0% of C18:3 [7]).

Table 5.3 The physical and chemical properties of RPO and UPO.

Oil type	Fatty acid composition (wt. %)							FFA content (wt. %)	Water content (wt. %)
	C12:0	C14:0	C16:0	C18:0	C18:1	C18:2	C18:3		
RPO	0.45	1.10	46.14	4.43	37.12	11.10	0.21	<0.01	<0.01
UPO	5.06	3.90	31.28	3.91	39.50	11.51	0.34	4.56	0.18

The triglyceride conversion and ester content in biofuel productions of RPO and UPO were compared in Figure 5.7. The %FAME contents of RPO and UPO samples increase with residence time and reached a maximum value of 90 % at a residence time of 18 min and 80% at 20 min, respectively. It clearly noticed that the reaction rate of RPO was slightly higher than that of UPO due to the lower levels of unsaturated fatty acids. It has been reported that reaction rate was dictated by the level of unsaturated fatty acids (C18:1 < C18:2 < C18:3) [68]. However, the level of esters in RPO samples was higher than that of UPO, which was probably due to the higher triglyceride content

in RPO compared with UPO (Table 5.3). Besides, the remains of glyceride compositions in the UPO sample were also observed under the standard after a residence time of 20 min, as illustrated in Figure 5.6 (b).
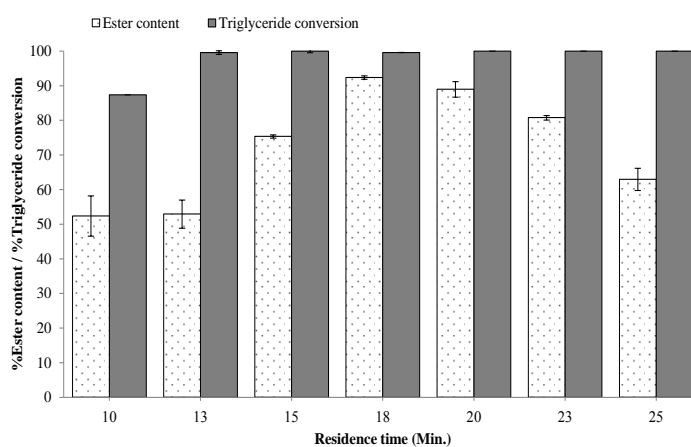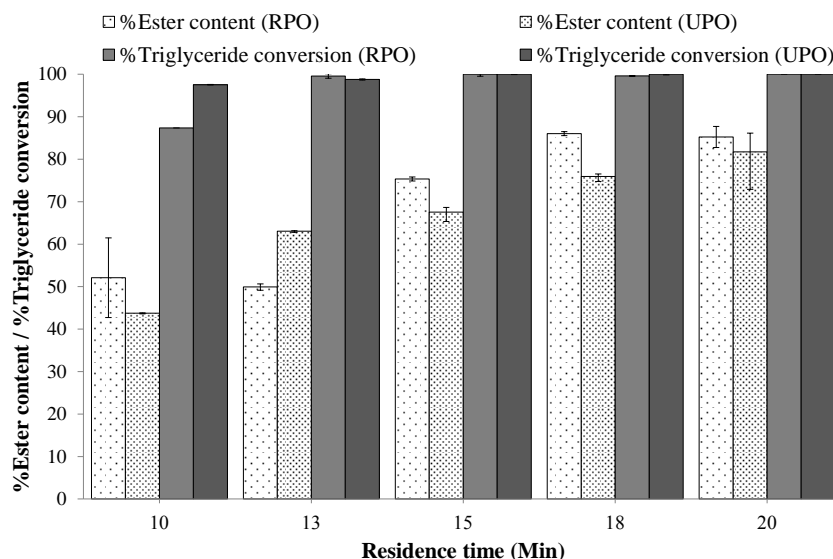

Figure 5.7. $\%X_{TG}$ and %ester content of biofuel samples from RPO and UPO as a function of residence time (reaction conditions: 400 °C at 15MPa, and 12:1 methanol to oil molar ratio).
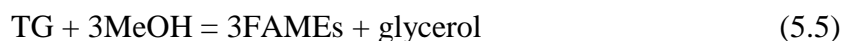
The mass balance was also evaluated based on the basic transesterification reactions involved in the process in order to compare the biofuel product from RPO and UPO. According to Table 5.3, the triglyceride content of RPO was assumed as 100 wt. %, thus, 100 kg of RPO feedstock will react as in Equation (5.6). Note that the average molecular weight of TG is 858 which was calculated based on the fatty acid composition of palm oil.

100.00 kg TG + 11.20 kg MeOH = 99.64 kg FAMEs +11.56 kg (glycerol) (5.6)
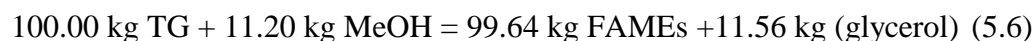
In the basis of 100 kg UPO feedstock, the triglyceride content is 95.44 kg and the FFA content is 4.56 kg. Therefore, the transesterification of TG and esterification reactions of FFA with methanol will also take place in the same time, as follows:

95.44 kg TG + 10.69 kg MeOH = 95.10 kg FAMEs + 11.03 kg (glycerol) (5.7)

4.56 kg FFA + 0.54 kg MeOH = 4.80 kg FAME + 0.30 kg H_2O (5.8)

Considering Equation (5.7) and Equation (5.8), the overall mass balance of UPO is given as

95.44 kg TG + 4.56 kg FFA + 11.23 kg MeOH = 99.90 kg FAMEs

$$+ 11.33 \text{ kg } (H_2O + \text{glycerol}) \qquad (5.9)$$

Table 5.4 summarized the experimental mass balances of biofuel samples from both RPO and UPO. Compared to the theoretical values from Equation (5.6) and Equation (5.9), the fuel yield was increased by approximately 7.84% and 2.61% for RPO and UPO, respectively. Because the higher triglyceride content of RPO compared with UPO, the increase in fuel yield from RPO was higher than that obtained from UPO. Moreover, the glycerol phase was observed to less than the theoretical value in both RPO and UPO feedstocks due to the etherification of glycerol and methanol at 400 °C, as described in Chapter IV.

Table 5.4 Simplified mass balance of biofuel production from RPO and UPO with SCM at 400 °C, 12:1 methanol to oil molar ratio, and 15 MPa.

Oil type	Feed (kg)		Outlet (kg)			
	Oil	Methanol	Fuel phase	Methanol Phase	Glycerol +water phase	Gas phase
RPO	100	44.80	107.28	24.63	3.64	9.25
UPO	100	44.92	102.51	27.81	3.52	11.08

According to thermal cracking of unsaturated fatty acids at 400 °C, the gas products were observed approximately 9.25% and 11.08% for RPO and UPO, respectively, which were calculated by weight loss method. These gaseous products compose with methane, ethane, and carbon dioxide, as reported in our previously study [9].

CHAPTER VI
CONTINUOUS BIOFUEL PRODUCTION IN SUPERCRITICAL ETHANOL
WITH WATER MIXTURE

As observed in batch reactor study, the SCE process has been successful synthesized the biofuel at low molar ratio with the prospect of produce an entirely renewable fuel. However, the cost of absolute ethanol (>99.8 wt. %) is still higher than methanol. Thus, hydrated ethanol (ethanol with water mixture) was applied as reacting alcohol in order to reduce the production cost. Hydrated ethanol is cheaper in the regional context than absolute ethanol. In this chapter, the refined palm oil (RPO) was selected as feedstock for the biofuel production with this SCE. The ethanol with water mixture was varied between 99.8% and 85%. The influences of molar ratio on $\%X_{TG}$ and %FAEEs were investigated from 9:1 to 15:1 to minimize the use of ethanol to oil molar ratio.

6.1. Effects of ethanol to oil molar ratio and residence time

In this section, the effect of ethanol to oil molar ratio on $\%X_{TG}$ and %FAEEs were investigated in the SCE by using hydrated ethanol (96 wt. %). The molar ratios were examined by varying from 9:1 to 15:1. Figure 6.1 presents the triglyceride and ester content changing with the various molar ratios and the residence time between 25 min and 70 min. At the residence time from 25 to 30 min, it can be clearly found that %FAEEs increase with the ethanol to oil molar ratios from 9:1 to 12:1 and relatively constant at 15:1. Similar to the SCM process, the critical point of mixtures was reduced when ethanol was increased into the reaction mixture. As observed in the pressure-temperature diagram of the ethanol and palm olein oil system (Figure 6.2), the phase transition region decreases with the increasing of ethanol to oil molar ratio. According to the constant of both values at 15:1; therefore, the 12:1 was chosen as the optimal molar ratio to elude the surplus of alcohol usage.

The influence of residence time on %X_{TG} and %FAEEs were evaluated and also shown in Figure 6.1. Note that the residence time of all ethanol to oil molar ratio were determined using Equation (5.1). The %X_{TG} was observed to increase with residence time and the conversion was almost complete with the value of 99% after 60 min for all ethanol to oil molar ratio. The ester content also sharply increased with the residence time; however, it rapidly decreased with a longer residence time after 40 min, especially in 12:1 to 15:1 molar ratios. Similar with the SCM process, the reduction of ester content is a result of the thermal decomposition at 400 °C coupling with prolonging residence times. Vieitez et al reported that the reaction temperature above 300 °C and lower flow rate (long residence time) had a strong effect on the decomposition of the final ethyl ester, especially for C18:2 and C18:3 [55].
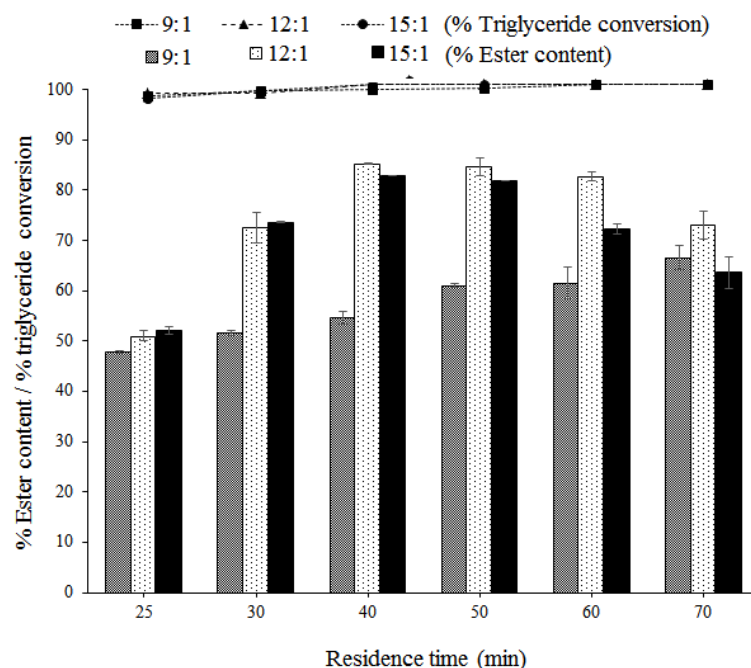
Figure 6.1 Ester and triglyceride contents of biofuel samples from RPO as a function of ethanol to oil molar ratio (reaction conditions: 400 °C at 15 MPa). Data are shown as means ± 1 SD, derived from 3 independent repeat measurements.
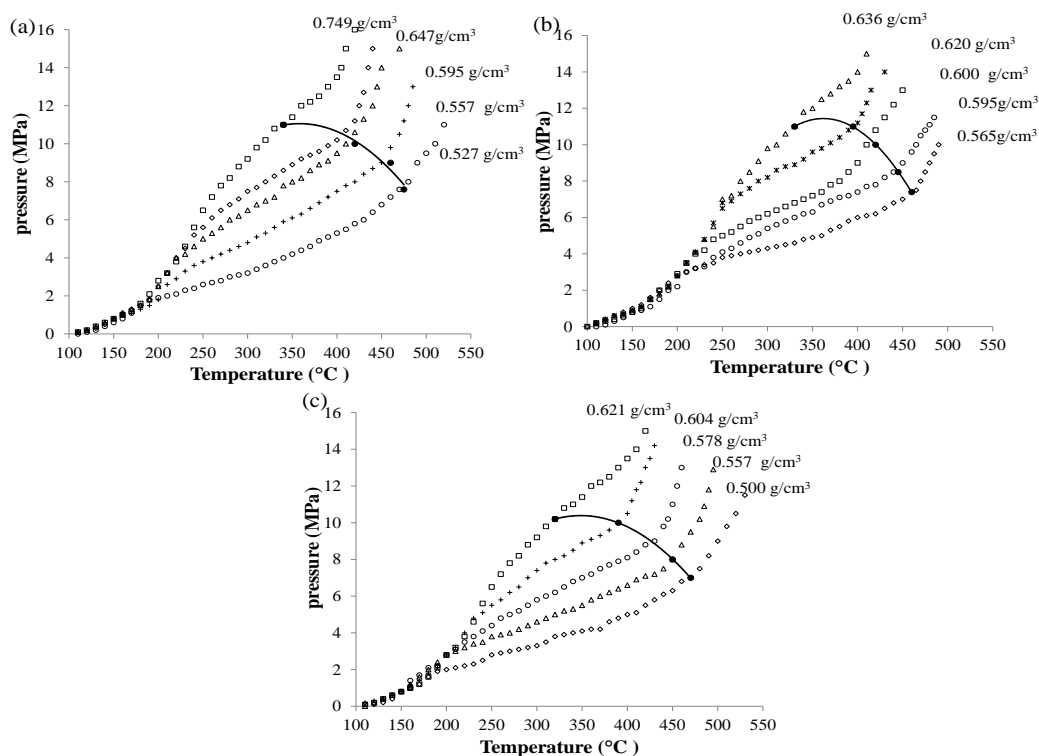
Figure 6.2. Pressure vs. temperature for the ethanol (96 wt.%) and palm olein oil system with a molar ratio of (a) 9:1, (b)12:1 and (c) 15:1 and (symbol ●) the phase transition point.

6.2. Effects of ethanol with water mixture

The influence of ethanol with water mixture on ester content (%FAEEs) was investigated by varying from 85 wt. % to 99.8 wt. % at 400 °C and 15 MPa with the fixed molar ratio of 12:1. Figure 6.3 displays the influence of ethanol with water mixture on the ester yield. For all of ethanol content, the highest ester yield was observed of approximately 85% within the residence time range investigated. Thus, it can be presumed that the presence of water in the reaction systems did not significant on the yield of FAEEs. With water in the system, the hydrolysis of triglyceride (TG) occurred, and then free fatty acid (FFA) and glycerol are produced. The esterification subsequently progress to form FAEE and water, as reported in the SCM with rapeseed

oil [2] and palm oil [104]. The hydrolysis and esterification reaction in the SCE are shown in Equation (6.1) and (6.2), respectively.

$$TG + H_2O = FFA + glycerol \qquad (6.1)$$

$$FFA + EtOH = FAEE + H_2O \qquad (6.2)$$

The maximum FAEEs yield was found at residence time of 50 min for 85, 90, and 96 wt.% of hydrated ethanol, while the maximum ester content was observed at residence tim of 60 min for absolute ethanol (99.8 wt.%). The observation has been demonstrated in SCE with water mixture of soybean [51, 55] and sunflower oil [53]. These results are in agreement with the hypothesis that the occurrence of water could enhance the formation of esters due to the faster esterification of FFA than the transesterification of TG [2]. In addition, the FFA can be played as the acid catalyst in a hydrolysis reaction to promote the faster reaction [83]. Beside, Velez et al. [53] also reported that the kinetic rate of transesterification with hydrated ethanol (96 wt. % ethanol, and 4% water) is higher than that with the pure ethanol at the supercritical condition of 320 °C.
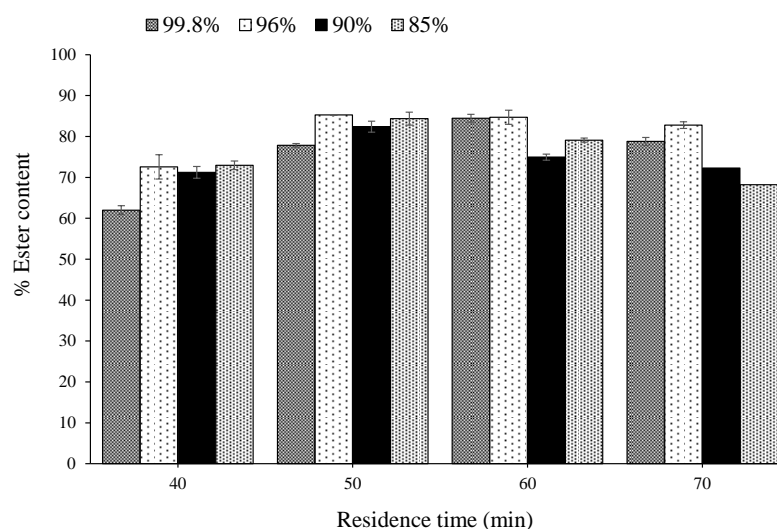
Figure 6.3. Ester contents of biofuel samples from RPO as a function of residence time (reaction conditions: 400 °C at 15 MPa, and 12:1 molar ratio of methanol to oil).

Figure 6.4 shows the change of mono-, di-, and triglycerides with residence time for different water content in ethanol. For all hydrated ethanol, the glycerides content tend to decrease with residence time and they are under the required levels of biodiesel standard after 60 min of residence time. Therefore, the residence time of 60 min is recommended for the biofuel production in the SCE with hydrated ethanol at 400°C and 15 MPa.
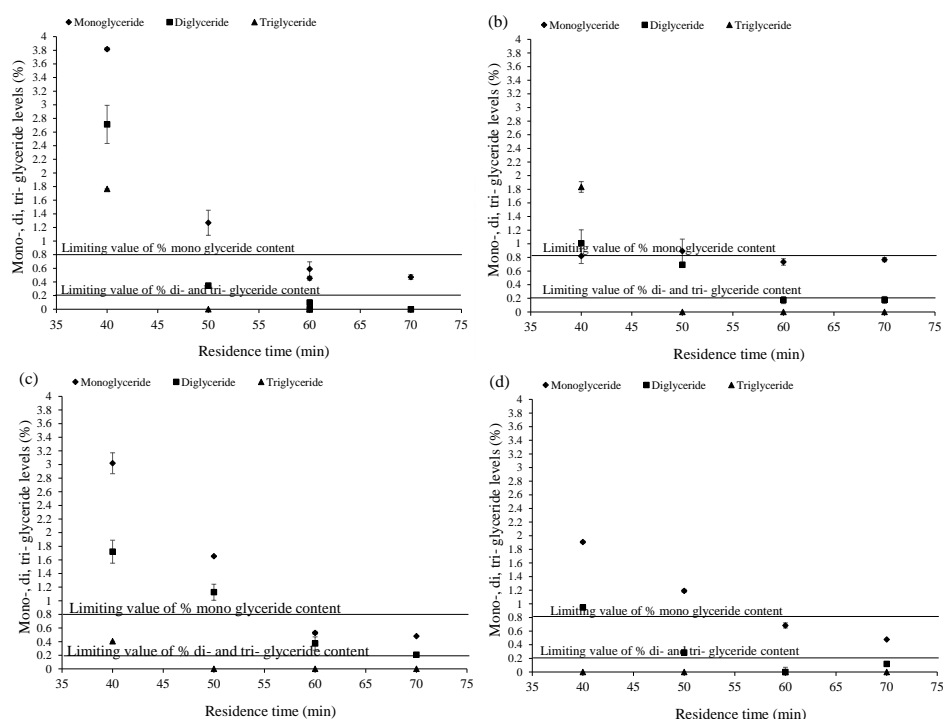
Figure 6.4. Glyceride levels: % monoglycerides (♦), diglycerides (■), and triglycerides (▲) in biofuel samples in SCE with water mixture of (a) 0.2 %, (b) 4%, (c) 10% , and (d) 15% as a function of the residence time (reaction conditions: 400 °C at 15MPa, and 12:1 ethanol to oil molar ratio).

6.3. Mass balance

According to the present of water in the system, three types of reaction took place; (i) transesterification, (ii) hydrolysis of triglycerides (TG) and (iii) ethyl esterification of free fatty acid (FFA) proceeded simultaneously under the supercritical condition. As previously mention, the TG was first hydrolyzed by water to form FFA

and subsequently esterified to FAEE. Finally, the transesterification of remaining TG will occur. At the selection molar ratio of 12:1; thus, 100 kg of RPO feed with 96 wt. % ethanol displays as follow:

$$40.90 \text{ kg TG} + 2.60 \text{ kg H}_2\text{O (4 wt. \%)} = 39.10 \text{ kg FFA} + 4.40 \text{ kg glycerol} \qquad (6.3)$$

$$39.10 \text{ kg FFA} + 6.93 \text{ kg EtOH (96 wt. \%)} = 41.06 \text{ kg FAEE} + 4.97 \text{ kg H}_2\text{O} \qquad (6.4)$$

$$59.10 \text{ kg TG} + 10.01 \text{ kg EtOH (96 wt. \%)} = 59.34 \text{ kg FAEEs} + 9.77 \text{ kg glycerol} \quad (6.5)$$

Considering Equation (6.3), (6.4) and (6.5), hence, the overall mass balance of RPO is given as:

$$100.00 \text{ kg TG} + 16.94 \text{ kg EtOH (96 wt. \%)} + 2.60 \text{ kg H}_2\text{O (4 wt. \%)}$$

$$= 100.40 \text{ kg FAEEs} + 19.83 \text{ kg (glycerol} + \text{H}_2\text{O)} \qquad (6.6)$$

In addition, the overall mass balance of RPO with 99.8 wt. % of ethanol is shows in Equation (6.7).

$$100.00 \text{ kg TG} + 16.30 \text{ kg EtOH (99.8 wt. \%)} + 0.13 \text{ kg H}_2\text{O (0.2 wt. \%)}$$

$$= 100.85 \text{ kg FAEEs} + 15.58 \text{ kg (glycerol} + \text{H}_2\text{O)} \qquad (6.7)$$

With regard to the ethanol with water mixture of 90 wt. % and 85 wt. %, the inputs of water are 8.85 kg and 9.87 kg, respectively. Assuming that the transesterification does not occur for these both ethanol due to the 6.36 kg is the minimum value of water for the complete conversion of TG to form FFA. Therefore, overall mass balance of the ethanol with water mixture of 90 wt. % and 85 wt. %, are shown in Equation (6.6) and (6.7), respectively.

$$100.00 \text{ kg TG} + 18.06 \text{ kg EtOH (90 wt. \%)} + 6.36 \text{ kg H}_2\text{O (10 wt. \%)}$$

$$= 100.40 \text{ kg FAEEs} + 24.02 \text{ kg (glycerol} + \text{H}_2\text{O)} \qquad (6.8)$$

$$100.00 \text{ kg TG} + 19.13 \text{ kg EtOH (85 wt. \%)} + 6.36 \text{ kg H}_2\text{O (10 wt. \%)}$$

$$= 100.40 \text{ kg FAEEs} + 25.09 \text{ kg (glycerol} + \text{H}_2\text{O)} \qquad (6.9)$$

The experimental mass balance of biofuel samples from SCM and SCE are summarized in Table 6.1. It can be seen that the fuel yield, basis on weight of RPO

input, increases about 8.45 wt. %, 11.49 wt. %, 18.37 wt. %, and 6.08 wt. % for ethanol with water mixture of 99.8 wt. %, 96 wt. %, 90 wt. % and 85 wt. %, respectively. In addition, fuel yield was indicated by the mass of the fuel phase divided by the mass of RPO. The glycerol and water phase was observed to less than the theoretical value for all ethanol with water mixture. Similar to SCM, the reduction of glycerol is a result from the etherification of glycerol and ethanol at 400 °C, as described in Chapter IV. Moreover, it has been reported that water can also react with glycerol in SCM at 280 °C to generate the volatile produce, possibly carbon dioxide [121].

Table 6.1 Simplified mass balance of biofuel production from RPO with SCE at 400 °C, 12:1 ethanol to oil molar ratio, and 15 MPa as observed in the experiment

Process	Feed (kg)		Outlet (kg)			
	RPO	Ethanol	Fuel phase	Ethanol	Glycerol + water phase	Gas phase
99.8 wt. % Ethanol	100.00	65.04	108.45	31.51	4.40	24.16
96 wt. % Ethanol	100.00	65.04	111.49	23.20	0.50	29.37
90 wt. % Ethanol	100.00	65.04	118.37	21.83	0.34	24.03
85 wt. % Ethanol	100.00	65.04	106.08	21.05	0.82	36.61

6.4. Fuel properties

In this section, the fuel properties of biofuel samples from both continuous SCM and SCE processes were analyzed, which were obtained from the optimal conditions of 400 °C, 15 MPa, and alcohol to oil molar ratio of 12:1. For the SCM, the biofuel samples derived from RPO and UPO at the optimal residence time of 20 and 18 min, respectively, while 50 min is the residence time to obtaining the biofuel samples in SCE with ethanol content of 85 wt.%, 90 wt.%, and 96 wt.% and 60 min for 99.8 wt. %. The

fuel properties were conducted according to American Standard of Testing Materials (ASTM) testing methods: D1298, D445, D93, D240 and D2887, including the density, kinematic viscosity, flash point, heating value and distillation characteristic, respectively. The analytical results of fuel properties are illustrated in Table 6.2. It can be seen that the properties are almost under the biodiesel specification. However, the ester content and viscosity properties are slightly outside these specifications.

According to EN 14214 for the European country, the ester content was required above 96.5 wt. % to employ as the pure biodiesel (B100) for the diesel engine. However, this property is not specific in some countries such as India and Brazil, which was followed the biodiesel standard of ASTM D6751. For all biofuel samples, the % ester content is approximately 85-90 wt. %, which are slightly lower than the EN 14214 standard. As previously mention, the approximately 10-15 wt. % is the product of etherification from glycerol with SCA and small hydrocarbon from the thermal decomposition, which can miscible in the fuel phase.

Compared to the vegetable oil, the lower kinematic viscosity is the main reason to used biofuel as an alternative fuel for transport engine. Since the viscosity is directly associated to the efficiency of a biofuel [122]. The high viscosity lead to generating the problems such as engine deposits, a larger mean liquid droplet diameter and a longer ignition delay [123]. The kinematic viscosity of all biofuel samples was observed slightly higher than the specification of biodiesel. This is probably due to the cis–trans isomerization of unsaturated FAMEs and FAEEs at 400 °C, which resulting in the increase of biofuel viscosity. It has been reported that the polymerization at a high temperature (> 300 °C) and a long reaction time is the main parameter to increase the viscosity of soybean biodiesel [124].

Table 6.2 Properties of biofuel sample and biodiesel standards.

Properties	Biofuel samples						Biodiesel Specification	
	MR	MU	E99.8	E96	E90	E85	EN 14214	ASTM D6751
Ester content (wt. %)	90	80	84	85	82	84	min 96.5	-
Density at 15 °C (kg/m³)	872	875	879	872	874	879	860-900	-
Kinematics viscosity at 40 °C (mm²/s)	6.0	6.8	7.2	6.8	7.4	7.9	3.5-5.0	1.9-6.0
Flash point (°C)	114	105	142	140	139	134	min 101	min 93
Heating value (MJ/kg)	39.6	40.5	39.1	39.1	39.2	40.8	-	-
Monoglyceride (%wt)	0.38	0.16	0.58	0.73	0.47	0.48	max 0.8	-
Diglyceride (%wt)	0.02	0.08	0.09	0.17	0.20	0.20	max 0.2	-
Triglyceride (%wt)	0.001	0.001	0.001	0.001	0.001	0.001	max 0.2	-
Distillation characteristics (°C)	90%, 335°C	90%, 356°C	N/A	N/A	N/A	N/A	-	90%, 360°C

CHAPTER VII

PHASE BEHAVIOR OF PALM OIL TRANSESTERIFICATION WITH SCM

To design optimal operating conditions, the knowledge of phase equilibria is necessary to control the possible phases coexisting in the reactor. In the previous studies, the phase equilibrium among compounds involved in the transesterification reaction, i.e. methanol, triglyceride, fatty acid esters and glycerol, have been investigated for the biodiesel production with SCA process. For example, the vapor-liquid equilibrium of methanol–triolein has been measured for the biodiesel synthesis under SCM by Glišić et.al. [73]. Fang et al. have reported the binary phase equilibrium data for supercritical methanol–C18 methyl esters [75]. Sawangkeaw et al. employed the vapor-liquid equilibrium data from the literature to find the best thermodynamic model for SCM transesterification in continuous tubular reactor [125]. However, the phase equilibria of methanol–tripalmitin system, which is suitable for applied with the biofuel production of palm oil in SCM, is not available. Therefore, the phase behavior for methanol–palm oil system was measured in the high-pressure view cell, as described in Chapter III. The effects of temperature and pressure on the solubility of methanol in palm oil were varied in a range from 363 to 393 K and pressure ranging from 1 to 4 MPa. The obtained experimental data were also compared and modeled with the same approach as done in our previous work concerning triolein [125]. Finally, the selected thermodynamic model was then applied to determine operating conditions favorable to the homogeneous phase transesterification of palm oil in SCM, model was confirmed by the experimental data obtained from isochoric method (Chapter V). For that purpose, the three binary sub-systems, i.e. methanol–tripalmitin, methanol–methyl palmitate and methanol–glycerol were considered in order to predict the phase envelope of the reacting mixture. The work diagram for phase behavior of palm oil transesterification with SCM is presents in Figure 7.1.
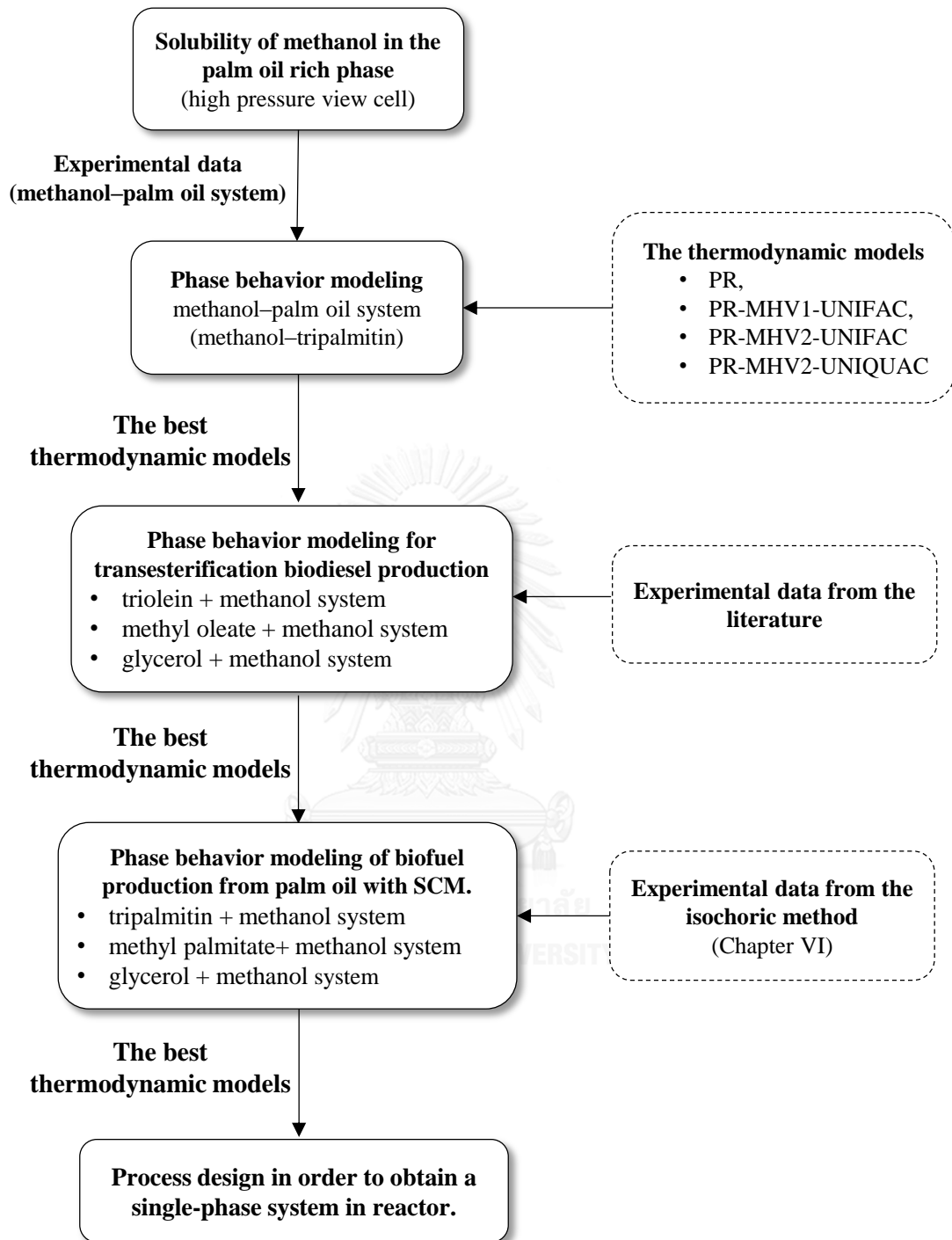
Figure 7.1. The work diagram for phase behavior of palm oil transesterification with SCM

7.1. Solubility of methanol in the palm oil rich phase

      The experimental concentration of methanol in the palm oil rich phase in the operation condition range of 363–393 K and the pressure range of 1–4 MPa, which obtained from FT-IR experiments, were illustrated in Table 7.1. As observed in this table, the solubility of methanol in palm oil rich phase increases with temperature. In other words, the miscibility of both compounds is enhanced at rising temperature. These data are in agreement well with the experimental results of methanol–sunflower oil and methanol–triolein systems as reported by Glišić et al. [73] and Tang et al. [71], respectively. In addition, the mole fraction of methanol in palm oil rich phase (x_i) deduced from the experimental data is also presented in Table 7.1.

Table 7.1 Experimental data of methanol solubility in palm oil rich phase.

Temperature (K)	Pressure (MPa)	C_{MeOH} (mol/L)	x_{MeOH}
363	1	0.6859	0.4026
383	1	0.7313	0.4215
383	1	0.6893	0.4071
383	1	0.7969	0.3902
393	1	0.7229	0.4429
393	1	0.6422	0.4190
363	2	0.6052	0.3729
383	2	0.6607	0.3970
393	2	0.6540	0.3948
393	2	0.7213	0.4184
393	2	0.7465	0.4226
363	4	0.5649	0.3569
383	4	0.7106	0.4145
383	4	0.7347	0.4226
393	4	0.6389	0.3892
393	4	0.8070	0.4647

7.2. Phase behavior modeling for methanol–palm oil system

In this study, the Peng–Robinson equation of state (PR EoS) was applied to modeling the phase equilibrium [126]. According to in our previous study [125], the PR EoS with the mixing rules of Modified Huron-Vidal 2 (MHV2) has proved to properly describe experimental fluid phase equilibria of the quaternary mixture (oil-alcohol-ester-glycerol) at high pressure. This approach, namely EoS/G^E mixing rules, allows the cubic equation of state, suitable for high pressure but poor for mixtures containing polar compounds, to be applied for high pressure calculations of mixture involving polar compounds. As the MHV2 mixing rules are based on the calculation of the excess Gibbs energy at zero pressure, an activity coefficient model is needed, in addition to the equation of state. In this study, the UNIQUAC activity coefficient model has been compared to predict group contribution model UNIFAC. The well-known Peng-Robinson equation of state is given by:

$$P = \frac{RT}{v-b} - \frac{a(T)}{v^2 + 2bv - b^2},$$

(7.1)

where P is pressure, R is the universal gas constant, T is temperature, a and b are the substance-specific constants and v is molar volume. The expression of equation of state parameters, attractive term, a (T), and co-volume, b, are depending on the chosen mixing rules. In the general case of MHV mixing rules, the attractive term is obtained by solving:

$$q_1 \left(\alpha - \sum_i z_i \alpha_i \right) + q_2 \left(\alpha^2 - \sum_i z_i \alpha_i^2 \right) = \frac{g_0^E}{RT} + \sum_i z_i \ln(\frac{b}{b_i})$$

(7.2)

$$\alpha = \frac{a}{bRT}$$

With:

(7.3)

$$\alpha_i = \frac{a_i}{b_i RT}$$

(7.4)

$$b = \sum_{i=1}^{n} z_i b_i \tag{7.5}$$

$$a_i = 0.45724 \frac{R^2 T_{c,i}^2}{P_{c,i}} [1 + (0.37464 + 1.5422 \omega_i - 0.266992 \omega_i^2)(1 - \sqrt{T_r})]^2 \tag{7.6}$$

$$b_i = 0.0777960739 \; \frac{R T_{c,i}}{P_{c,i}} \tag{7.7}$$

where ω is the acentric factor of the species, and z is compressibility factor. In the case of PR EOS, q_1=-0.4347 and q_2=-0.003654 for MHV2 (implicit calculation of α). Then an activity coefficient model has to be chosen to determine the value of the excess Gibbs energy at zero pressure (reference pressure) g_0^E. At their initial development, authors of MHV mixing rules coupled the SRK or PR equation of state with the UNIFAC predictive activity coefficient model, leading to a predictive way to use cubic equations of state. In the present study, MHV mixing rules have been used with the original UNIFAC and modified UNIFAC (Dortmund) 1993 model and with UNIQUAC activity coefficient model. When UNIQUAC model is used in the mixing rule, two binary interaction coefficients (A_{ij} and A_{ji}) have to be fitted on experimental data.

According to the composition of palm oil, tripalmitin (46.14 wt. %) was selected as a pseudo component to represent this oil to simplify the modeling of the methanol–palm oil binary systems. The group-contribution method [127] was applied to estimate the critical properties of tripalmitin, including methyl palmitate, methanol and glycerol, as shown in Table 7.2.

Table 7.2 Characteristic parameters of pure compounds used in PR-EoS. In that table, precise data are taken from databank (DiPPr if taken from Simulis) and other estimated from a group contribution method (and precise the corresponding method, such as Lydersen or Joback.)

Compound	T_c (K)	P_c (MPa)	V_c (cm^3/mol)	ω
Tripalmitin	965.00	0.250	2947.9	0.14
Triolein	943.23	3.22	3251.0	0.13
Methyl palmitate	717.63	1.255	1007.1	0.21
Methyl oleate	738.21	10.89	1108.1	0.2
Methanol	512.60	8.009	118.0	0.57
Glycerol	850.00	7.500	264.0	0.56

In this chapter, the thermodynamic models of PR, PR-MHV1-UNIFAC, PR-MHV2-UNIFAC and PR-MHV2-UNIQUAC were employed to correlate the experimental data. In case of the UNIQUAC model, the molecular volume (r_i) and molecular surface area parameters (q_i) of each compound is required. The group contribution method of Bondi [128] was used to estimating these compounds:

$$r_i = \sum_{k=1} v_k^{(i)} R_k \qquad (7.8)$$

$$q_i = \sum_{k=1} v_k^{(i)} Q_k \qquad (7.9)$$

where; $v_k^{(i)}$ is the number of group k in molecule i, R_k and Q_k are the UNIFAC subgroup parameters as given in Table 7.3. For all components used in this study, the values of r_i and q_i are given in Table 7.4.

Table 7.3 UNIFAC group volume and surface area parameters for this work [129]

Main group	Sub group	R_k	Q_k
CH_2	CH_3	0.9011	0.8480
	CH_2	0.6744	0.5400
	CH	0.4469	0.2280
C=C	CH=CH	1.1167	0.8670
COOC	CH_2COO	1.6764	1.4200
OH	OH	1.0000	1.2000
CH_3OH	CH_3OH	1.4311	1.4320

Table 7.4 Parameters r_i and q_i for the studied systems

Compound	UNIFAC group assignment	r_i	q_i
Tripalmitin	1[CH] 3 [CH$_3$] 41 [CH$_2$] 3 [CH$_2$COO]	35.829	29.172
Triolein	1[CH] 3 [CH$_3$] 41 [CH$_2$] 3 [CH$_2$COO] 3 [CH=CH]	39.179	31.773
Methyl palmitate	2 [CH$_3$] 13 [CH$_2$] 1 [CH2COO]	13.146	10.984
Methyl oleate	2 [CH$_3$] 13 [CH$_2$] 1 [CH$_2$COO] 1 [CH=CH]	14.263	11.851
Methanol	1 [CH$_3$OH]	1.431	1.432
Glycerol	1[CH] 2 [CH$_2$] 3 [OH]	4.795	4.908

The fitting of the thermodynamic model and experimental data have been done by minimizing of objective function with a Simulis® Thermodynamics MS- Excel add-in. The predicted phase equilibrium data for methanol-tripalmitin binary system of all thermodynamic models is illustrated in Table 7.5.The predicted values were then compared with the experimental data, as shown in Figure 7.2.

Table 7.5 Predicted phase equilibrium data for methanol-tripalmitin binary system and average absolute relative error

| T (K)	P (MPa)	Predicted values			
		PR	PR-MHV1-UNIFAC	PR-MHV2-UNIFAC	PR-MHV2-UNIQUAC
363	1	0.248	0.155	0.199	0.332
373	1	0.293	0.172	0.211	0.366
383	1	0.342	0.190	0.222	0.400
393	1	0.395	0.211	0.232	0.434
403	1	0.452	0.234	0.241	0.469
363	1	0.243	0.150	0.202	0.337
373	2	0.286	0.167	0.215	0.370
383	2	0.334	0.185	0.227	0.405
393	2	0.385	0.205	0.238	0.439
403	2	0.440	0.227	0.248	0.474
363	2	0.232	0.142	0.210	0.344
373	4	0.274	0.157	0.223	0.378
383	4	0.319	0.174	0.236	0.413
393	4	0.368	0.193	0.248	0.449
403	4	0.419	0.213	0.259	0.484
%AARE		16.26	50.89	44.09	5.58
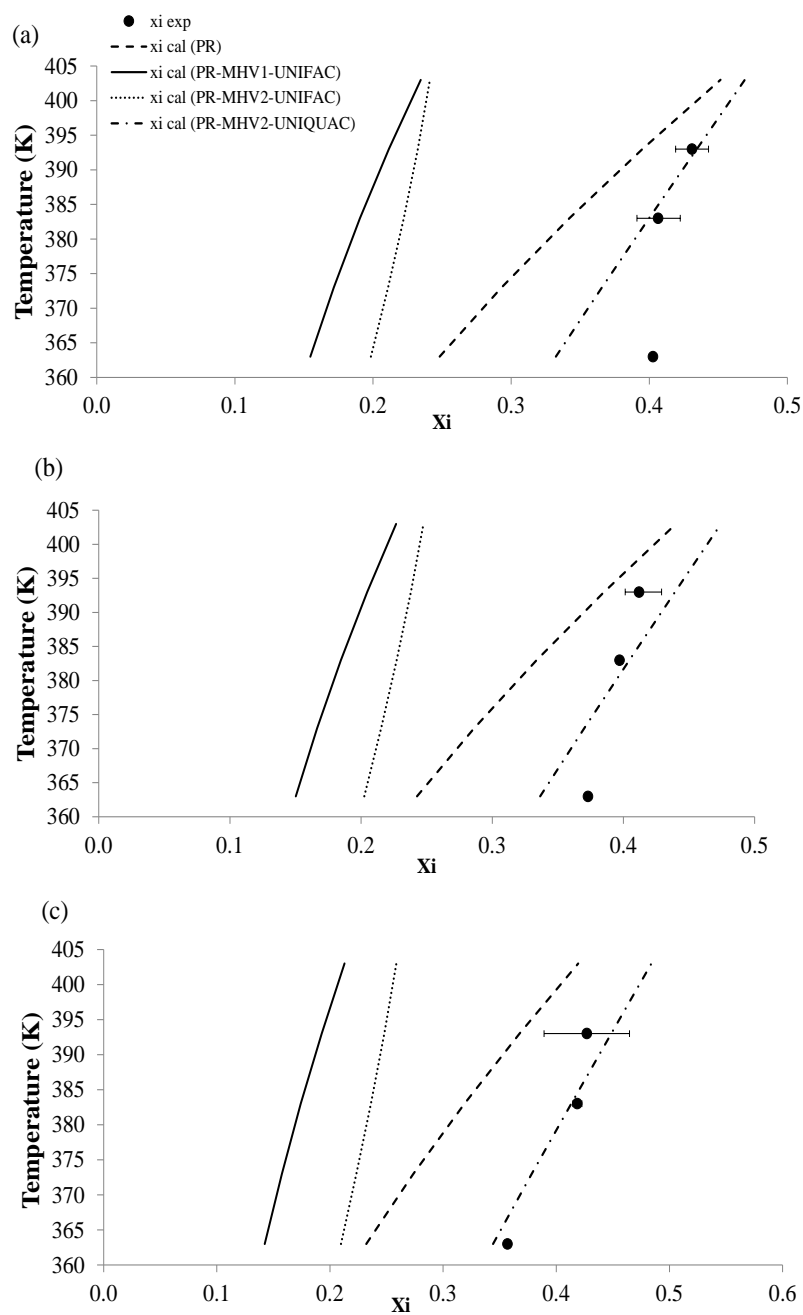
Figure 7.2. Experimental (doted) and calculated (lined) T-x diagram of methanol-tripalmitin system with (a) 1 MPa, (b) 2 MPa, and (c) 4 MPa.

The mean Average Absolute Relative Error (*AARE*) was calculated in order to evaluate the ability of the model to represent experimental data, as together illustrated in Table 7.5.

$$\%AARE = \frac{1}{N_p} \sum_{i=1}^{N_p} \left| \frac{x_i \, exp - x_i cal}{x_i \, exp} \right| \times 100 \,, \tag{7.10}$$

where; x_i is the molar solubility fraction of methanol in the palm oil and N_p is the number of experimental values.

It can be observed that the PR-MHV2-UNIQUAC model gave the best correlation of the experimental data with a minimum AARE of 5.58 % for the methanol–tripalmitin binary system. The binary interaction coefficients as a function of temperature were obtained from the UNIQUAC model and shown in Table 7.6. Considering to the phase envelope prediction, this observation suggests the temperature and pressure greater than the 662.29 K and 11.27 MP, respectively, to ensuring that the reaction is conducted in the homogeneous phase all along the reaction. Therefore, the PR-MHV2-UNIQUAC model can be applied to explore the operating conditions in order to guarantee running the reaction in a single-phase system all along the reactor This thermodynamic modeling agrees well with our previous studied [125], where the PR-MHV2-UNIQUAC model has been successfully used to evaluate phase equilibrium of the methanol–triolein binary, methanol–methyl oleate, and methanol–glycerol system with a relative error of less than 5%, 3%, and 10%, respectively. Note that the experimental data derived from the literature [73, 75, 76]. The experimental data for triolein + methanol, methyl oleate + methanol, and glycerol + methanol, and the results from PR-MHV2-UNIQUAC model are shown in Figure 7.3. Moreover, the UNIQUAC model was also has been reported to fit with the experimental data of soybean oil and methanol, including with three binary systems of oil–methanol, oil–glycerol, and FAMEs–glycerol [130].
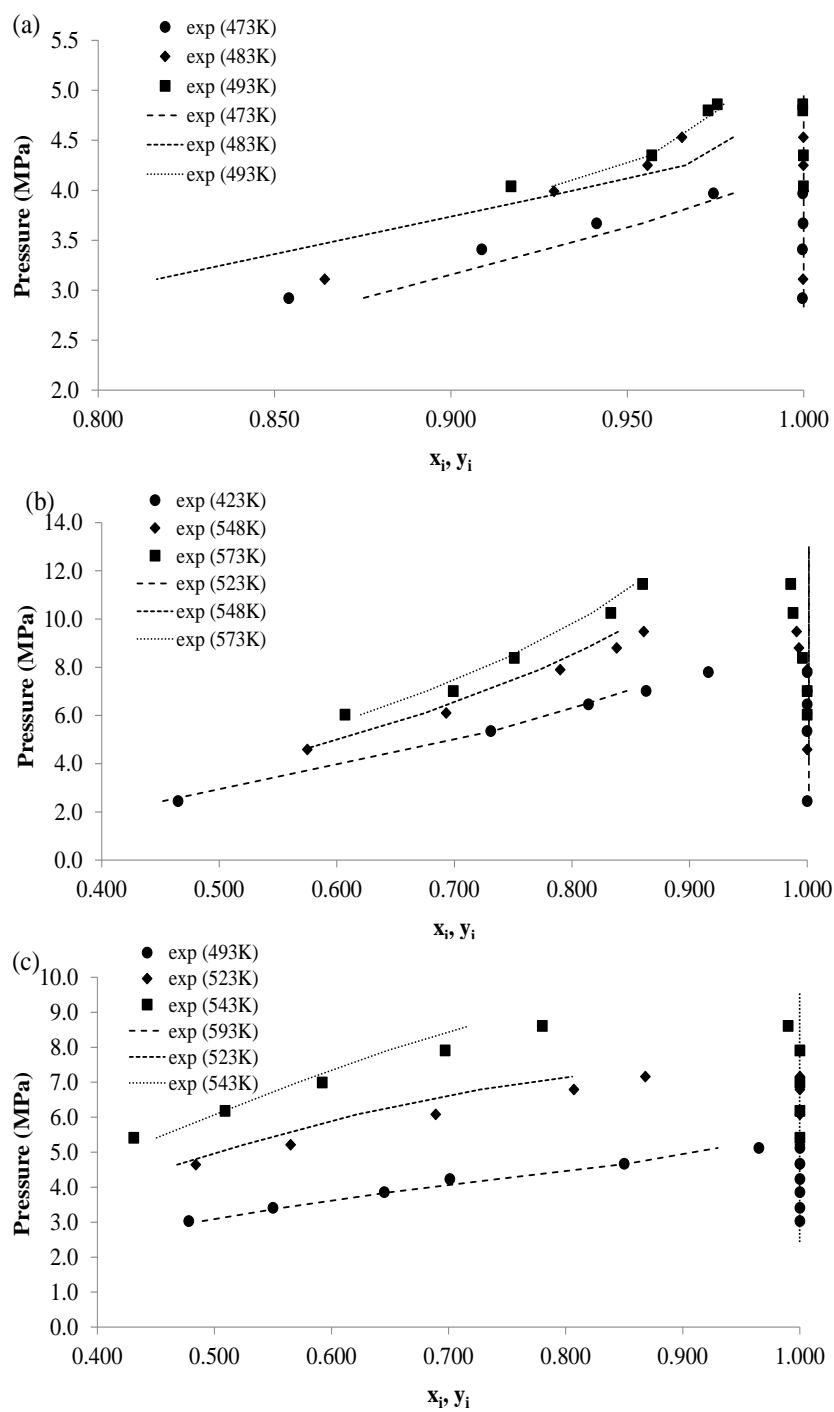
Figure 7.3. Experimental (doted) and calculated (lined) P-x, y diagram of (a) methanol-triolein system, (b) methanol-methyloleate system, and (c) methanol-glycerol system.

7.3. Phase behavior modeling of biofuel production from palm oil with SCM.

In this section, the best fitted of PR-MHV2-UNIQUAC model was applied to model the phase behavior of biofuel production from palm oil with supercritical methanol (SCM). Concerning to the transesterification reaction, the three-phase equilibrium binary systems of methanol–tripalmitin, methanol–methyl palmitate and methanol–glycerol binary were deduced from the correlation with isochoric experimental data. Note that the selected isochoric data is the methanol to oil molar ratio of 12:1.

In case of reactants (methanol and palm oil), the phase equilibrium of the methanol–tripalmitin binary system was considered. The phase envelope for reactants was predated based on the PR-MHV2-UNIQUAC model with the molar composition of 0.92 and 0.08 for methanol to tripalmitin molar ratio of 12:1. The comparative studies of predicted phase envelopes and the experimental isochoric data is show in Figure 7.4. Note that the prediction of P-T line was examined with LLV equilibria functions available in Simulis® Thermodynamics software. It is clearly that this prediction is in good agreement with the experimental trajectory at temperatures below 500 K.

To modeling the mixture of final products, the system is composed with tripalmitin, methanol, methyl palmitate and glycerol, the global mixture composition summarized in Table 7.7. Note that the global molar composition of final product mixture was derived by assuming different palm oil conversion values, varying between 10% and 100%. For example of 100% conversion, the global molar compositions are 0.23, 0.69 and 0.07 for methyl palmitate, methanol, and glycerol, respectively. The product phase envelope was constructed based on the PR-MHV2-UNIQUAC model with the critical properties presented in Table 7.2, as presented in Figure 7.4. The binary interaction coefficients fitted for each binary system were illustrated in Table 7.6. As observed in this table, the binary interaction coefficients values of methanol-methyl palmitate system are nearly close to the methanol-methyl oleate system. This is probably because of the characteristic critical parameters of methyl palmitate that are slightly different from methyl oleate.
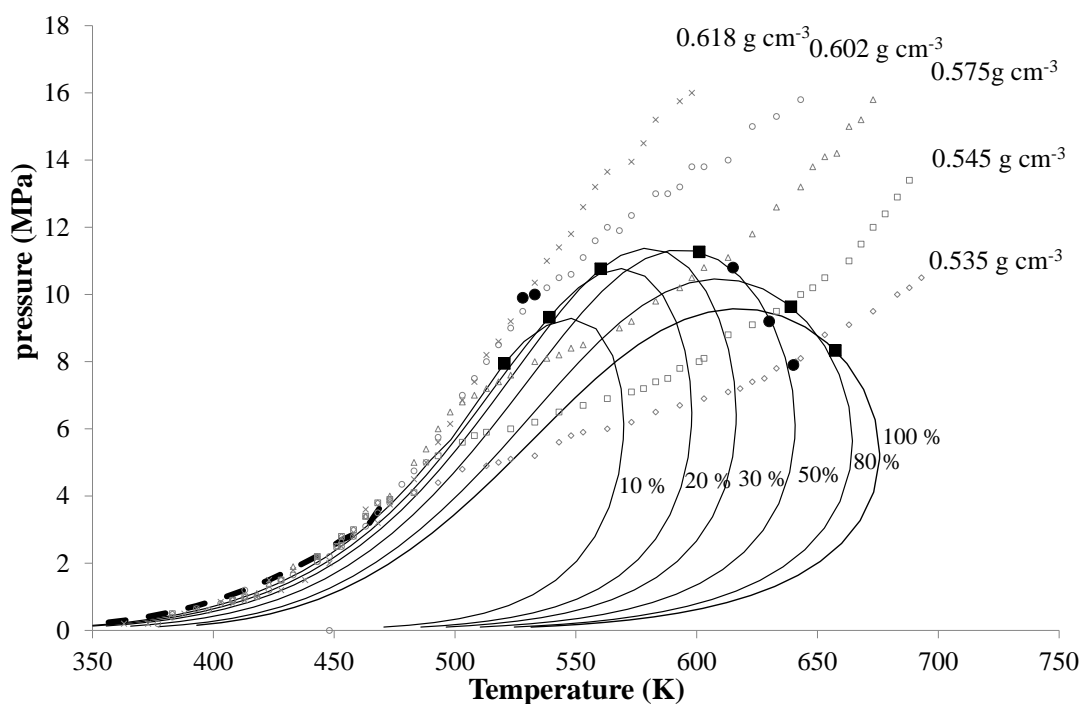
Figure 7.4. Phase behavior of supercritical transesterification for methanol and palm oil. Reactants (dashed line), products (solid line) phase envelopes and critical point (symbols ■) were predicted by the PR-MHV2-UNIQUAC model. The experimental trajectories (empty dots) and transition points (black dots) for the methanol and palm oil system with a molar ratio of 12:1.

As observed in Figure 7.4, the predicted phase envelope of product has the two regions of heterogeneous (enclosed area) and homogeneous phases. It can be observed that all of phase envelope predictions with PR-MHV2-UNIQUAC model is well-matched with the experimental data in the LV region at moderate conditions. Whatever the mixture composition, the system can be considered as homogeneous at temperature above 623 K and pressure above 10 MPa. Moreover, the critical points of mixtures were predicted and displayed in the symbols ■ (Figure 7.4). The results demonstrated that the critical temperature increases from 539.03 K to 662.29 K with the progress of the palm oil conversion; because methanol was consumed by the transesterification reaction (Table 8). As reported in the previous study, the critical point of reaction mixture is increased when decreases methanol content in the reaction mixture[4].

Considering to the phase envelope prediction, this observation suggests the temperature and pressure greater than the 662.29 K and 11.27 MP, respectively, to ensuring that the reaction is conducted in the homogeneous phase all along the reaction. Therefore, the PR-MHV2-UNIQUAC model can be applied to explore the operating conditions in order to guarantee running the reaction in a single-phase system all along the reactor.

Table 7.6 Calculated binary interaction coefficients for the UNIQUAC model.

Binary mixture	A_{12} (K)	A_{21} (K)
Methanol–tripalmitin	0.007+0.05T	1505+0.07T
Methanol–triolein	−8072+16.85T	11559–23.43T
Methanol–methyl palmitate	−5703+12.60T	1694–3.65T
Methanol–methyl oleate	−5713+12.06T	1698–3.60T
Methanol–glycerol	−4801.17+10.48T	1850–4.02T

Table 7.7 Product composition for the phase envelope modeling at the methanol to oil molar ratio of 12:1.

Conversion (%)	Product composition (mole fraction)				Critical point prediction	
	TP	MeOH	FAME	GL	T_C (K)	P_C (MPa)
10	0.07	0.90	0.02	0.01	528	9.9
20	0.06	0.88	0.05	0.02	539	9.3
30	0.05	0.85	0.07	0.02	560	10.7
50	0.04	0.81	0.12	0.04	601	11.3
80	0.02	0.74	0.18	0.06	638	9.5
100	0.00	0.69	0.23	0.08	662	8.1

TP is tripalmitin, MeOH is methanol, FAME is methyl palmitate, and GL is glycerol.

CHAPTER VIII
CONCLUSIONS AND RECOMMENDATION

8.1. Conclusions

8.1.1. Biofuel production with SCA using batch reactor

The optimal operating parameters of biofuel production from UPO in SCM, which were investigated by the response surface methodology, are temperature of 395 °C, methanol to oil molar ratio of 12:1, and reaction time of approximately 9 min. From the modified quadratic regression model, the operating temperature and reaction time were found as the most significant effect on the reaction. The predicted values of $\%X_{TG}$ and $\%FAME$ at the optimal reaction were in agreement with the experimental values of 99.99 % and 70.93 %, respectively.

The biofuel production in SCM and SCE from UPO was compared at the optimal operating parameters of 400 °C and reaction time of 10 min. Under this condition, the alcohol to oil molar ratio can be reduced to 12:1 and almost 99% triglycerides conversion was attained for both SCM and SCE. Moreover, the levels of mono-, di-, and tri-glycerides were within the maximum limits set by the European Standard (EN 14214) for biodiesel fuel. However, the ester contents were reduced due to the degradation of unsaturated fatty acids at the high temperature and long reaction time. The reaction products of glycerol with SCM and SCE were completely miscible with the fuel phase and increase the fuel yield by approximately 6% and 8%, respectively. The chemical kinetics study of both SCM and SCE indicated that reactions followed the pseudo-first-order reaction kinetics. Therefore, the optimal conditions and chemical kinetics data indicate the potential to develop a continuous production process of biofuel in SCA at 400 °C.

8.1.2. Continuous biofuel production with SCA

To scale-up reactor, biofuel production from palm oil was investigated in SCA at the temperature of at 400 °C and 15 MPa with low proportion of alcohol to oil molar

ratio. Under this condition, phase transition of the mixture indicated that the methanol-oil and ethanol-oil mixtures are a monophasic mixture. A residence time in the range 18–20 min is recommended to achieve the triglyceride conversion up to 99.99% and avoid the thermal decomposition of FAMEs. The maximum ester contents are 90% and 80% for RPO and UPO, respectively.

The effect of ethanol with water mixture was also investigated by varying between 85 wt. % and 99.8 wt. %. The presence of water in the reaction system was not a significant effect on ester content. The obtained ester contents were approximately 85% for all biofuel samples. The recommendation of residence time is 50 min for 85-96 wt. % ethanol-water mixture and 60 min for 99.8 wt. % ethanol-water mixtures.

According to the fuel properties of all biofuel samples, it should be blended with petro-diesel fuel before use in vehicles due to the slightly low of ester content and high viscosity.

8.1.3. Phase behavior of palm oil transesterification with SCM

The phase equilibrium of methanol–tripalmitin binary system was experimentally investigated and modeled using PR-MHV2-UNIQUAC thermodynamic model with EoS/GE approaches. The PR-MHV2-UNIQUAC model shows the best-fitted equilibrium data with a minimum average absolute relative error of 5.58 %. Besides, the PR-MHV2-UNIQUAC model is applied to the prediction of phase behavior in biofuel production from palm oil in SCM. The phase envelops predictions agree well with experimental data. Therefore, the PR-MHV2-UNIQUAC is found to be a suitable model for process design in order to obtain a single-phase system in the reactor.

8.2. Recommendation

In this study, the continuous biofuel production from palm oil with SCM and SCE was investigated. It could be presumed that the biofuel has a possibility to employ

as alternative fuel for diesel engine. However, some issues have originated from this study and warrant further researches as following aspects:

8.2.1. Mechanism and kinetics of the reactions in the biofuel production in SCA at 400 °C.

As found in the biofuel production in SCA at 400 °C, there are not only the transesterification of triglyceride but also the side reactions of hydrolysis and esterification, are simultaneously occurred during the process, including the etherification reaction of glycerol. The study of kinetics for all reactions is recommended to gain a better understanding of the mechanism for the biofuel production.

8.2.2. Phase behavior of biofuel production in the view cell

Since the study phase behavior for biofuel production with SCA, i.e. the phase transition in chapter IV and phase equilibrium in chapter VII, can be provided to explore the operating conditions to guarantee of running the reaction in a single-phase system all along the reactor. However, the direct observation of the phase behavior during the reaction process has not been possible. Thus, phase behavior was recommended to investigate in the view cell in order to confirm the real single-phase system in the reactor.

8.2.3. The effect of biofuel composition on fuel properties.

According to the biofuel samples in this study comprise with both the fatty acid alkyl ester and several minor compounds from the thermal decomposition reaction and etherification of glycerol. The fuel properties of biofuel are directly influenced by fatty ester composition and the presence of the minor compounds. Thus, the effect of biofuel composition on fuel properties should be considered and further investigated in order to improve and to control the quality of biofuel production with SCA at 400 °

REFERENCES

[1] Carraretto, C., Macor, A., Mirandola, A., Stoppato, A., Tonon, S. Biodiesel as alternative fuel: Experimental analysis and energetic evaluations. Energy 29 (2004): 2195-2211.

[2] Kusdiana, D., Saka, S. Effects of water on biodiesel fuel production by supercritical methanol treatment. Bioresource technology 91 (2004): 289-295.

[3] Ma, F., Hanna, M.A. Biodiesel production: a review. Bioresource Technology 70 (1999): 1-15.

[4] Anitescu, G., Deshpande, A., Tavlarides, L.L. Integrated Technology for Supercritical Biodiesel Production and Power Cogeneration. Energy & Fuels 22 (2008): 1391-1399.

[5] Kiwjaroun, C., Tubtimdee, C., Piumsomboon, P. LCA studies comparing biodiesel synthesized by conventional and supercritical methanol methods. Journal of Cleaner Production 17 (2009): 143-153.

[6] Marulanda, V.F., Anitescu, G., Tavlarides, L.L. Biodiesel fuels through a continuous flow process of chicken fat supercritical transesterification. Energy & Fuels 24 (2009): 253-260.

[7] Marulanda, V.F., Anitescu, G., Tavlarides, L.L. Investigations on supercritical transesterification of chicken fat for biodiesel production from low-cost lipid feedstocks. J Supercrit Fluid 54 (2010): 53-60.

[8] Anitescu, G., Bruno, T.J. Fluid properties needed in supercritical transesterification of triglyceride feedstocks to biodiesel fuels for efficient and clean combustion − A review. The Journal of Supercritical Fluids 63 (2012): 133-149.

[9] Sawangkeaw, R., Teeravitud, S., Bunyakiat, K., Ngamprasertsith, S. Biofuel production from palm oil with supercritical alcohols: effects of the alcohol to oil molar ratios on the biofuel chemical composition and properties. Bioresource technology 102 (2011): 10704-10710.

[10] Demirbas, A. The importance of bioethanol and biodiesel from biomass. Energy Sources, Part B 3 (2008): 177-185.

[11] UTCC, C. Thailand Regional Economic Report and Outlook: 4th Quarter (2013) and 2014. (2013):

[12] Dallinger, J. Oil palm development in Thailand: economic, social and environmental considerations. Oil Palm Expansion in South East Asia: Trends and Implications for Local Communities and Indigenous Peoples (2011): 24-51.

[13] Lee, K.T., Ofori-Boateng, C., Sustainability of biofuel production from oil palm biomass, Springer2013.

[14] Enweremadu, C.C., Mbarawa, M.M. Technical aspects of production and analysis of biodiesel from used cooking oil—A review. Renewable and Sustainable Energy Reviews 13 (2009): 2205-2224.

[15] Sawangkeaw, R., Ngamprasertsith, S. A review of lipid-based biomasses as feedstocks for biofuels production. Renewable and Sustainable Energy Reviews 25 (2013): 97-108.

[16] Hamze, H., Akia, M., Yazdani, F. Optimization of biodiesel production from the waste cooking oil using response surface methodology. Process Safety and Environmental Protection 94 (2015): 1-10.

[17] Diya'uddeen, B.H., Abdul Aziz, A.R., Daud, W.M.A.W., Chakrabarti, M.H. Performance evaluation of biodiesel from used domestic waste oils: A review. Process Safety and Environmental Protection 90 (2012): 164-179.

[18] Balat, M., Balat, H. Progress in biodiesel processing. Applied Energy 87 (2010): 1815-1835.

[19] Diasakou, M., Louloudi, A., Papayannakos, N. Kinetics of the non-catalytic transesterification of soybean oil. Fuel 77 (1998): 1297-1302.

[20] Coniglio, L., Coutinho, J.A., Clavier, J.-Y., Jolibert, F., Jose, J., Mokbel, I., Pillot, D., Pons, M.-N., Sergent, M., Tschamber, V. Biodiesel via supercritical ethanolysis within a global analysis "feedstocks-conversion-engine" for a sustainable fuel alternative. Progress in Energy and Combustion Science 43 (2014): 1-35.

[21] Semwal, S., Arora, A.K., Badoni, R.P., Tuli, D.K. Biodiesel production using heterogeneous catalysts. Bioresource Technology 102 (2011): 2151-2161.

[22] Kansedo, J., Lee, K.T., Bhatia, S. Biodiesel production from palm oil via heterogeneous transesterification. Biomass and Bioenergy 33 (2009): 271-276.

[23] Fukuda, H., Kondo, A., Noda, H. Biodiesel fuel production by transesterification of oils. Journal of Bioscience and Bioengineering 92 (2001): 405-416.

[24] Kusdiana, D., Saka, S. Methyl Esterification of Free Fatty Acids of Rapeseed Oil as Treated in Supercritical Methanol. Journal of chemical engineering of Japan 34 (2001): 383-387.

[25] Saka, S., Kusdiana, D. Biodiesel fuel from rapeseed oil as prepared in supercritical methanol. Fuel 80 (2001): 225-231.

[26] Demirbaş, A. Biodiesel from vegetable oils via transesterification in supercritical methanol. Energy conversion and management 43 (2002): 2349-2356.

[27] Pinnarat, T., Savage, P.E. Assessment of noncatalytic biodiesel synthesis using supercritical reaction conditions. Industrial & Engineering Chemistry Research 47 (2008): 6801-6808.

[28] Tan, K.T., Gui, M.M., Lee, K.T., Mohamed, A.R. An optimized study of methanol and ethanol in supercritical alcohol technology for biodiesel production. The Journal of Supercritical Fluids 53 (2010): 82-87.

[29] Warabi, Y., Kusdiana, D., Saka, S. Reactivity of triglycerides and fatty acids of rapeseed oil in supercritical alcohols. Bioresource Technology 91 (2004): 283-287.

[30] Demirbas, A. Biodiesel from waste cooking oil via base-catalytic and supercritical methanol transesterification. Energy Conversion and Management 50 (2009): 923-927.

[31] Shin, H.-Y., Lee, S.-H., Ryu, J.-H., Bae, S.-Y. Biodiesel production from waste lard using supercritical methanol. The Journal of Supercritical Fluids 61 (2012): 134-138.

[32] Iijima, W., Kobayashi, Y., Takekura, K., Taniwaki, K., Presented at the 2004 ASAE/CSAE Annual International Meeting2004.

[33] Cao, W., Han, H., Zhang, J. Preparation of biodiesel from soybean oil using supercritical methanol and co-solvent. Fuel 84 (2005): 347-351.

[34] Han, H., Cao, W., Zhang, J. Preparation of biodiesel from soybean oil using supercritical methanol and CO 2 as co-solvent. Process biochemistry 40 (2005): 3148-3151.

[35] Wang, L., He, H., Xie, Z., Yang, J., Zhu, S. Transesterification of the crude oil of rapeseed with NaOH in supercritical and subcritical methanol. Fuel Processing Technology 88 (2007): 477-481.

[36] Bunyakiat, K., Makmee, S., Sawangkeaw, R., Ngamprasertsith, S. Continuous Production of Biodiesel via Transesterification from Vegetable Oils in Supercritical Methanol. Energy & Fuels 20 (2006): 812-817.

[37] He, H., Sun, S., Wang, T., Zhu, S. Transesterification Kinetics of Soybean Oil for Production of Biodiesel in Supercritical Methanol. J Amer Oil Chem Soc 84 (2007): 399-404.

[38] Zhou, C., Wang, C., Wang, W., Wu, Y., Yu, F., Chi, R.a., Zhang, J. Continuous Production of Biodiesel from Soybean Oil Using Supercritical Methanol in a Vertical Tubular Reactor: I. Phase Holdup and Distribution of Intermediate Product along the Axial Direction. Chinese Journal of Chemical Engineering 18 (2010): 626-629.

[39] Imahara, H., Minami, E., Hari, S., Saka, S. Thermal stability of biodiesel in supercritical methanol. Fuel 87 (2008): 1-6.

[40] Shin, H.-Y., Lim, S.-M., Bae, S.-Y., Oh, S.C. Thermal decomposition and stability of fatty acid methyl esters in supercritical methanol. Journal of Analytical and Applied Pyrolysis 92 (2011): 332-338.

[41] Quesada-Medina, J., Olivares-Carrillo, P. Evidence of thermal decomposition of fatty acid methyl esters during the synthesis of biodiesel with supercritical methanol. The Journal of Supercritical Fluids 56 (2011): 56-63.

[42] Patil, P.D., Gude, V.G., Mannarswamy, A., Deng, S., Cooke, P., Munson-McGee, S., Rhodes, I., Lammers, P., Nirmalakhandan, N. Optimization of direct conversion of

wet algae to biodiesel under supercritical methanol conditions. <u>Bioresource Technology</u> 102 (2011): 118-122.

[43] Samniang, A., Tipachan, C., Kajorncheappun-ngam, S. Comparison of biodiesel production from crude Jatropha oil and Krating oil by supercritical methanol transesterification. <u>Renewable Energy</u> 68 (2014): 351-355.

[44] Kulkarni, M.G., Dalai, A.K., Bakhshi, N.N. Transesterification of canola oil in mixed methanol/ethanol system and use of esters as lubricity additive. <u>Bioresource Technology</u> 98 (2007): 2027-2033.

[45] Madras, G., Kolluru, C., Kumar, R. Synthesis of biodiesel in supercritical fluids. <u>Fuel</u> 83 (2004): 2029-2033.

[46] Varma, M.N., Madras, G. Synthesis of Biodiesel from Castor Oil and Linseed Oil in Supercritical Fluids. <u>Industrial & Engineering Chemistry Research</u> 46 (2007): 1-6.

[47] Vieitez, I., da Silva, C., Alckmin, I., Borges, G.R., Corazza, F.C., Oliveira, J.V., Grompone, M.A., Jachmanián, I. Continuous catalyst-free methanolysis and ethanolysis of soybean oil under supercritical alcohol/water mixtures. <u>Renewable Energy</u> 35 (2010): 1976-1981.

[48] Santana, A., Maçaira, J., Larrayoz, M.A. Continuous production of biodiesel using supercritical fluids: A comparative study between methanol and ethanol. <u>Fuel Processing Technology</u> 102 (2012): 110-115.

[49] Silva, C., Weschenfelder, T.A., Rovani, S., Corazza, F.C., Corazza, M.L., Dariva, C., Oliveira, J.V. Continuous production of fatty acid ethyl esters from soybean oil in compressed ethanol. <u>Industrial & Engineering Chemistry Research</u> 46 (2007): 5304-5309.

[50] Gui, M.M., Lee, K.T., Bhatia, S. Supercritical ethanol technology for the production of biodiesel: Process optimization studies. <u>The Journal of Supercritical Fluids</u> 49 (2009): 286-292.

[51] Vieitez, I., da Silva, C., Borges, G.R., Corazza, F.C., Oliveira, J.V., Grompone, M.A., Jachmanián, I. Continuous Production of Soybean Biodiesel in Supercritical Ethanol−Water Mixtures. <u>Energy & Fuels</u> 22 (2008): 2805-2809.

[52] Vieitez, I., Pardo, M.J., da Silva, C., Bertoldi, C., de Castilhos, F., Oliveira, J.V., Grompone, M.A., Jachmanián, I. Continuous synthesis of castor oil ethyl esters under supercritical ethanol. The Journal of Supercritical Fluids 56 (2011): 271-276.

[53] Velez, A., Soto, G., Hegel, P., Mabe, G., Pereda, S. Continuous production of fatty acid ethyl esters from sunflower oil using supercritical ethanol. Fuel 97 (2012): 703-709.

[54] Ngamprasertsith, S., Laetoheem, C.-e., Sawangkeaw, R. Continuous production of biodiesel in supercritical ethanol: a comparative study between refined and used palm olein oils as feedstocks. Journal of the Brazilian Chemical Society 25 (2014): 1746-1753.

[55] Vieitez, I., da Silva, C., Alckmin, I., de Castilhos, F., Oliveira, J.V., Grompone, M.A., Jachmanián, I. Stability of ethyl esters from soybean oil exposed to high temperatures in supercritical ethanol. The Journal of Supercritical Fluids 56 (2011): 265-270.

[56] Vieitez, I., Irigaray, B., Casullo, P., Pardo, M., Grompone, M., Jachmanián, I. Effect of free fatty acids on the efficiency of the supercritical ethanolysis of vegetable oils from different origins. Energy & Fuels 26 (2012): 1946-1951.

[57] Muppaneni, T., Reddy, H.K., Ponnusamy, S., Patil, P.D., Sun, Y., Dailey, P., Deng, S. Optimization of biodiesel production from palm oil under supercritical ethanol conditions using hexane as co-solvent: A response surface methodology approach. Fuel 107 (2013): 633-640.

[58] Sawangkeaw, R., Teeravitud, S., Piumsomboon, P., Ngamprasertsith, S. Biofuel production from crude palm oil with supercritical alcohols: comparative LCA studies. Bioresour. Technol. 120 (2012): 6-12.

[59] Rodríguez-Guerrero, J.K., Rubens, M.F., Rosa, P.T.V. Production of biodiesel from castor oil using sub and supercritical ethanol: Effect of sodium hydroxide on the ethyl ester production. The Journal of Supercritical Fluids 83 (2013): 124-132.

[60] Balat, M. Biodiesel Fuel Production from Vegetable Oils via Supercritical Ethanol Transesterification. Energy Sources, Part A: Recovery, Utilization, and Environmental Effects 30 (2008): 429-440.

[61] Lee, S., Posarac, D., Ellis, N. An experimental investigation of biodiesel synthesis from waste canola oil using supercritical methanol. Fuel 91 (2012): 229-237.

[62] He, H., Wang, T., Zhu, S. Continuous production of biodiesel fuel from vegetable oil using supercritical methanol process. Fuel 86 (2007): 442-447.

[63] Demirbas, A. Thermal degradation of fatty acids in biodiesel production by supercritical methanol. Energy, Exploration & Exploitation 25 (2007): 63-70.

[64] Song, E.S., Lim, J.W., Lee, H.S., Lee, Y.W. Transesterification of RBD palm oil using supercritical methanol. J Supercrit Fluid 44 (2008): 356-363.

[65] Hegel, P., Andreatta, A., Pereda, S., Bottini, S., Brignole, E.A. High pressure phase equilibria of supercritical alcohols with triglycerides, fatty esters and cosolvents. Fluid Phase Equilibria 266 (2008): 31-37.

[66] Valle, P., Velez, A., Hegel, P., Mabe, G., Brignole, E.A. Biodiesel production using supercritical alcohols with a non-edible vegetable oil in a batch reactor. The Journal of Supercritical Fluids 54 (2010): 61-70.

[67] Demirbas, A. Biodiesel production via non-catalytic SCF method and biodiesel fuel characteristics. Energy Conversion and Management 47 (2006): 2271-2282.

[68] Rathore, V., Madras, G. Synthesis of biodiesel from edible and non-edible oils in supercritical alcohols and enzymatic synthesis in supercritical carbon dioxide. Fuel 86 (2007): 2650-2659.

[69] Ghoreishi, S.M., Moein, P. Biodiesel synthesis from waste vegetable oil via transesterification reaction in supercritical methanol. The Journal of Supercritical Fluids 76 (2013): 24-31.

[70] Choi, C.-S., Kim, J.-W., Jeong, C.-J., Kim, H., Yoo, K.-P. Transesterification kinetics of palm olein oil using supercritical methanol. The Journal of Supercritical Fluids 58 (2011): 365-370.

[71] Tang, Z., Du, Z., Min, E., Gao, L., Jiang, T., Han, B. Phase equilibria of methanol–triolein system at elevated temperature and pressure. <u>Fluid Phase Equilibria</u> 239 (2006): 8-11.

[72] Negi, D.S., Sobotka, F., Kimmel, T., Wozny, G., Schomäcker, R. Liquid−Liquid Phase Equilibrium in Glycerol−Methanol−Methyl Oleate and Glycerol−Monoolein−Methyl Oleate Ternary Systems. <u>Industrial & Engineering Chemistry Research</u> 45 (2006): 3693-3696.

[73] Glišić, S., Montoya, O., Orlović, A., Skala, D. Vapor-liquid equilibria of triglycerides-methanol mixtures and their influence on the biodiesel synthesis under supercritical conditions of methanol. <u>Journal of the Serbian Chemical Society</u> 72 (2007): 13-27.

[74] Hegel, P., Andreatta, A., Pereda, S., Bottini, S., Brignole, E.A. with triglycerides, fatty esters and cosolvents. <u>Fluid Phase Equilibria</u> 266 (2008): 31-37.

[75] Fang, T., Shimoyama, Y., Abeta, T., Iwai, Y., Sasaki, M., Goto, M. Phase equilibria for the mixtures of supercritical methanol+ C18 methyl esters and supercritical methanol+ α-tocopherol. <u>The Journal of Supercritical Fluids</u> 47 (2008): 140-146.

[76] Shimoyama, Y., Iwai, Y., Jin, B.S., Hirayama, T., Arai, Y. Measurement and correlation of vapor–liquid equilibria for methanol + methyl laurate and methanol + methyl myristate systems near critical temperature of methanol. <u>Fluid Phase Equilibria</u> 257 (2007): 217-222.

[77] Shimoyama, Y., Abeta, T., Iwai, Y. Prediction of vapor–liquid equilibria for supercritical alcohol + fatty acid ester systems by SRK equation of state with Wong–Sandler mixing rule based on COSMO theory. <u>The Journal of Supercritical Fluids</u> 46 (2008): 4-9.

[78] Shimoyama, Y., Abeta, T., Zhao, L., Iwai, Y. Measurement and calculation of vapor–liquid equilibria for methanol + glycerol and ethanol + glycerol systems at 493–573 K. <u>Fluid Phase Equilibria</u> 284 (2009): 64-69.

[79] Almagrbi, A.M., Glisic, S.B., Orlovic, A.M. The phase equilibrium of triglycerides and ethanol at high pressure and temperature: The influence on kinetics of ethanolysis. The Journal of Supercritical Fluids 61 (2012): 2-8.

[80] Glišić, S.B., Skala, D.U. Phase transition at subcritical and supercritical conditions of triglycerides methanolysis. The Journal of Supercritical Fluids 54 (2010): 71-80.

[81] Glisic, S.B., Orlovic, A.M. Modelling of non-catalytic biodiesel synthesis under sub and supercritical conditions: The influence of phase distribution. The Journal of Supercritical Fluids 65 (2012): 61-70.

[82] Kusdiana, D., Saka, S. Two-step preparation for catalyst-free biodiesel fuel production. Appl Biochem Biotechnol 115 (2004): 781-791.

[83] Minami, E., Saka, S. Kinetics of hydrolysis and methyl esterification for biodiesel production in two-step supercritical methanol process. Fuel 85 (2006): 2479-2483.

[84] Sawangkeaw, R., Bunyakiat, K., Ngamprasertsith, S. Effect of co-solvents on production of biodiesel via transesterification in supercritical methanol. Green Chemistry 9 (2007): 679-685.

[85] Muppaneni, T., Reddy, H.K., Patil, P.D., Dailey, P., Aday, C., Deng, S. Ethanolysis of camelina oil under supercritical condition with hexane as a co-solvent. Applied Energy 94 (2012): 84-88.

[86] da Silva, C., de Castilhos, F., Oliveira, J.V., Filho, L.C. Continuous production of soybean biodiesel with compressed ethanol in a microtube reactor. Fuel Processing Technology 91 (2010): 1274-1281.

[87] Bertoldi, C., da Silva, C., Bernardon, J.P., Corazza, M.L., Filho, L.C., Oliveira, J.V., Corazza, F.C. Continuous production of biodiesel from soybean oil in supercritical ethanol and carbon dioxide as cosolvent. Energy & Fuels 23 (2009): 5165-5172.

[88] Trentin, C.M., Lima, A.P., Alkimim, I.P., Da Silva, C., De Castilhos, F., Mazutti, M.A., Oliveira, J.V. Continuous production of soybean biodiesel with compressed ethanol in a microtube reactor using carbon dioxide as co-solvent. Fuel Processing Technology 92 (2011): 952-958.

[89] Sun, J., Ju, J., Ji, L., Zhang, L., Xu, N. Synthesis of biodiesel in capillary microreactors. Industrial & Engineering Chemistry Research 47 (2008): 1398-1403.

[90] Guan, G., Kusakabe, K., Moriyama, K., Sakurai, N. Transesterification of sunflower oil with methanol in a microtube reactor. Industrial & Engineering Chemistry Research 48 (2009): 1357-1363.

[91] da Silva, C., de Lima, A.P., de Castilhos, F., Cardozo Filho, L., Oliveira, J.V. Non-catalytic production of fatty acid ethyl esters from soybean oil with supercritical ethanol in a two-step process using a microtube reactor. Biomass and Bioenergy 35 (2011): 526-532.

[92] Ngamprasertsith, S., Sawangkeaw, R. Transesterification in supercritical conditions. Biodiesel-Feedstocks and Processing Technologies. Rijeka: InTech (2011): 247-268.

[93] Lima, D.G., Soares, V.C., Ribeiro, E.B., Carvalho, D.A., Cardoso, É.C., Rassi, F.C., Mundim, K.C., Rubim, J.C., Suarez, P.A. Diesel-like fuel obtained by pyrolysis of vegetable oils. Journal of Analytical and Applied Pyrolysis 71 (2004): 987-996.

[94] Ltd., K.I. Fluidized Baths http://www.keison.co.uk/techneprecisionfluidisedsand baths.shtml.

[95] Brunner, G., Gas extraction: an introduction to fundamentals of supercritical fluids and the application to separation processes, Springer1994.

[96] Camy, S., Pic, J.S., Badens, E., Condoret, J.S. Fluid phase equilibria of the reacting mixture in the dimethyl carbonate synthesis from supercritical CO2. The Journal of Supercritical Fluids 25 (2003): 19-32.

[97] Esteban, B., Riba, J.-R., Baquero, G., Rius, A., Puig, R. Temperature dependence of density and viscosity of vegetable oils. Biomass and Bioenergy 42 (2012): 164-171.

[98] Kuehl, R.O., Kuehl, R., Design of experiments: statistical principles of research design and analysis, Duxbury/Thomson Learning Pacific Grove, CA:2000.

[99] Myers, R.H., Montgomery, D.C., Anderson-Cook, C.M., Response surface methodology: process and product optimization using designed experiments, John Wiley & Sons2009.

[100] EN 141032003.

[101] D2887, A., ASTM D2887, ASTM International West Conshohocken, PA2008.

[102] Bastida, S., Sanchez-Muniz, F.J. Polar content vs. TAG oligomer content in the frying-life assessment of monounsaturated and polyunsaturated oils used in deep-frying. J Am Oil Chem Soc 79 (2002): 447-451.

[103] Encinar, J.M., Sanchez, N., Martinez, G., Garcia, L. Study of biodiesel production from animal fats with high free fatty acid content. Bioresource Technology 102 (2011): 10907-10914.

[104] Tan, K.T., Lee, K.T., Mohamed, A.R. Effects of free fatty acids, water content and co-solvent on biodiesel production by supercritical methanol reaction. J Supercrit Fluid 53 (2010): 88-91.

[105] Vieitez, I., Irigaray, B., Casullo, P., Pardo, M.J., Grompone, M.A., Jachmanian, I. Effect of Free Fatty Acids on the Efficiency of the Supercritical Ethanolysis of Vegetable Oils from Different Origins. Energy & Fuels 26 (2012): 1946-1951.

[106] Knothe, G. "Designer" biodiesel: Optimizing fatty ester (composition to improve fuel properties. Energy & Fuels 22 (2008): 1358-1364.

[107] Sawangkeaw, R., Bunyakiat, K., Ngamprasertsith, S. Continuous production of biodiesel with supercritical methanol: Optimization of a scale-up plug flow reactor by response surface methodology. Fuel Processing Technology 92 (2011): 2285-2292.

[108] Tan, K.T., Lee, K.T., Mohamed, A.R. Optimization of supercritical dimethyl carbonate (SCDMC) technology for the production of biodiesel and value-added glycerol carbonate. Fuel 89 (2010): 3833-3839.

[109] Steel, R.G., Torrie, J.H. Principles and procedures of statistics. Principles and procedures of statistics. (1960):

[110] de Boer, K., Bahri, P.A. Supercritical methanol for fatty acid methyl ester production: A review. Biomass and Bioenergy 35 (2011): 983-991.

[111] Sawangkeaw, R., Bunyakiat, K., Ngamprasertsith, S. A review of laboratory-scale research on lipid conversion to biodiesel with supercritical methanol (2001-2009). J Supercrit Fluid 55 (2010): 1-13.

[112] Hegel, P., Mabe, G., Pereda, S., Brignole, E.A. Phase Transitions in a Biodiesel Reactor Using Supercritical Methanol. Industrial & Engineering Chemistry Research 46 (2007): 6360-6365.

[113] Yurttas, L., Holste, J.C., Hall, K.R., Gammon, B.E., Marsh, K.N. Semiautomated Isochoric Apparatus for p-V-T and Phase Equilibrium Studies. Journal of Chemical & Engineering Data 39 (1994): 418-423.

[114] Duarte-Garza, H.A., Holste, J.C., Hall, K.R., Marsh, K.N., Gammon, B.E. Isochoric pVT and Phase Equilibrium Measurements for Carbon Dioxide + Nitrogen. Journal of Chemical & Engineering Data 40 (1995): 704-711.

[115] Zhou, J., Patil, P., Ejaz, S., Atilhan, M., Holste, J.C., Hall, K.R. (p, V m, T) and phase equilibrium measurements for a natural gas-like mixture using an automated isochoric apparatus. Journal of Chemical Thermodynamics 38 (2006): 1489-1494.

[116] Velez, A., Pereda, S., Brignole, E.A. Isochoric lines and determination of phase transitions in supercritical reactors. The Journal of Supercritical Fluids 55 (2010): 643-647.

[117] Velez, A., Hegel, P., Mabe, G., Brignole, E.A. Density and Conversion in Biodiesel Production with Supercritical Methanol. Industrial & Engineering Chemistry Research 49 (2010): 7666-7670.

[118] Haynes, W.M., CRC handbook of chemistry and physics, CRC press2013.

[119] Barrufet, M.A., Eubank, P.T. New physical constraints for fluid mixture equations of state and mixture combining rules. Fluid Phase Equilibria 37 (1987): 223-240.

[120] Ka, H., Sa, K., AYa, T. The Management of Waste Cooking Oil: A Preliminary Survey.

[121] Manuale, D.L., Mazzieri, V.M., Torres, G., Vera, C.R., Yori, J.C. Non-catalytic biodiesel process with adsorption-based refining. <u>Fuel</u> 90 (2011): 1188-1196.

[122] Moser, B.R., Biodiesel production, properties, and feedstocks, Biofuels, Springer2011, pp. 285-347.

[123] Hoekman, S.K., Broch, A., Robbins, C., Ceniceros, E., Natarajan, M. Review of biodiesel composition, properties, and specifications. <u>Renewable and Sustainable Energy Reviews</u> 16 (2012): 143-169.

[124] Lin, R., Zhu, Y., Tavlarides, L.L. Effect of thermal decomposition on biodiesel viscosity and cold flow property. <u>Fuel</u> 117, Part B (2014): 981-988.

[125] Sawangkeaw, R., Satayanon, W., Bunyakiat, K., Camy, S., Condoret, J.-S., Ngamprasertsith, S. Continuous Production of Biodiesel with Supercritical Methanol: a Simple Compressible Flow Model for Tubular Reactors. <u>International Journal of Chemical Reactor Engineering</u> 9 (2011):

[126] Peng, D.-Y., Robinson, D.B. A new two-constant equation of state. <u>Industrial & Engineering Chemistry Fundamentals</u> 15 (1976): 59-64.

[127] Sales-Cruz, M., Aca-Aca, G., Sánchez-Daza, O., López-Arenas, T., Proceedings of the 20th European Symposium on Computer Aided Process Engineering, Elsevier BV, Amsterdam2010.

[128] Kontogeorgis, G.M., Folas, G.K., Thermodynamic models for industrial applications: from classical and advanced mixing rules to association theories, John Wiley & Sons2009.

[129] Magnussen, T., Rasmussen, P., Fredenslund, A. UNIFAC parameter table for prediction of liquid-liquid equilibriums. <u>Industrial & Engineering Chemistry Process Design and Development</u> 20 (1981): 331-339.

[130] Casas, A., Rodríguez, J.F., del Peso, G.L., Rodríguez, R., Vicente, G., Carrero, A. Liquid–Liquid Phase Equilibria for Soybean Oil Methanolysis: Experimental, Modeling, and Data Prediction. <u>Industrial & Engineering Chemistry Research</u> 53 (2014): 3731-3736.

APPENDIX

APPENDIX A

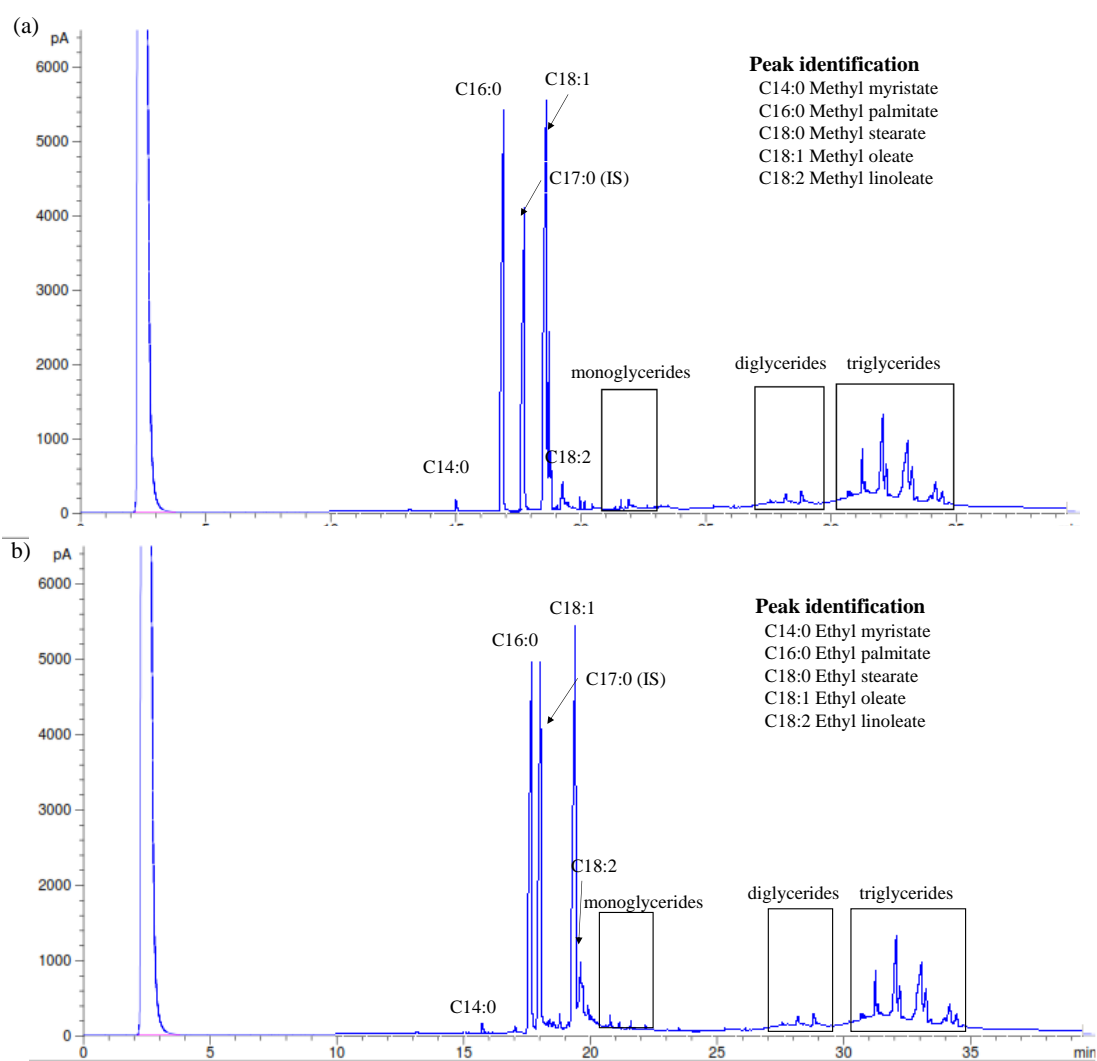# DETERMINATION OF TOTAL FATTY ACID ALKYL ESTER AND MONO-, DI-, AND TRI- GLYCERIDES IN BIOFUEL

Figure A1. The GC-chromatogram of (a) FAME and (b) FAEE

According to European standard method EN 14103:2003[100], methyl heptadecanoate was employed as the internal standard to determine the %FAME and %FAEE of each biofuel sample using Equation (A1),

$$\%FAM(E)E = \frac{\Sigma A - A_{IS}}{A_{IS}} \times \frac{C_{IS} \times V_{IS}}{m} \times 100, \tag{A1}$$

where ΣA is the total peak area of the alkyl ester (C14:0–C18:3), A_{IS} is the area of the peak corresponding to methyl heptadecanoate, C_{IS} is the concentration of methyl heptadecanoate in heptane (mg/mL), V_{IS} is the volume of methyl heptadecanoate solution (mL), and m is the mass of biofuel sample (mg).

The amount of mono-, di-, and tri-glyceride in each biofuel samples was calculated with the calibration function derived from the calibration curved (Figure A3). The triolein, diolein, and monoolein were employed as the standard for calibration solutions and the chromatogram displays Figure A2.
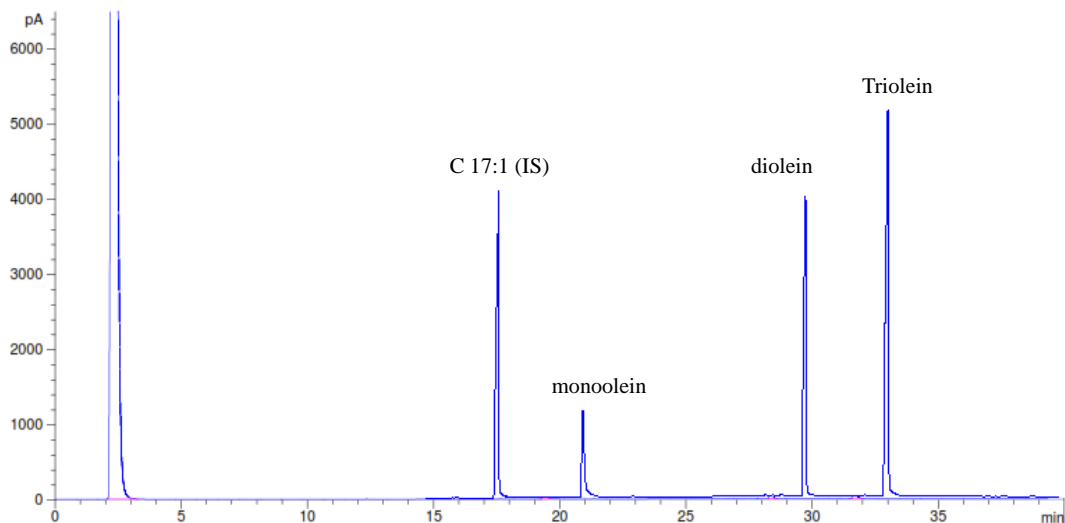
Figure A2. The GC-chromatogram of mixture standard solutions.
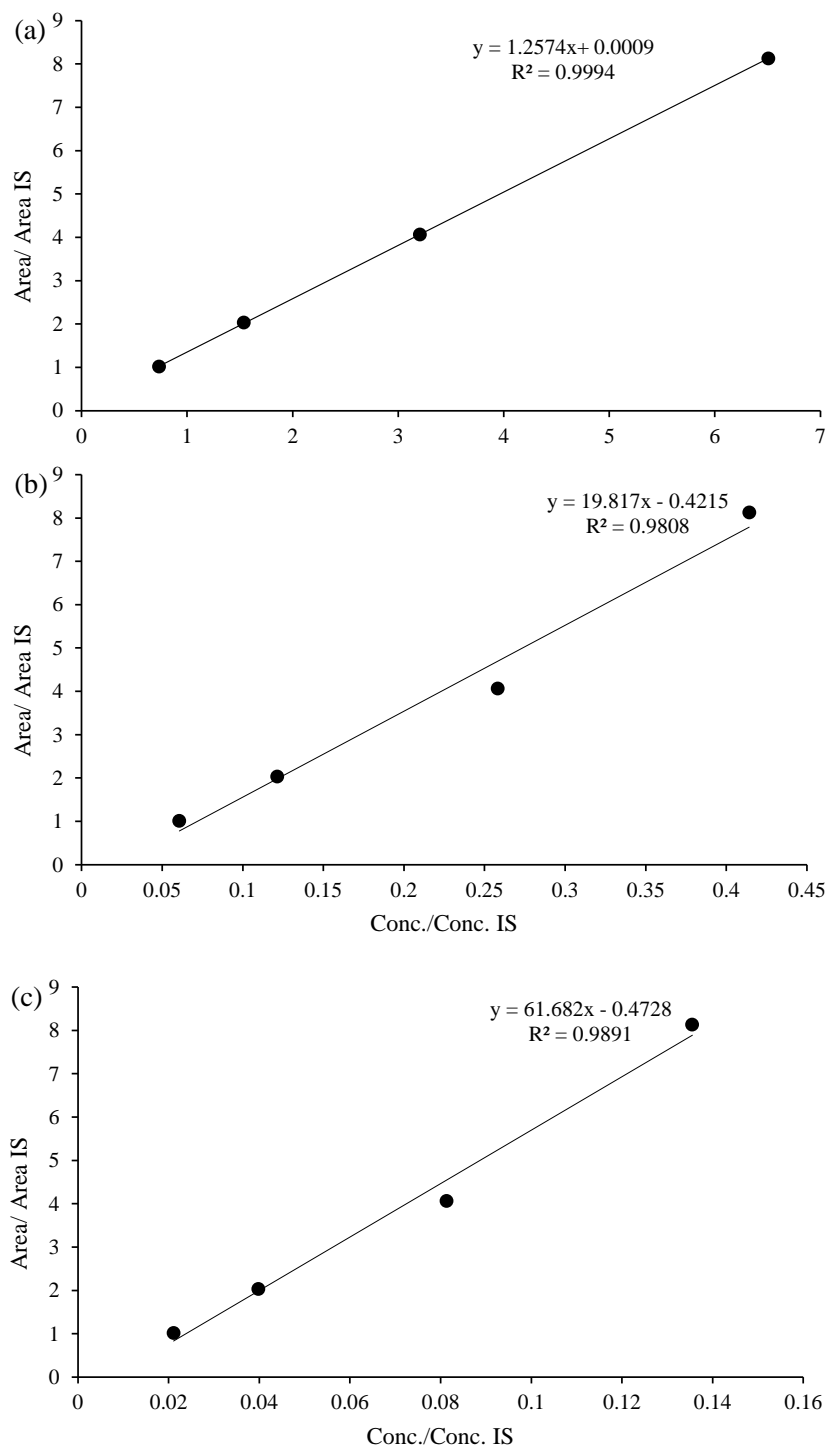
Figure A3. Calibration curves for (a) triolein, (b) diolein, and (c) triolein

APPENDIX B

THE STATISTICAL ANALYSIS OF THE REGRESSION MODEL

As indicated in Chapter IV, the normality and randomness of the residuals were considered to checking the model adequacy. Figure B1 and Figure B2 show the normal plot of the residuals, the relationship between residuals and run number, and the relationship betwee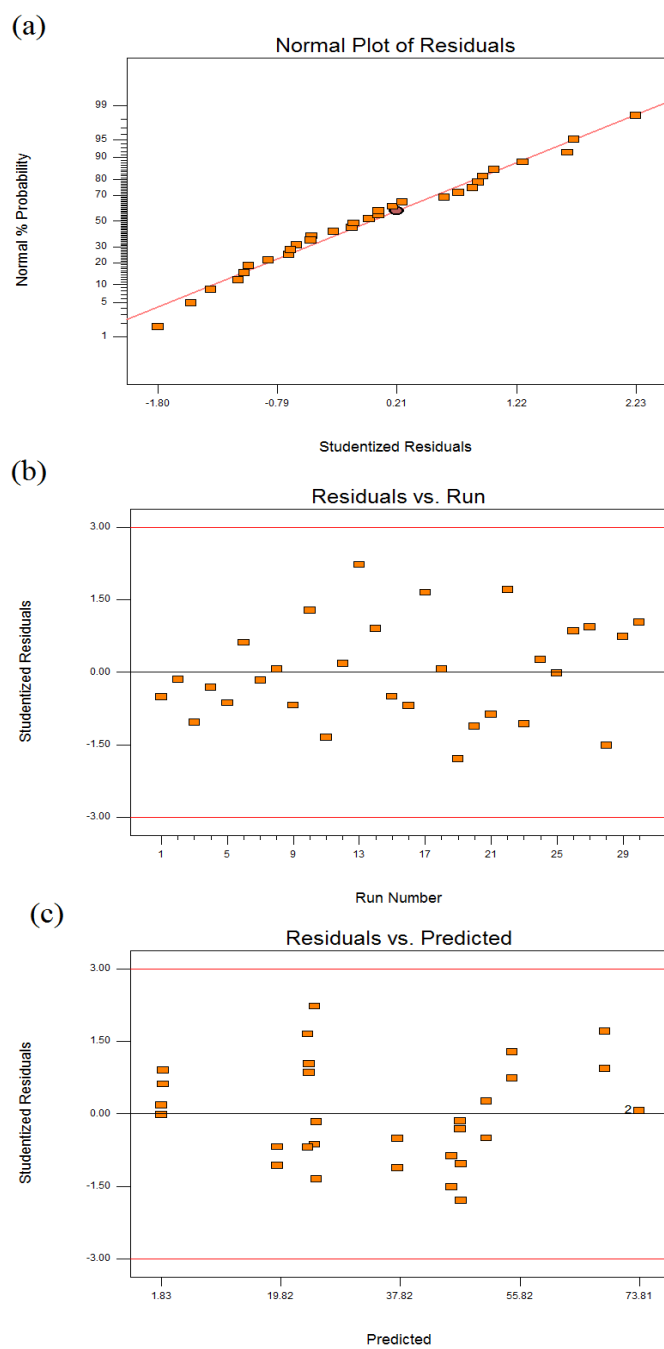n residuals and predicted values for triglyceride conversion and ester content, respectively. All data obtained from Design Expert ® 6.0 software. The results from the normal plot demonstrated that the residuals commonly follow a straight line for both triglyceride conversion and ester content in Figure B1 (a) and Figure B2 (a), respectively. Therefore, it can be implied that the errors are normally distributed.

Moreover, the relationship between residuals and run number and the relationship between residuals and predicted values were observed to have the unusual structure and pattern in Figure B1 (b-c) and Figure B2 (b-c). It is indicated that the model of both responses are adequate and not have to suppose the violation of independence or constant variance assumption.
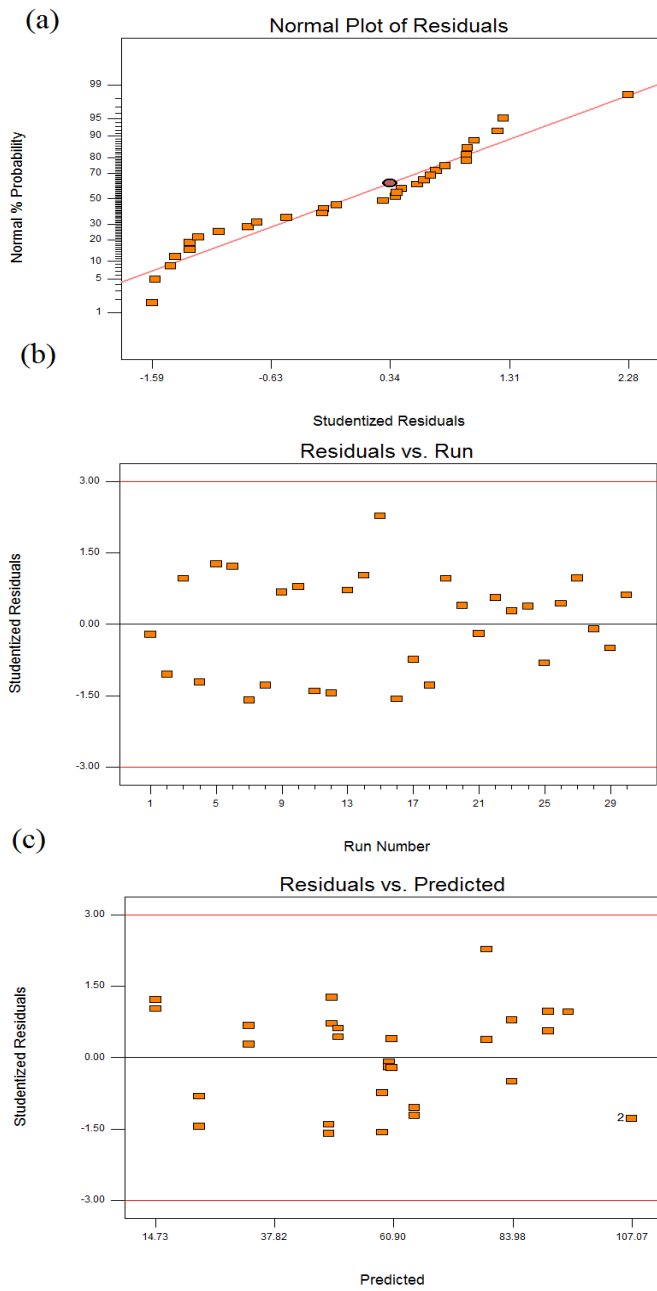
Figure B1. (a) The normal plot of the residuals, (b) The relationship between residuals and run number, and (c) The relationship between residuals and predicted values for triglyceride conversion.

Figure B2. (a) The normal plot of the residuals, (b) The relationship between residuals and run number, and (c) The relationship between residuals and predicted values for ester content

APPENDIX C
CALCULATION OF MASS BALANCE

In this study, three type of mass balance were performed, which depend on the type of feedstocks (RPO and UPO) and type of alcohol used (SCM and SCE). Firstly, the mass balance of biofuel production from RPO with SCM and SCE display in Figure C1. In this case, the transesterification reaction took place. For instance, the calculation of RPO with SCM was calculated as follow:
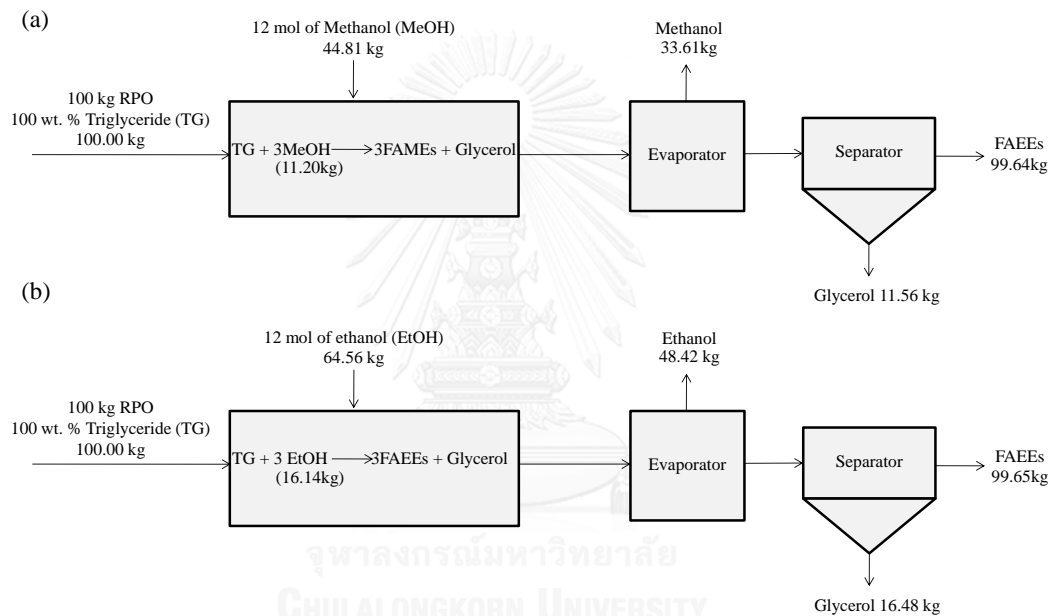
Figure C1. Flow sheet of the process with mass balance of biofuel production from RPO under the optimal molar ratio of 12:1 with (a) SCM and (b) SCE

Basis 100 kg of oil feeds

For RPO → Transesterification reaction: TG + 3MeOH = 3FAMEs + glycerol

The requirement of MeOH is

From, $\dfrac{1\,mole\,of\,TG}{3\,mole\,of\,MeOH} = \dfrac{\dfrac{100kg}{858\,g/mole}}{\dfrac{MeOH\,kg}{32.04\,g/mole}}$

Hence,
$$MeOH \ required = \frac{100\,kg}{858\ g/mole} \times 32.04\ g/mole \times \frac{3\ mole}{1mole}$$

$$= \underline{\textbf{\textit{11.20 kg}}}$$

With the alcohol to oil molar ratio of 12:1

The supplement of MeOH is

From,
$$\frac{1\,mole\ of\ TG}{12\,mole\ of\ MeOH} = \frac{\dfrac{100kg}{858\ g/mole}}{\dfrac{MeOH\ g}{32.04\ g/mole}}$$

Hence,
$$MeOH \ supplied = \frac{100\,kg}{858\ g/mole} \times 32.04\ g/mole \times \frac{12\ mole}{1mole}$$

$$= \underline{\textbf{\textit{44.81 kg}}}$$

The formation of FAMEs is

From,
$$\frac{1\,mole\ of\ TG}{3\,mole\ of\ FAMEs} = \frac{\dfrac{100.00kg}{858\ g/mole}}{\dfrac{FAMEs\ kg}{284.98\ g/mole}}$$

Hence,
$$FAMEs \ formed = \frac{100.00kg}{858\ g/mole} \times 284.98\ g/mole \times \frac{3\ mole}{1mole}$$

$$= \underline{\textbf{\textit{99.64 kg}}}$$

And the formation of glycerol is

From,   mass input   =   mass out put

TG (kg) + MeOH (kg) = FAMEs (kg) + Glycerol (kg)

Hence,   Glycerol formed = (100.00 + 11.20) -99.64

$$= \underline{\textbf{\textit{11.56 kg}}}$$

Therefore, 100 kg of RPO feedstock will react with SCM as follows:

100.00 kg TG + 11.20 kg MeOH = 99.62 kg FAMEs +11.20 kg (glycerol) (C1)

Secondly, the mass balance of biofuel production from UPO with SCM and SCE display in Figure C2. In this case, the transesterification of triglyceride and esterification of free fatty acid simultaneously took place. For instant, the calculation of UPO with SCM was calculated as follow:
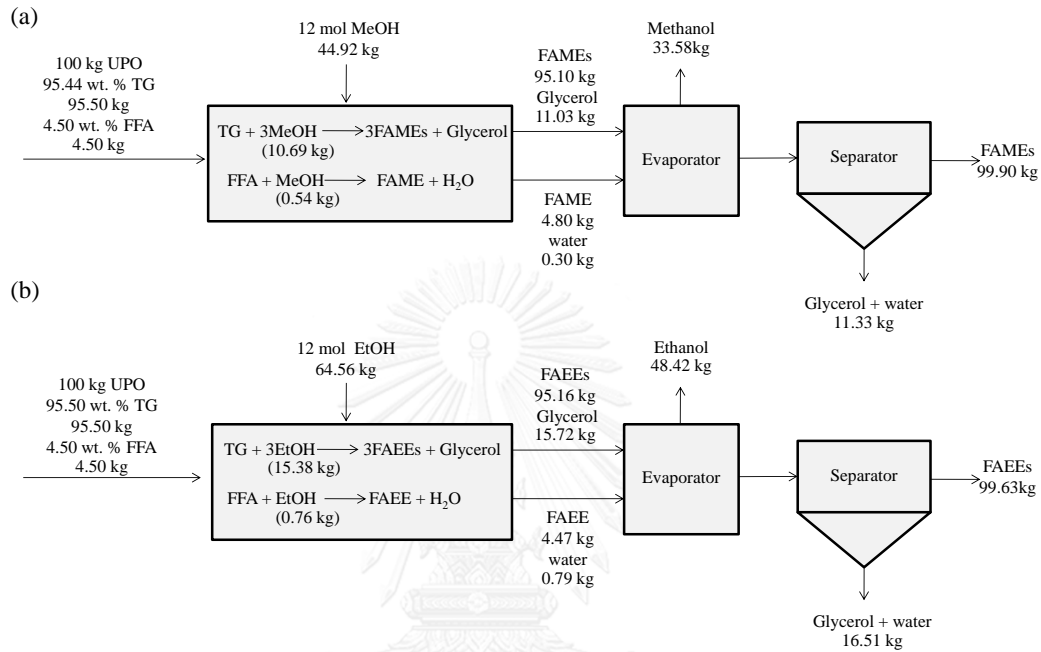

Figure C2. Flow sheet of the process with mass balance of biofuel production from UPO under the optimal molar ratio of 12:1 with (a) SCM and (b) SCE

Basis 100 kg of oil feeds

For UPO →   Transesterification reaction: TG + 3MeOH = 3FAMEs + glycerol

Esterification reaction: FFA + MeOH = FAMEs + H2O

The requirement of MeOH for the transesterification reaction is

From, $$\frac{1\ mole\ of\ TG}{3\ mole\ of\ MeOH} = \frac{\dfrac{95.44kg}{858\ g/mole}}{\dfrac{MeOH\ kg}{32.04\ g/mole}}$$

$$MeOH\ required\ for\ TG = \frac{95.44\,kg}{858\ g/mole} \times 32.04\ g/mole \times \frac{3\ mole}{1mole}$$

$$= \underline{\textbf{\textit{10.69 kg}}}$$

The requirement of MeOH for the esterification reaction is

From,
$$\frac{1\,mole\,of\,FFA}{1\,mole\,of\,MeOH} = \frac{\frac{4.56kg}{270.89\,g/mole}}{\frac{MeOH\,kg}{32.04\,g/mole}}$$

$$MeOH\,required\,for\,FFA = \frac{4.56\,kg}{270.89\,g/mole} \times 32.04\,g/mole \times \frac{1\,mole}{1\,mole}$$

$$= \underline{\textbf{0.54 kg}}$$

Therefore, the total requirement of MeOH = 10.69+0.54 = **11.22 kg**

The formation of FAMEs is

From,
$$\frac{1\,mole\,of\,TG}{3\,mole\,of\,FAMEs} = \frac{\frac{95.44kg}{858\,g/mole}}{\frac{FAMEs\,kg}{284.98\,g/mole}}$$

$$FAMEs\,formed\,from\,TG = \frac{95.44\,kg}{858\,g/mole} \times 284.98\,g/mole \times \frac{3\,mole}{1\,mole}$$

$$= \underline{\textbf{95.10 kg}}$$

From,
$$\frac{1\,mole\,of\,MeOH}{1\,mole\,of\,FAME} = \frac{\frac{0.54kg}{32.04\,g/mole}}{\frac{FAME\,kg}{270.89\,g/mole}}$$

$$FAME\,formed\,from\,FFA = \frac{0.54\,kg}{32.04\,g/mole} \times 270.89\,g/mole \times \frac{1\,mole}{1\,mole}$$

$$= \underline{\textbf{4.80 kg}}$$
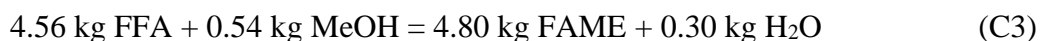
Therefore, the total formed of FAMEs = 95.10+4.80 = **99.90 kg**

And the formation of glycerol and water are

$$Water\,formed\,from\,FFA = 4.56\text{-}4.55$$

$$= \underline{\textbf{0.01 kg}}$$

$$Glycerol\,formed = 95.44g +10.69g\text{-}95.10g$$

$$= \underline{\textbf{11.03 kg}}$$

Therefore, 100 kg of UPO feedstock will react as follows:

95.44 kg TG + 10.69 kg MeOH = 95.10 kg FAMEs +11.03 kg (glycerol)   (C2)

4.56 kg FFA + 0.54 kg MeOH = 4.80 kg FAME + 0.30 kg H_2O (C3)

Considering Equation (C2) and Equation (C3), a mass balance of the overall reaction of UPO is given as

95.44 kg TG + 4.56 kg FFA + 11.23 kg MeOH = 99.90kg FAMEs

+ 11.33 kg (H_2O + glycerol) (C4)
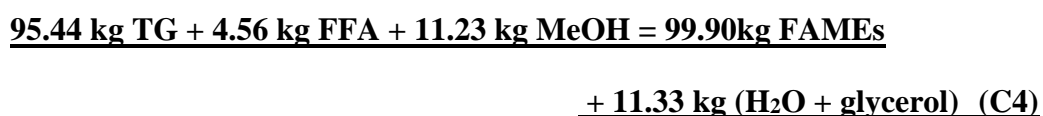
Finally, the mass balance of biofuel production from RPO with SCE (ethanol with water mixture) display in Figure C3. In this case, three types of reaction took place; transesterification and hydrolysis of triglycerides and ethyl esterification of free fatty acid proceeded simultaneously under the supercritical condition. For instance, the calculation of RPO with SCE (96 wt. %) was calculated as follow:
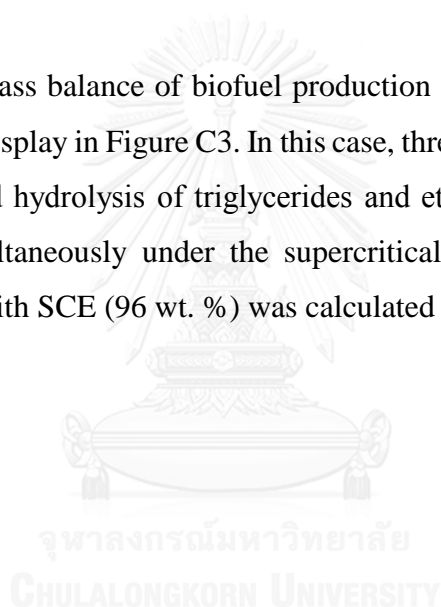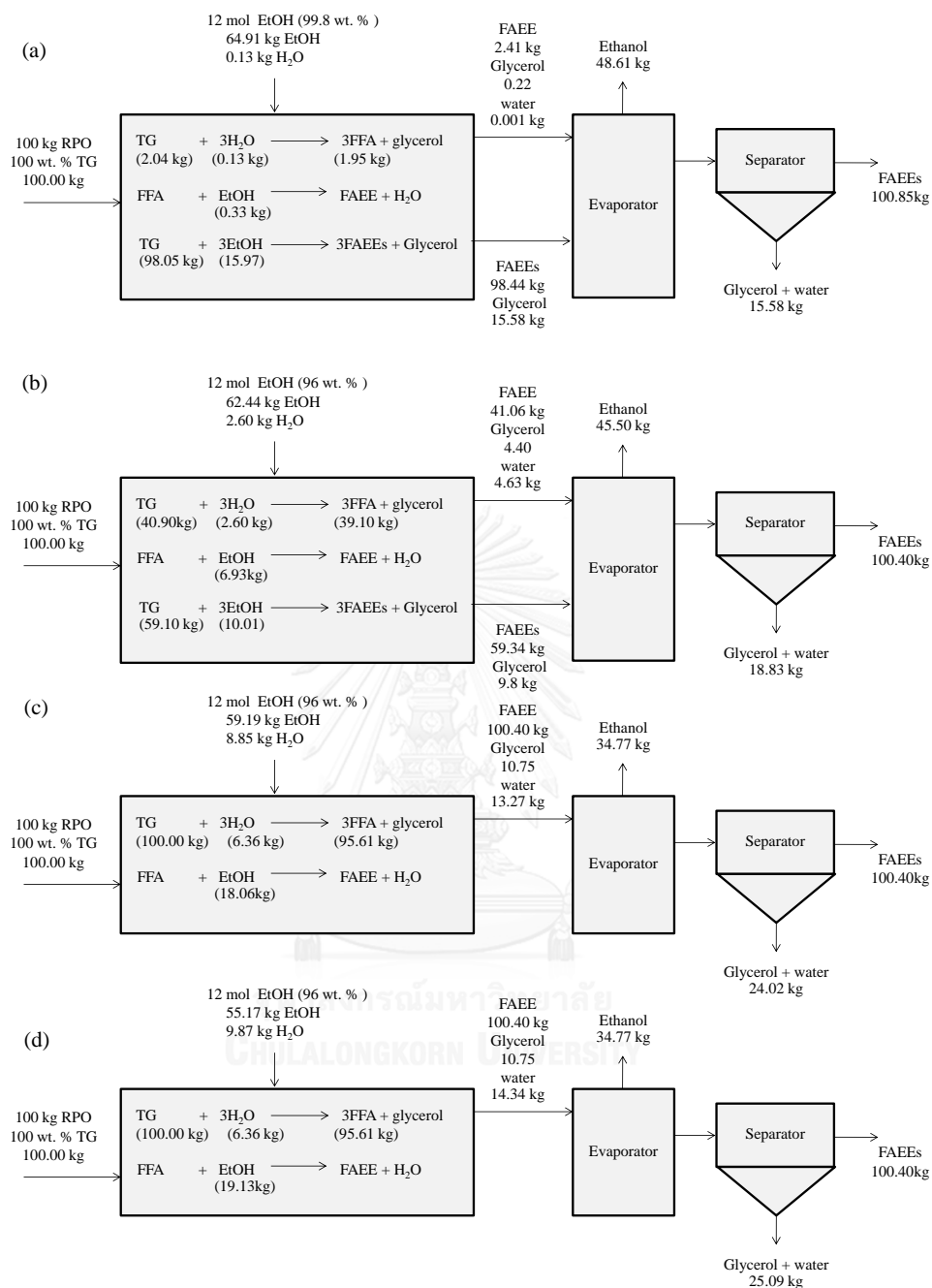
Figure C3. Flow sheet of the process with the mass balance of biofuel production from RPO under the optimal molar ratio of 12:1 with SCM with water mixture of (a) 99.8 wt. % and (b) 96 wt. %, (c) 90 wt. %, and (d) 85 wt. %.

Basis 100 kg of oil feeds

<u>For RPO</u> →   Hydrolysis: TG +3H2O = 3FFA + glycerol

             Esterification reaction: FFA + EtOH = FAEE + H2O

             Transesterification reaction: TG + 3EtOH = 3FAEEs + glycerol

The requirement of TG for the hydrolysis reaction with 2.60 kg of water is

From, $\dfrac{1\,mole\ of\ TG}{3\,mole\ of\ H_2O} = \dfrac{\dfrac{TG\,kg}{850\ g/mole}}{\dfrac{2.60\,kg}{18.01\ g/mole}}$

$$TG = \dfrac{2.60\,kg}{18.01\ g/mole} \times 850\ g/mole \times \dfrac{1\,mole}{3\,mole}$$

$$\underline{\boldsymbol{=40.90\ kg}}$$

The formation of FFA is

From, $\dfrac{1\,mole\ of\ TG}{3\,mole\ of\ FFA} = \dfrac{\dfrac{40.90\,kg}{850\ g/mole}}{\dfrac{FFA\,kg}{270.89\ g/mole}}$

$$FFA = \dfrac{40.90\,kg}{850\ g/mole} \times 270.89\ g/mole \times \dfrac{3\,mole}{1\,mole}$$

$$\underline{\boldsymbol{=39.10\ kg}}$$

The requirement of EtOH for esterification reaction is

From, $\dfrac{1\,mole\ of\ EtOH}{1\,mole\ of\ FFA} = \dfrac{\dfrac{EtOH\,kg}{46.07\ g/mole}}{\dfrac{39.10\,kg}{270.89\ g/mole}}$

$$EtOH\ require\ for\ FFA = \dfrac{39.10\,kg}{270.89\,g/mole} \times 46.07\ g/mole \times \dfrac{1\,mole}{1\,mole}$$

$$= 6.64\ /\ (0.96\ wt.\ \%\ Ethanol) = \underline{\boldsymbol{6.93\ kg}}$$

The formation of FAMEs via the esterification reaction is

From, $\dfrac{1\ mole\ of\ FFA}{1\ mole\ of\ FAEE} = \dfrac{\dfrac{39.10 kg}{270.89\ g/mole}}{\dfrac{X\ kg}{284.48\ g/mole}}$

$$FAEEs\ from\ FFA = \dfrac{39.10 kg}{270.89\ g/mole} \times 297.50\ g/mole \times \dfrac{1\ mole}{1 mole}$$

$$= \underline{\textbf{\textit{41.06 kg}}}$$

Thus, the formation of FAMEs via the transesterification reaction is

From, $\dfrac{1\ mole\ of\ TG}{3\ mole\ of\ FAEEs} = \dfrac{\dfrac{59.10 kg}{850\ g/mole}}{\dfrac{X\ kg}{297.50\ g/mole}}$

$$FAEEs\ formed\ from\ TG = \dfrac{59.10 kg}{850\ g/mole} \times 284.48\ g/mole \times \dfrac{3\ mole}{1 mole}$$

$$= \underline{\textbf{\textit{59.34 kg}}}$$

The requirement of EtOH for transesterification reaction is

From, $\dfrac{3\ mole\ of\ EtOH}{1\ mole\ of\ TG} = \dfrac{\dfrac{EtOHkg}{46.07\ g/mole}}{\dfrac{59.10\ kg}{850\ g/mole}}$

$$EtOH\ require\ for\ TG = \dfrac{59.10 kg}{850\ g/mole} \times 46.07\ g/mole \times \dfrac{3\ mole}{1 mole}$$

$$= 9.60\ /\ (0.96\ wt.\ \%\ Ethanol) = \underline{\textbf{\textit{10.01 kg}}}$$

Therefore, the total formed of FAEEs = *41.06+59.34*=$\underline{\textbf{\textit{100.40 kg}}}$

And, Water formed from FFA = *(39.10+6.93)-41.06*

$$= \underline{\textbf{\textit{4.63 kg}}}$$

Glycerol formed = *(40.90+2.60-39.10) + (59.10+10.01-59.34)*

$$= \underline{\textbf{\textit{14.20 g}}}$$

Therefore, 100 kg of RPO feedstock will react with 96 wt.% Ethanol as follows:

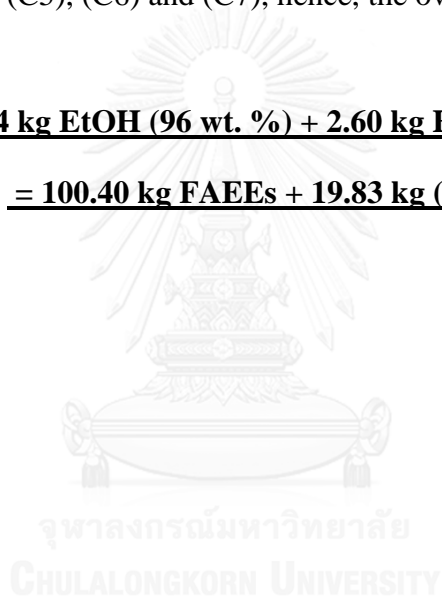40.90 kg TG + 2.60 kg H_2O (4 wt. %)

$$= 39.10 \text{ kg FFA} + 4.40 \text{ kg glycerol} \quad\quad (C5)$$

39.10 kg FFA + 6.93 kg EtOH (96 wt. %)

$$= 41.06 \text{ kg FAEE} + 4.97 \text{ kg } H_2O \quad\quad (C6)$$

59.10 kg TG + 10.01 kg EtOH (96 wt. %)

$$= 59.34 \text{ kg FAEEs} + 9.77 \text{ kg glycerol} \quad\quad (C7)$$

Considering Equation (C5), (C6) and (C7), hence, the overall mass balance of RPO is given as:

100.00 kg TG + 16.94 kg EtOH (96 wt. %) + 2.60 kg H_2O (4 wt. %)

$$\underline{\mathbf{= 100.40 \text{ kg FAEEs} + 19.83 \text{ kg (glycerol} + H_2O) \quad (C8)}}$$

VITA

Miss Winatta Sakdasri was born on 2nd December 1987 at Nan Province, Thailand. She received her Bachelor degree in Industrial Chemistry from the Faculty of Science, Chiang Mai University, Thailand. Winatta started her doctorate program in the 2010 academic year in Department of Chemical Technology, Faculty of Science, Chulalongkorn University. She has received the Royal Golden Jubilee Ph.D. scholarship from Thailand Research Fund (TRF) and Chulalongkorn University (2010-2014) and Teaching Assistant Scholarship from Graduate School (2015) for her Ph.D. study. Winatta also served as a teaching assistant for undergraduate course "Physicochemical Measurements I (2012)", "Unit operations laboratory (2012)", "Fuels testing laboratory (2014), and "Physicochemical Measurements II (2015)".

Winatta also received a Co-financial grant from The France Government's contribution to RGJ for doing research in Université de Toulouse, Institut National Polytechnique de Toulouse (INPT), Laboratoire de Génie Chimique, Toulouse, France. She also presented her work on the topic of "Experimental study and modelling of phase behavior of palm oil transesterification with supercritical methanol" at the international conference Chemical and Biochemical Engineering, Paris, France.

Her first article entitled "Continuous production of biofuel from refined and used palm olein oil with supercritical methanol at a low molar ratio" has been published in "Energy Conversion and Management, Volume 103, 2015, Pages 934–942". She also presented her work in two international conferences in Thailand.